

# UC San Diego

## UC San Diego Electronic Theses and Dissertations

### Title

Hybrid Power System: Grid Stability Through Spinning Reserve

### Permalink

<https://escholarship.org/uc/item/64373402>

### Author

Chauhan, GB Singh

### Publication Date

2022

Peer reviewed|Thesis/dissertation

UNIVERSITY OF CALIFORNIA SAN DIEGO

Hybrid Power System: Grid Stability Through Spinning Reserve

A dissertation submitted in partial satisfaction of the  
requirements for the degree Doctor of Philosophy

in

Engineering Sciences (Mechanical Engineering)

by

GB Singh Chauhan

Committee in charge:

Professor Miroslav Krstic, Chair  
Professor Robert Bitmead  
Professor Raymond De Callafon  
Professor George Tynan  
Professor David Victor

2022

Copyright

GB Singh Chauhan, 2022

All rights reserved.

The Dissertation of GB Singh Chauhan is approved, and it is acceptable in quality and form for publication on microfilm and electronically.

University of California San Diego

2022

## TABLE OF CONTENTS

### CONTENTS

DISSERTATION APPROVAL PAGE.....	iii
LIST OF FIGURES .....	vii
LIST OF TABLES.....	x
LIST OF ABBREVIATIONS.....	xi
ACKNOWLEDGEMENTS .....	xiii
ABSTRACT OF THE DISSERTATION .....	xv
Chapter 1 .....	1
Project Overview .....	1
1.1    Background.....	1
1.2    Research Goals.....	3
1.3    Research Contributions through GTG-BESS Integration:.....	3
Chapter 2 .....	7
Hybrid Power System Framework.....	7
2.1    HPS Architecture .....	7
2.2    Advantages of HPS.....	12
2.3    Grid and Island Mode Transition.....	13
2.4    HPS Application in Combined Heat and Power.....	14
2.5    Blackout Avoidance .....	15
2.6    Grid Support Functions .....	17
Chapter 3 .....	21
Spinning Reserve Application .....	21
3.1    Introduction.....	21
3.2    Literature Review .....	22
3.3    System Overview.....	23
3.4    Plant Operation.....	26

A.	Start-Up Condition.....	26
B.	Normal Operation .....	26
C.	Loss of Generation.....	27
D.	KW/KVAR Dispatch.....	27
E.	Recharging .....	28
3.5	Control Philosophy .....	28
A	Inertia (H) & Rate of Change of Frequency (RoCoF).....	29
B	Calculating Rate of Change of Frequency (RoCoF).....	32
Chapter 4	.....	35
Hybrid Power System Model	.....	35
4.1	Model Background & Literature Review .....	35
4.2	Inverter Model .....	38
4.3	Gas Turbine Generator Model .....	49
4.4	Exciter Model.....	58
4.5	Transformer Model.....	61
Chapter 5	.....	63
Loopback Dynamical Simulation	.....	63
5.1	Introduction.....	63
5.2	Model Configuration .....	64
5.3	Preferred Governor Power Flow Models .....	66
5.4	High Fidelity T60-7901S Power Flow Models.....	69
5.5	Dynamic Performance.....	70
5.5.1	Preferred Governor Power Flow Models.....	71
5.5.2	High Fidelity T60-7901S Power Flow Models .....	72
5.5.3	Multiple Fidelity Comparison .....	73
5.6	Software Requirements .....	75

5.6.1	MATLAB® Simulink® .....	75
5.6.2	RSLogix 5000® .....	76
5.6.3	Studio 5000® Simulation Interface .....	77
Chapter 6 .....		78
Results & Technical Analysis .....		78
6.1	Test Setup of loop back PLC and CHIL .....	78
Chapter 7 .....		95
Economic & Policy Analysis .....		95
7.1	Feasibility & Adoption .....	95
7.2	Policy Potential .....	95
Chapter 8 .....		97
Field Validation and Conclusion .....		97
8.1	Site Testing.....	97
8.2	Results and Discussion .....	98
8.3	Conclusion.....	100

## LIST OF FIGURES

Figure 1	Flexible hybrid power system operation in a microgrid .....	2
Figure 2	Overview of proposed modular HPS with 3 levels of control .....	11
Figure 3	Microgrid operation in grid-connected and islanded modes.....	14
Figure 4	Real power step response measured in power units of HPS .....	16
Figure 5	Hybrid power system application portfolio .....	20
Figure 6	High level control architecture .....	24
Figure 7	Upon loss of one generator remaining three units will start sharing the load .....	25
Figure 8	Upon loss of one GTG, BESS will start dispatching the power.....	26
Figure 9	Dynamic response of a grid upon loss of generation .....	30
Figure 10	Dynamic response of a grid upon loss of a generation .....	34
Figure 11	HPS model simulated in typhoon simulator .....	38
Figure 12	Grid connected inverter model block diagram .....	40
Figure 13	Grid connected inverter electrical diagram.....	41
Figure 14	id and iq controller model block diagram .....	45
Figure 15	Inverter switching frequency setting in model .....	46
Figure 16	Grid forming inverter electrical diagram .....	47
Figure 17	Simplified gas turbine generator model .....	49
Figure 18	Governor model of gas turbine generator set.....	51
Figure 19	PID control subsystem .....	54
Figure 20	Derivative term configuration.....	55
Figure 21	Internal term configuration .....	56
Figure 22	Rotor model .....	57

Figure 23	Load model .....	58
Figure 24	Exciter model of diesel generator set .....	59
Figure 25	Standalone preferred governor model .....	65
Figure 26	Preferred governor block, output NGP .....	66
Figure 27	Preferred governor power flow model, generator driven by mechanical power .....	67
Figure 28	Preferred governor power flow model, generator driven by rotor speed .....	68
Figure 29	High-fidelity electrical system model, speed driven .....	69
Figure 30	High-fidelity electrical system model, mechanical power driven .....	70
Figure 31	Load transient analysis .....	71
Figure 32	Load transient analysis, governor power flow models .....	72
Figure 33	Load transient analysis, high fidelity power flow models .....	73
Figure 34	Load transient analysis, multiple fidelity comparison .....	74
Figure 35	Controller hardware in loop (CHIL) simulation set up using GTG and BESS .....	79
Figure 36	Primary and secondary control loops of hybrid power system.....	79
Figure 37	Discharge-charge of BESS in scenario 1 .....	83
Figure 38	Inverter PI controller performance .....	84
Figure 39	Export-import control in scenario 2 .....	85
Figure 40	When load breaker is closed,GT1/2 share 800KW under isochronous control mode	86
Figure 41	GTG 1 and 2 ramp-up to provide black start charging for BESS .....	87
Figure 42	BESS is fully discharged, GTG will load share and charge .....	88
Figure 43	Scenario 4, GTG 1 trips and BESS immediately takes over the load .....	89
Figure 44	GTG1 trips, GTG2 tries to pickup the load however BESS immediately takes over .	90
Figure 45	Frequency drop with active frequency control from BESS .....	90

Figure 46	Frequency control with BESS and GTG .....	91
Figure 47	Impact of gain adjustment of BESS on islanding .....	93
Figure 48	Solar Kearny Mesa facility one-line diagram .....	97
Figure 49	Test showing exhaust temperature rise due to significant on-load ramp up.....	98
Figure 50	Only gradual step load changes allowing better control for the plant.....	99
Figure 51	System response without any gas turbine load acceptance limitation .....	100
Figure 52	Plant capacity without BESS .....	101
Figure 53	Plant capacity with BESS .....	102

## LIST OF TABLES

Table 1	IEEE AC8B AVR/Exciter Parameters.....	33
Table 2	Gas turbine GT2 governor model parameters .....	33
Table 3	Generator Exciter Settings.....	60
Table 4	Transformer Settings.....	62
Table 5	Scenario Testing Table .....	82
Table 6	System load response.....	100
Table 7	Carbon Footprint and Operational Cost Reduction .....	103

## LIST OF ABBREVIATIONS

BESS	Battery Energy Storage System
CHIL	Controller Hardware In-the-Loop Simulation
DERs	Distributed Energy Resources
ESS	Energy Storage System
$f_n$	Nominal Frequency
GT	Gas Turbine
GTG	Gas Turbine Generator
H	Inertia of Power System
HIL	Hardware In-the-Loop Simulation
$J_s$	Moment of Inertia
kVar	Reactive Power
LS	Load Shedding
MW	Mega-Watts
$N_{gp}$	Gas Producer/Turbine Speed
PID	Proportional Integral Derivative
PLC	Programmable Logic Controller
PMS	Power Management System
PV	Photovoltaic
RoCoF	Rate of Change of Frequency
S	Rated Power (MVA)
Sys	System

T5 Exhaust Temperature of Gas Turbine

$\omega$  Angular Frequency

## ACKNOWLEDGEMENTS

I want to start by thanking Prof. Miroslav Krstic who has been my Chair and Guide on this journey to pursue my educational goals. Without his support I wouldn't have made it this far. I would also like to thank Prof Raymond de Callafon, for sharing his ideas that motivated me to work on the core area of this research; his coaching and direction helped me bridge some gaps in report writing. While working on this dissertation I had to rely on many individuals at my workplace and I will not be able to thank each of them starting from design, analysis, facilities, testing and my leadership team but, want to highlight amazing support that I have received from Habib Abdulelah and Robert Moroto at every step.

Finally, I want to thank my family for their unconditional support in helping me pursue my passion.

## VITA

- 1997 Bachelor of Engineering, Instrumentation & Control, University of Pune, India
- 2001 Master of Business Administration, South Gujarat University, India
- 2019 Master of Science, Mechanical Engineering, University of California San Diego
- 2022 Doctor of Philosophy, Mechanical Engineering, University of California San Diego

## Publications

Energy Storage in Oil and Gas, a Spinning Reserve Application“*5<sup>th</sup> International Hybrid Power Systems Workshop, Germany*, GB Singh, Abdullah Habib, Solar Turbines<sup>®</sup>, USA, HYB21-81

Hybrid Gas Turbine Applications, Gas Machinery Research Council Conference, 2020, GB Singh , Solar Turbines<sup>®</sup>, USA

Annual Hybridization and Electrification forum, 2020, Berlin, Germany, GB Singh, Abdulla Habib, Eric Waters , Solar Turbines<sup>®</sup>, USA

Energy Storage and Battery Solutions during the 2020 crisis, Virtual Conference 2020, GB Singh, Solar Turbines<sup>®</sup>, USA

Hybrid Power Systems: Grid Stability Through Spinning Reserve, Proceedings of ASME Turbomachinery Technical Conference and Exposition, Rotterdam, The Netherlands GT2022- 83419, GB Singh, Solar Turbines<sup>®</sup>

Hybrid Power System: Carbon reduction through spinning reserve, 6th Hybrid Power Systems Workshop, Madeira, Portugal ,26 – 27 April 2022, HYB\_22\_2, GB Singh, UCSD

ABSTRACT OF THE DISSERTATION

Hybrid Power System: Grid Stability Through Spinning Reserve

by

GB Singh Chauhan

Doctor of Philosophy in Engineering Sciences (Mechanical Engineering)

University of California San Diego, 2022

Professor Miroslav Krstic, Chair

The objective of this Doctorate Thesis is to provide a framework for developing and testing modular, fast-acting, coordinated, real-time, power control methodology which can be extended to myriad of Hybrid Power System (HPS) applications. End goal of such hybridization is to offer grid stability, resiliency, higher efficiency and smaller carbon footprint.

As the variable energy sources become predominant in the energy mix, power system stability and resiliency have become the topics of prime research. Grid connected or island systems face similar challenges for multiple applications like frequency control, economic dispatch, peak shaving, black start or spinning reserve. Grid stability is interlinked with grid inertia and the reaction time of an electrical power network. We have studied an island microgrid application consisting of a BESS (Battery Energy Storage System) and Gas Turbine Generator (GTG) system used for spinning reserve application. In this research we present the integrated architecture of Hybrid Power System and determine the control algorithm for such operation. We ascertain the response time for the power system, ensuring there is enough spinning reserve available on the grid for smooth operation of the plant. Later these results are verified through the theoretical framework of Rate of Change of Frequency (RoCoF) and physical testing through Hardware in-the-Loop simulation (HIL).

The modular design of the control algorithms should allow a variety of new and existing Distributed Energy Resources (DERs) in the 1-20 MWe size range to adopt the technology. To accomplish this objective, a Hybrid Power System is modeled and simulated on Controller Hardware in Loop (CHIL) simulator and various operating scenarios and plant disturbance conditions are tested to validate the design. A market assessment of the proposed hybrid power system is also reviewed highlighting the technical challenges, policy issues, economic and market benefits to global plant operators and the larger electric grid.

Scope of Project: In this dissertation, a Hybrid Power System (HPS) consists of Gas Turbine Generator (GTG) and a Battery Energy Storage System (BESS). It is assumed that Battery Storage could be charged through GTG or if the site had a provision, it could be charged through feature specific, renewable energy resources like PV or Wind.

Test Bed: This dissertation was completed through the implementation of control algorithms developed using Rockwell® Programmable Logic Controller (PLC) and validation of the various operation modes of the Microgrid were performed on Typhoon® Hardware In Loop (HIL) simulator.

As a final step the simulated test results were also validated on actual test facility consisting of GTG and BESS. The proposed hybrid power system technology and control methods will provide an effective solution for islanded microgrids and grid operators looking to strengthen grid stability with lowest emissions.

Chapter 1 provides the introduction of Hybrid Power System (HPS), this is further expounded in Chapter 2 highlighting the proposed system description, followed by its architecture and applications. Chapter 3 builds upon the spinning reserve application and concepts of grid inertia. We later discuss the control algorithms used to optimize the operation and provide a theoretical framework for calculating system reaction time. In Chapter 4 we layout the building blocks of modelling. In Chapter 5 theoretical calculations of reaction and response time are validated by Hardware In-the-Loop-Simulation(HIL) and loop back dynamical simulation assuring reliable operation of the proposed hybrid power system. The results of these simulation runs are discussed in Chapter 6. Policy potential for this technology adoption is addressed in Chapter 7. Finally, the data from HPS model is validated through field testing and conclusion is provided in Chapter 8 of this dissertation.

# Chapter 1

## Project Overview

### 1.1 Background

Most power plant installations are designed to produce onsite, base load electrical power and thermal energy at lowest possible cost. These Power plants can be based on Fossil Fuel technology (Diesel Engine, Gas Engine, Gas Turbine, Boilers etc) in open cycle or combined cycle configuration or can be based on renewable resources like hydro, wind or solar energy. When these technologies are combined with an energy storage technology they provide a very powerful energy solution widely termed as Hybrid Power System (HPS). These HPS form a Microgrid, benefits of which can extend beyond cost savings to include system reliability, resilience, and grid services that align with grid modernization objectives.

A formal definition of Hybrid Power System is given as “A Hybrid Power System describes the local association of at least two different types of power generation equipment in a closed grid. The energy supply comes directly via a grid connection point (GCP) to the public transmission or distribution network. As far as renewable generators are integrated into the hybrid power plant, this allows a combination with flexible power generation units, such as a gas turbine or combined cycle plants, to balance volatile feed. The public grid is therefore less stressed”[1].

In the future, HPS can be leveraged to support grid modernization and provide maximum value beyond baseload thermal and electrical power generation. With the advancement of inverter technology, the addition of distributed energy resources, the development of cost-effective storage systems, and the connection of a large number of microgrid systems to the main

grid, there is a need to develop new controls technology that can manage multiple types of DERs. These systems must not only manage low frequency load fluctuations, but also be responsive to high frequency fluctuations. This must be accomplished while optimizing facility operations in response to manufacturing demands and tariff swings.

In this research, a specific hybrid collection of DERs will consist of a Gas Turbine Generator (GTG) and a Battery Energy Storage System (BESS). For coordinated control we developed and tested a modular control algorithm using PLC to dispatch energy. The modular control algorithm is designed to integrate with a variety of power electronics equipment. The technology development embodies a modular approach enabling adaptation with other DERs such as renewable energy sources (Solar/Wind Farm). Finally, the technology aims to support an integrated implementation that enables application of the technology into a variety of existing and future HPS without major modification.

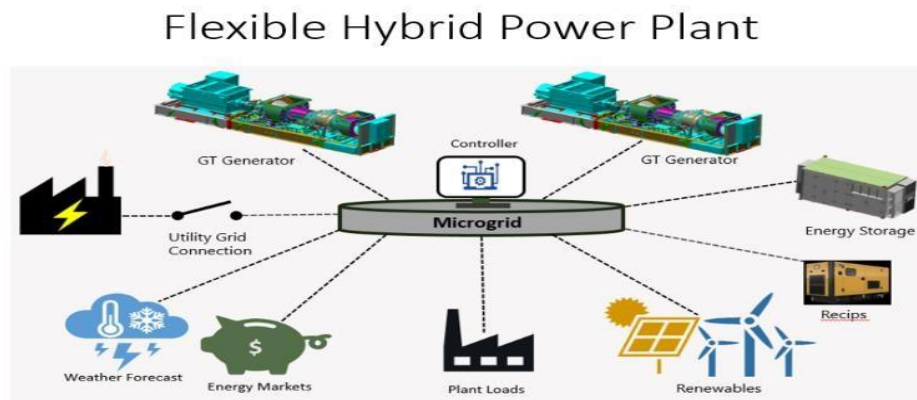


**Figure 1 Flexible hybrid power system operation in a microgrid**

The figure shows multiple Distributed Energy Resources (DER) connected along with Utility connection. Weather forecasting, load profile and operating flexibility of Power Generator Sets (PGS) are few inputs that determine the objective function for the plant operation.

## **1.2 Research Goals**

The specific goals of this research are:

Goal 1: Study and validate HPS models for microgrid capabilities. Develop a library of first principle system components that offer scalability and modularity. The modeling framework includes different HPS configurations consisting of Gas Turbine Generator (GTG) & inverter-based Battery Energy Storage System (BESS).

Goal 2: Develop a modular HPS control system architecture that demonstrates grid supporting function and island voltage/frequency control. This will expound power flow control for grid stability leveraging a unique application in island mode.

Goal 3: Identify site specific model and parameters for the application selected in Goal 2 above. Understand the plant operation and control philosophy and determine the response and reaction time for this HPS.

Goal 4: Validation of the modular HPS developed in Goal 3 above through Control Hardware In-the-Loop (CHIL) testing using the Typhoon HIL simulator and integrated loop back testing with the Programmable Logic Controller (PLC).

Goal 5: Validation of the simulated test results in Goal 4 above, by conducting site testing and ensuring the end result of grid stability and lower carbon footprint.

## **1.3 Research Contributions through GTG-BESS Integration**

Before the work conducted through this dissertation, a strong and broad intuition has existed in the research community that the incorporation of energy storage (in the form of battery systems or other forms of storage—thermal, pneumatic, flywheels, potential energy of water storage at height) into energy generation from conventional, on-demand sources would be

beneficial in multiple ways: for grid stability, fuel efficiency, carbon and other emissions, and cost savings. A fully developed integrated system design, accompanied by an objective comparison with a system comprising entirely of conventional generation sources, has not been conducted before. One of the reasons is the significant cost of such equipment and access to it, which is not possible in the academic environment but only in industry where such resources exist and are being further advanced.

With this dissertation we develop a system in which a storage system (battery-based) supplants a portion of a conventional generation systems consisting of several gas turbines and demonstrate the benefit of this system re-design. We specifically contribute in system design, the accompanying controller design, the development of scenarios for which a fair comparison with the baseline system can be made, and the conduct of tests and comparisons at scale.

We demonstrate primarily an improvement in grid stability, as this improvement is most directly attributable to the control system of the integrated architecture. In addition, accompanying improvements are also made in system efficiency (fuel consumption) and emission reduction.

The advance presented in the dissertation extends beyond research. One needs to envision the societal benefit derived from the introduction and penetration of such systems into energy production across the globe and in a wide range of industrial and residential use sectors. The potential for benefits to the society and the environment are vast, regardless of which companies deliver these technological advances through products.

Next, we spell out in further detail the contributions and tangible outcomes of this work:

### 1) Grid Stability & Frequency Control

Tightly coupled GTG and BESS refer to physically connected technologies having various time constants. They can provide a range of services to the grid, including spinning reserve, power on demand, black start and power phase, frequency, and voltage regulation.

### 2) Cost and siting synergies

Linking Gas Turbine Generator (GTG) and Battery Energy Storage System (BESS) has enabled the sharing of costs and infrastructure, the latter of which has led to increased utilization and defer the need for additional capital and operational expenditure. By using BESS, we can decommission a Gas Turbine unit and avoid its operational expenditure for overhaul, maintenance and upgrade.

### 3) Policies and mandates

The federal investment tax credit or tax avoidance can offset the capital costs associated with an energy storage device that is coupled with GTG. In the real-life use case for this research, customer was able to obtain permits for operation based on the emission avoidance due to this integration.

### 4) Operational benefits

Besides a very effective frequency control provided by the inverter of the BESS, it can capture otherwise clipped energy and have the potential to reduce wear and tear from gas turbine generator cycling.

### 5) Resilience

Integration of gas turbine generation and storage systems can increase plant-level and system resilience by maintaining power quality during an event and providing additional recovery services (e.g., spinning reserve).

#### 6) Environmental sustainability

Hybridization of GTG and BESS allows to displace high emission thermal units. Hybridization with conventional baseload thermal allows for resource operational optimization to avoid off-design/part load operations that result in emissions increases and increased unit operating costs.

#### 7) Testing and Simulation

A key challenge for the wide-scale adoption of integrated storage and GTG solution is in the complexity associated with developing and testing robust and efficient hybrid control solution. This research has provided a methodical approach to leverage Hardware in Loop (HIL) and dynamical loopback simulation through Simulink modeling.

#### 8) Controls Architecture Development

In this research we have optimized control strategy, divided in two different but interdependent layers: a fast control layer (e.g., 10–100 Hz control speed) that will send setpoints and receive feedback from GTG and BESS. The Plant Management System (PMS) layer (millisecond-minutes-hour speed) determines the setpoints to GTG and BESS for different plant modes.

Given the current challenges grid operators face due to the increased penetration of DERs and intermittent renewable resources on the grid, the need for these essential grid stabilization and demand response services are increasing. Transformative solutions developed through this dissertation would facilitate the growth and understanding of this important integration opportunity.

# Chapter 2

## Hybrid Power System Framework

### 2.1 HPS Architecture

The proposed HPS solution is based on the idea of augmenting a traditional Power Generation Unit with energy storage capability to increase the flexibility and agility of the whole system. The application of energy storage could offer unprecedented advantages and flexibilities that are currently being explored and implemented.

To achieve the objective of grid support in the form of primary frequency response, additional services should become available for an HPS. First, grid support demands successful and reliable integration of a HPS plant into the main grid and the ability for fast power flow control following the grid operator's requests. This will be made possible by employing energy storage capability and developing control algorithms to provide smooth and controllable power flow at the grid connection. Next, effective communication should be enabled between the main grid operator with the HPS plant. The function of this communication would be to inform the HPS plant regarding current and future demands that could possibly be met by the HPS plant. Most HPS facilities are interested in disconnected (islanded) operation capability as a resiliency measure to serve their own demand during possible blackouts. This disconnection and reconnection process will also require robust control algorithms to ensure the successful transition between the two states.

Microgrids consisting of Gas turbines in combined heat and power (CHP) plants operating in connected and islanded mode from the main electricity grid have existed for many

decades. These systems have been controlled via classical control methodologies such as droop control, where there is a droop relationship established between speed(frequency) and power. Reader will be able to get further insight into traditional power plant control modes in this reference[2]. With the advancement of inverter technology, the addition of renewable sources of energy, development of economical energy storage systems, and the expectation of a large number of such microgrid systems connected to the main grid, there is a need to develop new controls technology that can manage multiple types of DERs and not only control low frequency load fluctuations, but also the high frequency fluctuations, optimize the operation of the microgrid and be able to manage phase fluctuations as well as voltage and frequency fluctuations.

A hybrid collection of distributed energy resources (DERs) inside a microgrid provide challenges for power flow control at the main Grid Connection Point (GCP) to the utility grid. For proper system integration and coordinated control of the DERs it is imperative to consider the various operational constraints of each DER to properly dispatch power commands according to the requirements summarized in the IEEE P1547 standard to satisfy the performance, operation, testing, safety considerations, and maintenance of the interconnection of the DERs. In this research, the specific hybrid collection of DERs will consist of a Gas Turbine Generator (GTG) and a Battery Energy Storage System (BESS).

For an overview of the HPS we refer to figure 2, where a conventional CHP/PGS is combined with energy storage to produce power for a manufacturing facility. To support modularity, the control system is separated in three levels of functionality, based on the time scale and speed of response required:

**1.** Level 1 also known as Unit Level Control indicates a high bandwidth (10Hz or more update rate) real (P) and reactive (Q) power control of the flex-CHP system consisting of a fast battery storage system combined with a much slower DER like Gas Turbine Generator (GTG) or heat & power turbine system. Each of these DERs have their independent Unit Level Controllers (ULCs) which are tied to Station Microgrid Controller (SMC) command during grid- connected mode operation but keep the autonomy to perform local optimization on the power exchange of the DER units, as well as implement fast load tracking following transition to an autonomous mode[3]. In a decentralized operation, the goal is to provide the maximum autonomy to the DER units and loads inside the microgrid. In this case, the ULCs are intelligent, make decisions locally and can communicate with each other to create a larger intelligent entity. The task of these controllers is not to maximize the performance of an individual unit, but to optimize the overall performance of the microgrid. This decentralized operation is often approached by researchers through multi-agent systems, an area of possible future research in the field of Microgrid Controllers. In order to implement autonomous systems or functions, intelligent agent technologies can be a good solution. An intelligent agent (abbreviated as an *agent*) can sense external environmental changes, effectively make decisions based on designed purposes against the changes, and act autonomously according to the decision. A multiagent system is an autonomous system or society composed of multiple agents. In the multiagent system, agents can communicate using an agent communication language (ACL) and share knowledge for their cooperation [4]

**2.** Level 2 control also known as Station Level Control consists of a lower bandwidth (0.25Hz update rate) power or voltage/angle update control to regulate frequency and voltage at the Grid Connection Point (GCP) or sometimes called Point of Common Coupling (PCC). This

is where the Station Microgrid Controller is operating. As shown in figure 2, for the purpose of this dissertation and model simulation we have used Rockwell® PLC to simulate all the signals to different plant models and DERs. SMC will assign real and reactive power references for the DER units to appropriately share power among the DER units, respond to microgrid disturbances and transients, balance the power and restore the frequency, as well as enable synchronization of the microgrid with local utility network, perform islanding operation if needed. In the case of off-grid microgrids for electrification of remote areas, where fueled back up power and energy storage devices keep the balance of the system, the dispatch strategy is strongly related with the consumption of fuel and prolongation of the lifetime of the equipment. In Industry there are four commonly used dispatch strategies, which are related with the cooperation of the diesel generator and the batteries in the autonomous microgrid: the frugal dispatch strategy, the load following strategy, the state of charge (SOC) set point strategy and full power/minimum runtime strategy [5]. The Algorithms must cater to a combination of all these strategies. Detailed discussion of these strategies is outside the purview of this thesis however there is a lot of research being carried out on this subject especially leveraging linear observers[6].

**3. Level 3 control** also known as Aggregator Layer indicates the regulation of power flow at a slow time scale initiated by a Regional Transmission Organization (RTO) or Independent System Operator (ISO) as Calliso. Integrated energy exchange scheduling strategy between

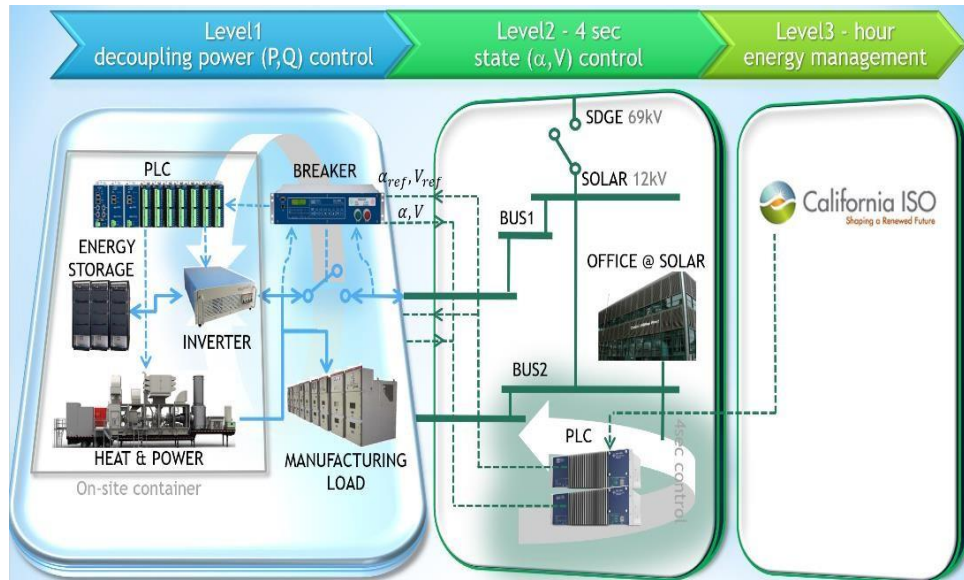


**Figure 2 Overview of proposed modular HPS with 3 levels of control**

a multi-microgrid system and the main grid is normally performed by an aggregator, who aims at minimizing the total electricity cost of the multi-microgrid system while meeting the market obligation. The aggregated scheduling problem is formulated as a linear programming constrained by physical requirements of microgrids. From this linear programming, several dual variables, which are representative of the marginal cost of proper constraints, are manipulated to form the adjusted price which is the modification of original electricity price[7]. This controller aims to increase utilization of available DER, reduce the daily variability of power flow to the main grid, while at the same time controlling power fluctuations at the point of connection. The controller is designed to utilize updating load and PV predictions on a receding time horizon and uses the flexibility of energy storage and PGS resources to compensate for fluctuations and prediction errors[8].

## 2.2 Advantages of HPS

Advantages of HPS compared to traditional power generation include[9]:

**Grid Reliability:** HPS can improve power quality, provide ancillary services, and relieve grid constraints, improving overall grid reliability. Having multiple DERs which are not relying on any single resource to generate power helps with reliability. If for some reason one particular type of DER was not available the grid may be able to leverage other available power resources.

**Customer Resilience:** HPS can provide baseload power for end-users and microgrids, allowing critical loads to continue operation during grid outages. Having fossil fuel based generation DER as a part of the microgrid further ensures resiliency if feature dependent resources were not available.

**Energy Efficiency:** HPS allows for better utilization of each DER thus helping maximize energy utilization and driving fuel/operation cost low. By leveraging operational costs, fuel costs, operating characteristics of each DER, the Station Microgrid Controller (SMC) can be programmed to leverage cost functions which can help improve efficiency.

**DER Integration:** HPS can assist utilities in integrating renewable DERs and help balance variable and intermittent loads. Having a central SMC helps in integrating DERs for coordinated dispatch, load, voltage and frequency control.

**Locational Value:** HPS can be deployed at strategic locations on the utility grid, reducing the need to add or upgrade distribution infrastructure, remote power islands consisting of HPS can help avoid building long power transmission lines and avoid multiple distribution infrastructure.

**Affordability:** HPS can often meet system needs more cost effectively than investments in traditional assets, thus lowering costs for ratepayers across the utility system. Combined Levelized Cost of Energy (LCOE) of multiple DERs can be optimized to reduce the overall installation and operation cost of HPS.

**Emissions Reductions:** Efficient HPS have lower emissions than conventional grid resources and can be used to meet emissions reduction targets. Standalone fossil fuel-based power generation sets, if combined with BESS, Solar/Wind, provide a fantastic opportunity to curtail the emissions based on the load profile. For e.g most gas turbine products generate higher emissions at part load but very low emissions at full load, thus SMC can ensure base load operation for gas turbines to help emission reduction and partial load demand can be managed by other renewable resources.

## **2.3 Grid and Island Mode Transition**

Seamless reconnection or blink-less transfer is a mode transfer scheme where the microgrid smoothly switches between the grid connected and islanded modes within a few cycles (typically < 10). Control methods for various cases such as unintended islanding and intended islanding can be handled by the SMC. It may be shown that the control algorithm can handle these mode transfers by minimizing the power transients through the interconnection breaker as demonstrated in figure 3. We have tried to simulate the islanding operation in this dissertation by creating line to line and line to neutral voltage faults and the results are discussed in Chapter 6.

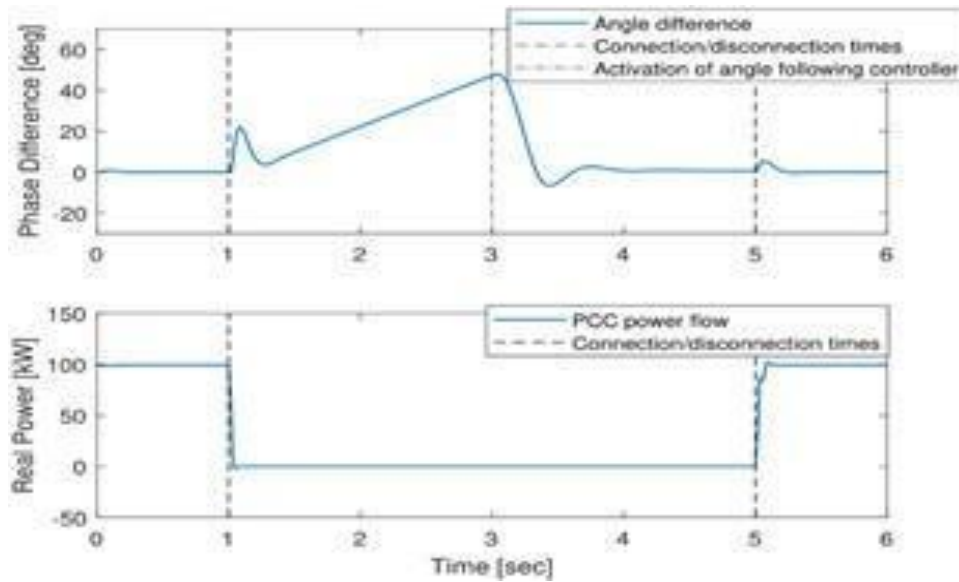


**Figure 3 Microgrid operation in grid-connected and islanded modes**

The top figure shows the angle difference between main grid and microgrid. Islanding occurs at  $t=1s$  and angle difference grows until  $t=3s$  at which point the following controller is activated to mitigate the angle difference. Microgrid switches back to connected mode at  $t=5s$ . The bottom figure shows real power exchange at GCP. Due to the small angle difference at reconnection time, power exchange has a smooth transition at  $t=5s$  without any surges

## 2.4 HPS Application in Combined Heat and Power

The outlook for the increased use and deployment of HPS is strong in many industrial manufacturing sectors. Increases in electricity rates and the long-term supply and price of North American natural gas – a preferred fuel for many HPS applications – have contributed to positive economics for HPS investments.

One of the most prime candidate for utilization of HPS technology are Combined Heat and Power plants (CHP). A recent DOE technical potential assessment for CHP in the U.S. [10] identified 9,325 industrial facilities with 32,603 MW of capacity having the technical potential

to install CHP. The industrial facility types with the most potential are chemicals, food processing, primary metals, paper, and textiles [10]. Industrial facilities that install CHP systems are currently limited by their on-site electrical requirements (because exporting electricity to the grid is not economically viable), leading to a limit on the overall capacity that CHP can provide, and requiring the facility to be subject to the utility for a portion of their power needs. As reliability and economic considerations for CHP systems installed at manufacturing facilities become more prevalent, HPS designed to provide grid support functions in addition to host electric and thermal requirements can offer significant benefits to the U.S. manufacturing sector and the electric grid.

Currently, most CHP systems are installed with operating controls that make them responsive to site electric and thermal loads, increasing and decreasing output based on signals from the host facility. Even systems that are designed with island capability so that they can operate independently of the grid, are only set up to receive signals from the site's loads. These current systems however are not designed to receive signals from the grid or electric utility about needed load adjustments. HPS technology will enable systems to receive signals from both the site loads as well as the grid and use algorithms to balance the needs of both in a manner that is optimized for cost effectiveness.

## **2.5 Blackout Avoidance**

Furthermore, as more renewable generation is added to the power grid, more conventional central power plants which utilize spinning turbines will be required to participate in power regulation at a much faster time scale than is currently done. These spinning turbine power plants provide spinning inertia on the contrary renewable generation such as

photovoltaic generation does not add spinning inertia, and thus the power grid can become less stable [11] and exhibit undamped oscillations as higher levels of renewable generation are added leading to blackout (disconnection) of the grids. HPS enables smart grids to solve this problem by creating a power control Power Generator Sets(PGS) work conjointly with PV/Wind renewable resources, allowing even greater penetration of renewables.

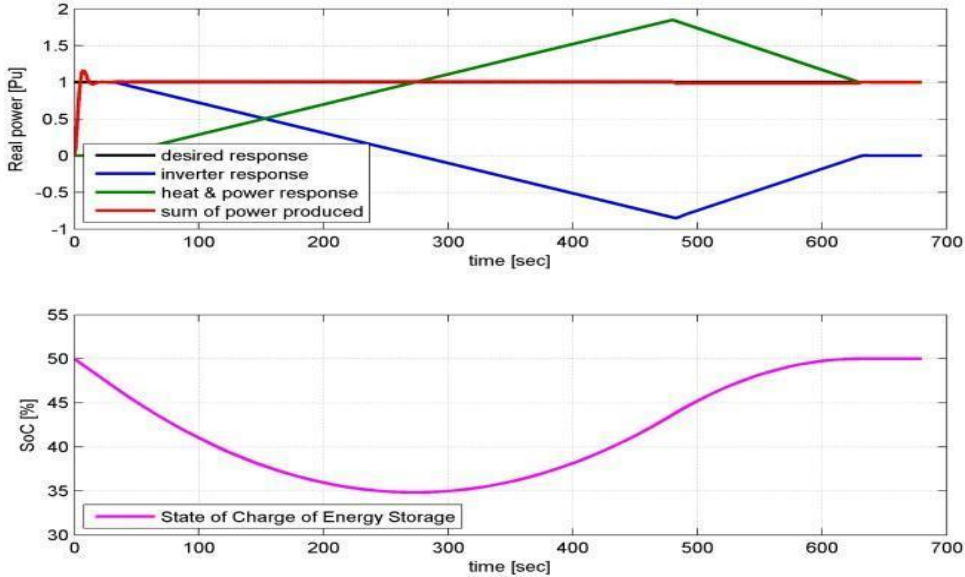


**Figure 4 Real power step response measured in power units of HPS**

Top figure shows desired step power response in comparison with power produced by HPS and bottom figure shows the SoC of the energy storage system. The simulated model of HPS tested in this research plays a crucial role in the selection of the control mode of the inverter to prescribe the dynamics of both voltage via reactive power control and frequency via real power control. Observations of real power, reactive power, voltage and frequency obtained are used to formulate control algorithms that take into account the dynamic aspects and constraints of the power producing components in the HPS. A simple but effective demonstration is illustrated in figure 4 where a desired stepwise change of power is created by the coordinated control of a HPS that consists of a fossil based PGS system combined with a fast inverter system.

Note how the fast inverter increases power within a second, while the much slower and rate-limited PGS comes in later with a ramp-rate that also restores the battery SoC to its initial value of 50%.

The combination of both power producing actuators in the HPS allows the heat and power system to operate around a favorable operating condition to maximize efficiency and reduce emissions, while the inverter is used to pick up volatile power demand fluctuations. HPS can significantly improve individual customer resilience and operational reliability. The advanced controls systems allow HPS to provide onsite generation more efficiently than traditional systems and are not subject to electric grid outages or system blackouts. HPS can also be sized greater than the thermal load of the host facility because of the ability to provide grid services and export power back to the grid, capturing additional revenue streams that are not typically viable with traditional HPS or grid power.

In addition to providing grid support functions, HPS can also facilitate the integration of DERs at the distribution system level or within microgrids. The standardized control algorithms utilized with HPS can be applied to other DERs to facilitate coordination among resources and balance variable loads. HPS can also serve as an ideal anchor for microgrids and district energy systems that serve multiple customers in downtown areas or industrial parks while potentially providing a competitive edge for manufacturers and institutions.

## **2.6 Grid Support Functions**

Grid Stability: As the inertia and reliability of the electricity grid drops, as renewable/intermittent resources replace conventional rotating synchronous machines, the grid will require more reliable voltage and frequency regulation resources to support it during times

of a power shortage. The role of HPS in this regard could become significant as they could easily increase/decrease their energy generation per the grid operator's request to support the grid. The distributed nature of such systems at different locations across the electricity grid offers additional opportunities for HPS to support the electric grid. Major grid support functions favorable by the grid operators are frequency control, reactive power control and voltage regulation. HPS of up to 20 MW capacity can provide such local grid support functions if financially compensated by the grid operator. HPS deployed at manufacturing facilities that have enough generating capacity to support electric grid needs can be an excellent tool in providing grid stability. HPS can provide a rapid response to transient events and enhance power quality in the form of frequency and voltage regulation, contribute real and reactive power to the grid, and serve as a demand response resource. Strategically installed HPS can also provide these services where they are needed most to reduce peak demand or congestion on transmission lines.

Operational Flexibility: Expanding the flexibility of HPS could be viewed from a variety of different aspects. In principle, a flexible HPS is expected to provide grid support by being able to respond to events/requests in a *fast* and *agile* manner and having the capacity to impose a significant impact on the grid variables. Therefore, a flexible HPS design should consider both issues of speed of response and magnitude of impact. Demand response, enhanced dispatchability, load shifting, curtailment prevention, are some of the applications where HPS offers flexibility to provide extremely fast and agile solution.

Frequency Control : One of the critical forms of grid support is frequency control in the first few seconds following a change in system frequency (disturbance) to stabilize the grid frequency. The most common type of disturbance in a grid has traditionally been associated with generator loss which causes a decline in frequency. More recently with the ever-

increasing share of renewable resources, frequency support will become more critical due to the intermittency of renewable generation. Frequency control attempts to help with adjusting for frequency deviations of the main grid. HPS plants are ideal candidates for grid support operations due to their locational distribution. Frequency control is often categorized into three different levels of control: primary, secondary, and tertiary depending on the time-scale of reaction with primary control having the fastest response. The role of a HPS plant in primary frequency control can become more significant if timely response and extensive response range is available. Spinning reserve and peak shaving are classical applications which help with frequency control. Spinning reserve is the application that has been selected as the primary focus area of this dissertation. Figure 5 below shows different applications that can be delivered by combining renewable, conventional and energy storage technologies.

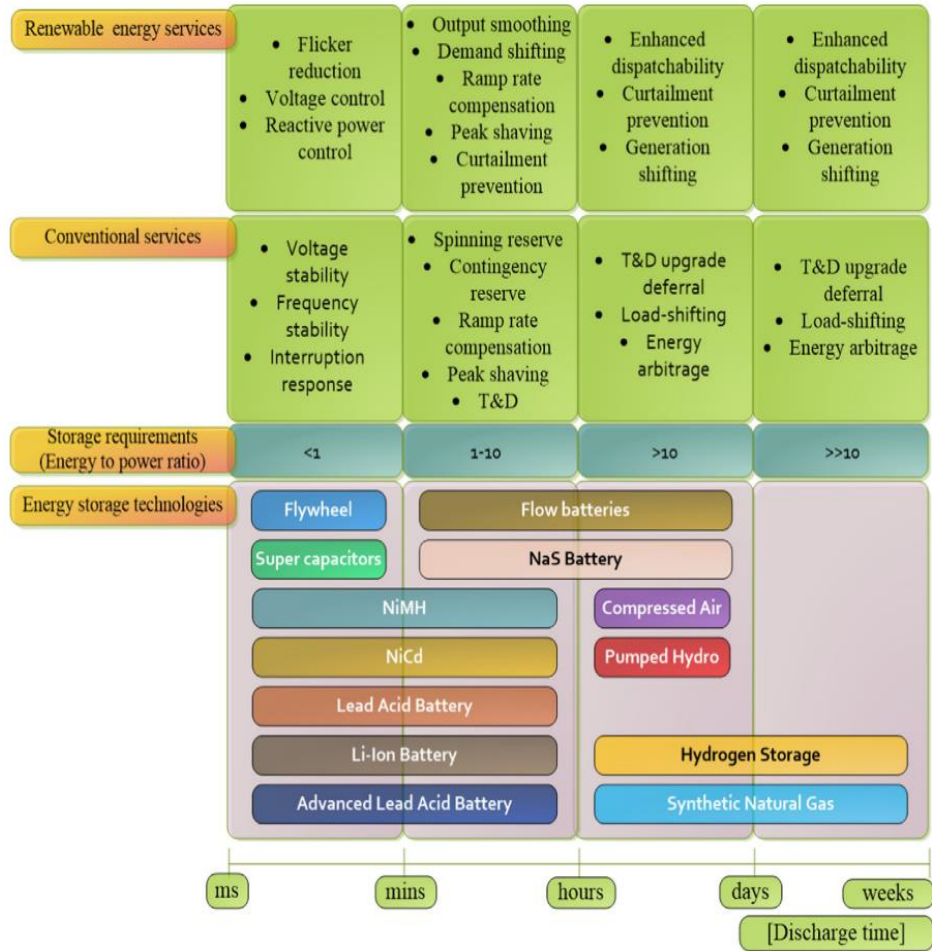


Figure 5 Hybrid power system application portfolio[12]

# Chapter 3

## Spinning Reserve Application

### 3.1 Introduction

In cases when an energy unbalance occurs in the power system the frequency deviates from its nominal value. A large deviation of frequency is expected to occur as the unbalance grows, thus, threatening normal power network operation. With the intention of confining deviation extension to safe levels, frequency surveillance and corrective actions are performed by conventional generators along with grid operator supervision – known as primary control and, if necessary, authorizing spinning reserve release – known as secondary control[12]. Spinning Reserve for frequency control is defined as an energy source that is on line, connected and ready to dispatch in seconds to maintain the frequency of the network.

Spinning reserve is a mandatory grid code requirement in almost all power generation applications. To illustrate the application and use of the research idea, we have considered a typical LNG (Liquified Natural Gas) plant installation with 5 x Taurus 60<sup>®</sup> gas turbines generator sets, supplied by Solar Turbines<sup>®</sup> operating in an N+1 configuration to ensure there is enough spinning reserve to pick up the generation if a Gas Turbine (GT) shuts down. The need to provide this spinning reserve results in the gas turbines operating at a lower efficiency than desired.

We introduce energy storage and change the operating philosophy from an N+1 to an N+BESS (Battery Energy Storage System). This will allow the turbines to operate at a higher efficiency point and consume less gas whilst emitting less CO<sub>2</sub>. An integrated GT + BESS

hybrid solution provides enhanced operational flexibility, significantly reduces the thermal stress on a gas turbine; with a positive effect on service life[13].The control algorithm is developed such that the energy storage will provide intermittent power if a loss of generation occurs.

## **3.2 Literature Review**

Hartmann, Bálint and others have studied the effect of decreasing synchronous inertia on power system dynamics[14] Kosmecki, Michał and others have described various techniques like inverters and storage systems can play by providing synthetic inertia and grid stability[15]. Kerdphol, Thongchart and others have proposed self-adaptive microgrid control techniques leveraging primary and secondary control loops[16]. Feng Xianyong, A. Shekhar, F. Yang, R. E. Hebner, and P. Bauer have offered hierarchical and distributed architecture of microgrid structures to ascertain grid stability[17]. Zhang, Hong and others have discussed the idea of spinning reserve optimization to maximize power system operational flexibility[18]. Usama, Muhammad Usman and others have proposed the idea of using spinning reserve as energy storage for renewable integration[19]. Majority of the research in the space of grid stability and renewable penetration is centered around wind power, solar power and battery storage integration. Bevrani, Hassan[20], Rodrigues.E [12], Ulbig, Andreas [21], Shair, Jan[22] have discussed microgrid stability pertaining to renewable energy resources like wind, solar and their integration with battery storage. Kamel, Rashad and others have discussed the stability of a microgrid consisting of a microturbine, fuel cell, solar and wind farm[23]. Research on leveraging Energy Storage System and Gas Turbine technology for Grid Stability has gained a lot of interest in recent years. Hebner, Robert E and others have presented the idea of Gas Turbine integration with battery storage for grid stability in a ship system[24]. Bahlawan, Hilal

and others have discussed integration of Gas Turbine in a Microgrid with renewable energy resources for optimal operation[25]. This paper has built upon these research areas and provides a novel method of hybrid power system integration using Gas Turbine and Battery Energy Storage System for spinning reserve application.

### **3.3 System Overview**

Figure 6 illustrates the basic control architecture of the LNG processing plant. On-site power generation system comprises five (5) Taurus 60<sup>®</sup> gas turbines with a site rating of 4.0 MW each. Each BESS module is rated for 1 MW, 0.5 hour each, a total four such BESS modules are used in this configuration making it a 4 MW x 0.5 hour system. Each gas turbine has an off-skid control system and all the turbine I/Os are directly wired back to the main turbine control panel. The BESS utilizes PLC based Turbotronic5<sup>®</sup> as the control system. It comprises on-skid I/Os controlled by a Multi-Unit-Controller located in the Control Room. Both the BESS and GTs are connected to the Load Shedding Panel via ethernet and data switch. The control objective is to optimize the onsite generation, detect a loss of generation event and discharge the energy storage system, maintaining the grid stability: thus avoiding system black out.

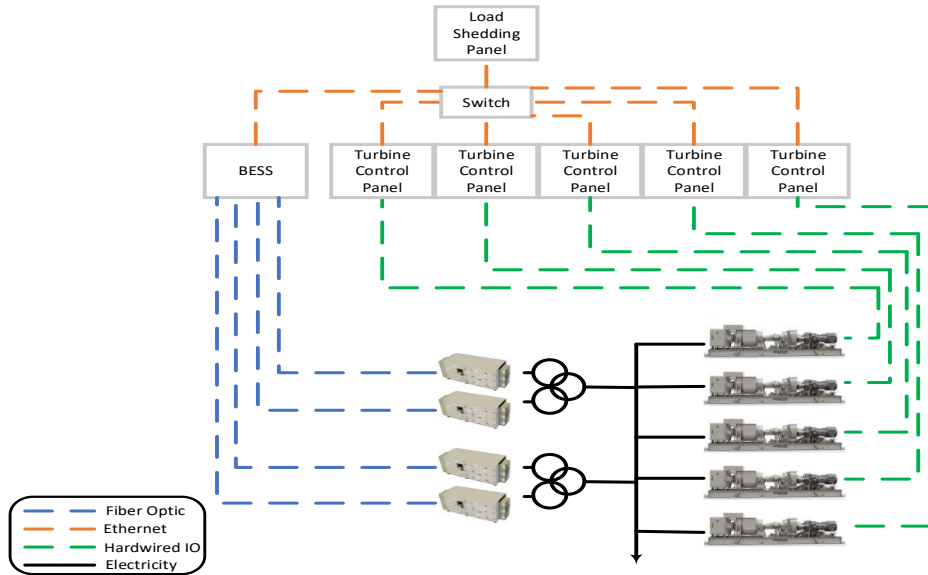


**Figure 6 High level control architecture**

Since the maximum plant load is about 15 MW and Normal plant load is 12 MW, 4 Units are normally operated at 3.5 MW capacity in load sharing mode, this is shown in figure 7 below. If one unit trips the remaining units share the load until the Spinning Reserve unit is brought into operation. As the Non-Spinning unit starts participating in load sharing the N+1 backup is not available and only means of avoiding blackout will be through plant wide load shedding scheme.

Load shedding is not a preferred operation since it impacts the production of the plant.

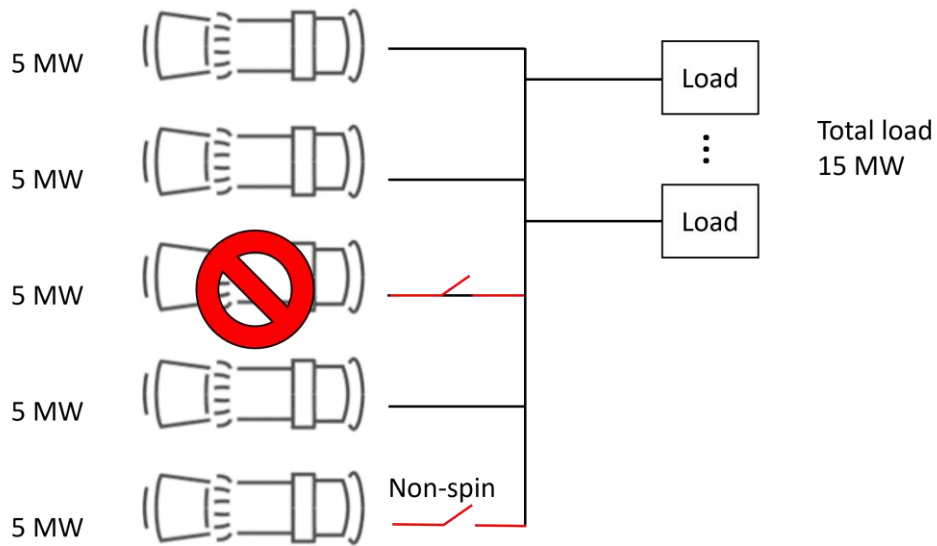


**Figure 7 Upon loss of one generator remaining three units will start sharing the load**

In the proposed Hybrid Power System shown in figure 8, Three (3) x GTG units are operating at their full capacity, BESS is deployed upon Gas Turbine trip, and it starts participating in Load Sharing. It's noteworthy, since most of the Gas Turbines are operating at their full capacity, they have better operational efficiency & lower emissions. Here, we can retain spinning reserve capacity for the plant and one gas turbine can be kept as an installed spare thus reducing the operational expenses. Upon loss of one GTG, BESS will start dispatching the power to the load and remaining two units will start sharing the load, non-spin unit remains available as standby capacity.

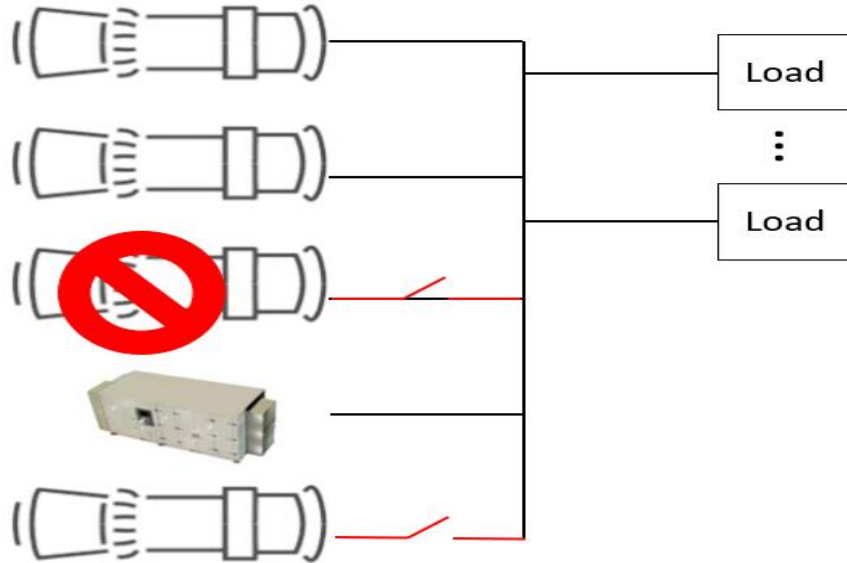


**Figure 8** Upon loss of one GTG, BESS will start dispatching the power

### **3.4 Plant Operation**

#### **A. Start-Up Condition**

Under normal start-up conditions, it is assumed the BESS is connected to a powered bus. In this instance, the upstream breakers will be closed, and the BESS inverter will automatically detect the voltage, frequency and sync to the bus.

#### **B. Normal Operation**

Under normal conditions, the energy storage system is connected and running online. The system will be optimized to maintain at least 30 minutes of charge time. BESS will be occasionally charging/discharging to ensure the correct state of charge (SoC). This charging/discharging current should not exceed 40kW per unit. Each gas turbine will be loaded up to 90% load as this will allow for any small disturbances to be managed by the gas turbines and avoid charging/discharging the batteries.

### **C. Loss of Generation**

The BESS system will monitor the following signals :

- i. Closed Status of GTG breakers x 5
- ii. Open Command from GTG to GTG breakers x 5
- iii. On-Line Status of GTG
- iv. Power Output of GTG
- v. Power Factor of GTG
- vi. Spinning Reserve of GTG
- vii. Exhaust (T5) Temperature of GTG

Based on these signals, the BESS unit will determine the dispatch control. The opening of the GTG breakers will have the longest detection time and hence recommended to be hardwired. The GTG breaker status will not be true until after a command is sent to the breaker and the breaker fully opens. Method of detection of loss of turbine generator will be a hard-wired loss of breaker closed status signal from the generator breaker aux contact, and hard-wired breaker open command signal from GTG. Either of these events will trigger a BESS dispatch.

### **D. KW/KVAR Dispatch**

As shown in figure 8, On loss of turbine generator, the BESS will immediately dispatch power to keep the plant spinning reserve above a minimum threshold. Initially the amount of power discharged by the BESS will correspond to the magnitude of real power being produced by the lost turbine generator immediately before loss, after a user configured time (e.g., 30 seconds), the BESS will ramp down so that the total plant spinning reserve is equal to the minimum spinning reserve threshold. Whenever possible, reactive power will be produced to

maintain a 0.9 PF. The kVar amount discharge will be based upon a 0.9 power factor. Based on the BESS capability curve, the BESS has the most capability to discharge at this power factor without reducing the kW capability.

#### **E. Recharging**

After a BESS dispatch event, and after another turbine generator is brought online, the BESS will use the excess spinning reserve to recharge to be ready for another event. BESS can either act as a fixed load and charge at a constant power, or act as a variable load and maintain a fixed plant spinning reserve. The recharge time will be dependent on the amount of energy required to be fully charged and the available power to charge it. The charge rate will be 4MW and this will ensure a fully discharged battery is fully charged in 30 mins. However, it is unlikely that the BESS will ever be charged at 4MW as this would require an entire GTG.

### **3.5 Control Philosophy**

Hybrid Power System control philosophy is focused on the entire system rather than just the energy storage, it has 4 key aspects :

- (i) Calculating Rate of Change of Frequency (RoCoF)
- (ii) Optimizing the onsite Distributed Energy Resources (DER)
- (iii) Detect a loss of generation
- (iv) Discharge DERs before the system black out.

Following sections describe the concept and calculation of RoCoF followed by a test setup environment that allows for testing of this algorithm on an efficient system architecture.

## A Inertia (H) & Rate of Change of Frequency (RoCoF)

As the amount of kinetic energy from the generators spinning masses lowers, the system becomes more prone to disturbances resulting in power imbalances, which leads to severe frequency deviations and a higher rate of change of frequency (RoCoF), reaching 6 Hz/s in extreme cases[26]. As shown in figure 9, during normal operation, the frequency fluctuates around the nominal value due to load variations. This leads to the mismatch between mechanical and electrical torque, causing change in the generator rotor speed (and, therefore, activating inertial dynamic response)[27]. System ability to address these constant changes in the power balance is defined by system inertia ( $H_{sys}$ ), which is dependent on the inertia constants ( $H_i$ ) of all synchronous generators in the system and system rated power ( $S_{sys}$ ).  $H_i$  represents the time in seconds a generator can provide rated power solely using the kinetic energy stored in the rotating mass [15] and  $S$  is rated power in MVA.

$$H_i = \frac{E_{kinetic}}{S} \quad (1)$$

$$H_i = \frac{\text{kinetic energy at rated speed [MWs]}}{\text{rated power [MVA]}} \quad (2)$$

$$H_{sys} = \frac{\sum_{i=1}^n H_i S_i}{S_{sys}} \quad (3)$$

In conventional power systems, the dynamic behavior of synchronous generators based on the swing equation can be expressed as[20]

$$J_S \frac{d\omega}{dt} = T_m - T_e = \frac{P_m}{\omega} - \frac{P_e}{\omega} \quad (4)$$

where  $J_s$  means the moment of inertia,  $\omega$  means the angular velocity of the synchronous rotor,  $T_m$  and  $T_e$  mean the mechanical and electrical torque for the generator,  $P_m$  and  $P_e$  mean the mechanical and electrical power for the generator. The inertia power response is usually generated using the stored kinetic energy in synchronous generators. Thus, the kinetic energy ( $E_{kinetic}$ ) of system rotating mass including spinning loads is formed as[27]

$$E_{kinetic} = \frac{1}{2} J_s \omega_{sys}^2 \quad (5)$$

$\omega_{sys}$  is the synchronous angular frequency.

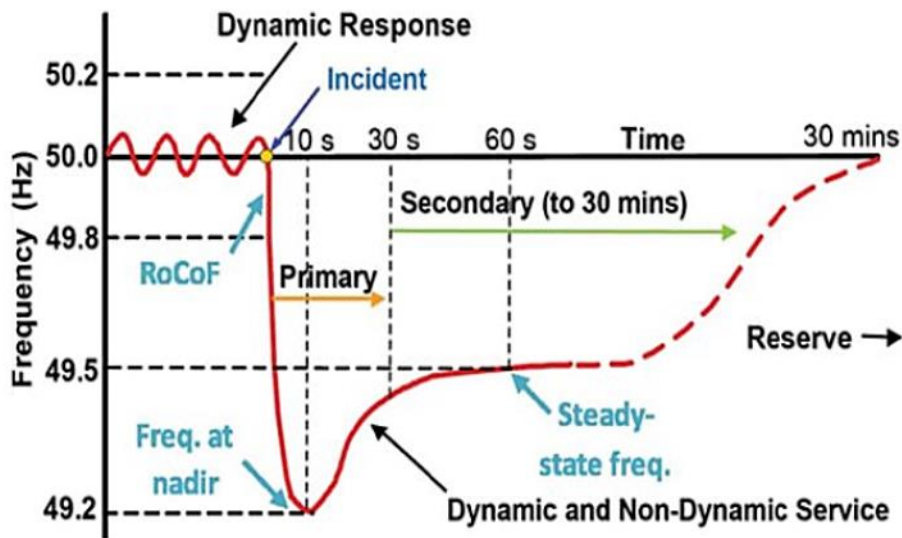


Figure 9 Dynamic response of a grid upon loss of generation

The rate of change of frequency, also known as RoCoF, is a very important variable inside the power system operation and control. The RoCoF has an intrinsic relationship to the magnitude of the power imbalance during the frequency response. As shown in figure 9 above the RoCoF defines how quickly the generator speed changes and the system frequency changes upon an incident. The RoCoF is expressed in Hertz per second (Hz/s); this might be used as a measure of the severity of a disturbance, it is the initial response to frequency deviations after the

disturbance is stabilized by the system inertia (H). If a power system's generation portfolio fully consists of synchronous generators, in case of a notable sudden change in the active power (eg, generator outage, loss of significant load, and system split), RoCoF can be calculated by the change in the kinetic energy stored inside the rotating masses of the machines [14].

$$\begin{aligned}
 P_{gen} = P_m - P_e &= \frac{d(E_{kinetic})}{dt} = \frac{d\left(\frac{1}{2}J_S\omega_{sys}^2\right)}{dt} \\
 &= J_S\omega_{gen} \frac{d\omega_{sys}}{dt} \quad (6)
 \end{aligned}$$

The RoCoF means the time derivative of the frequency signal, which is used to calculate the inertia response of the system as [16]

$$2HS = J_S\omega_{sys}^2 \quad (7)$$

$$P_{gen} = P_m - P_e = J_S\omega_{gen} \frac{d\omega_{sys}}{dt} \quad (8)$$

$$P_m - P_e = \frac{2HS}{\omega_n} \frac{d\omega_{sys}}{dt} \quad (9)$$

$$\frac{2H}{f_n} \frac{df_{sys}}{dt} = \frac{P_m - P_e}{S_{sys}} \quad (10)$$

$$ROCOF = \frac{d(\Delta f)}{dt} = \frac{f_n(P_m - P_e)}{2HS} \quad (11)$$

$$RoCoF = \frac{\Delta P f_n}{2H_{sys}S_{sys}} \quad (12)$$

As can be seen from the equation above, RoCoF is highly dependent on the system inertia and magnitude of power imbalance  $\Delta P$ . As we can see smaller inertia value causes higher RoCoF, The RoCoF calculation in real environments is a complex process, the numerical results shown above are based on an electrical frequency time-series recorded in the ETAP<sup>®</sup> transient model and then it is compared with real time data simulated through Hardware In-the-Loop (HIL). HIL is a real time simulation technique used by emulating signals from real time embedded systems. Conventional generators were not planned to withstand high RoCoF values therefore, measurements and tests should be carried out to identify the technically feasible limits[28]. The following section explains these tests and the determination of RoCoF which is the key parameter for accurate and tighter control of the Spinning Reserve application.

## **B Calculating Rate of Change of Frequency (RoCoF)**

The ETAP<sup>®</sup> transient model was built considering all major active elements of the power system including generators and induction motors. Also, several lumped loads are used for simulating a total plant load of 15.4 MW. The main components of the ETAP<sup>®</sup> transient model are the power generation units, i.e. the gas turbine generators. A standard IEEE AC8B AVR/exciter dynamic model has been selected for the GTs. Following Table 1 shows the exciter's parameters.

**Table 1 IEEE AC8B AVR/Exciter Parameters**

Parameter	Description	Value	Unit
VRmax	Maximum value of the regulator output voltage	16.80	pu
VRmin	Minimum value of the regulator output voltage	0	pu
SEmax	Saturation value of exciter at Efdmax	1.02	pu
SE0.75	Saturation value of exciter at 0.75xEfdmax	1.00	pu
Efdmax	Maximum exciter output voltage	8.00	pu
KP	Proportional control gain	40.00	pu
KI	Integral control gain	20.00	pu
KD	Derivative control gain	15.00	pu
KA	Regulator gain	1.20	pu
KE	Exciter constant for self-excited field	1.00	pu
TD	Derivative control time constant	0.01	sec
TA	Regulator amplifier time constant	0	sec
TE	Exciter time constant	0.212	sec
TR	Regulator input filter time constant	0	sec
RC	Resistive component of load compensation	0	pu
XC	Reactive component of load compensation	0	pu

ETAP® GT2 dynamic model has been used for this study, with the following parameters

**Table 2 Gas turbine GT2 governor model parameters**

Parameter	Description	Value	Unit
P <sub>ref</sub>	Load reference	1	pu
P <sub>limit</sub>	Ambient temperature load limit (calculated)	0.84	pu
V <sub>max</sub>	Maximum fuel valve opening	1.1	pu
V <sub>min</sub>	Minimum fuel valve opening	-0.07	pu
Base	Governor's base MW (ISO 20°C)	5	MW
R	Speed drop	0.1	pu
TR	Load setting time constant	0.005	sec
T1	Governor time constant	0.1	sec

As shown in figure 10 below plant load is considered at 15.5 MW, with 4 GTs online. At second 2, one GT trips. After the GT trips the active power per GT increases from 3.88 MW to 5.17 MW, exceeding the GT's maximum output (4 MW), consequently the power system's frequency collapses requiring load shedding or equivalent amount of Load injection through BESS. A 2.5 MW load shedding at 250 ms after the GT trip stabilizes the system frequency and recovers to 100%. The active power per GT decreases from 5.17 MW to 4.33 MW. The Figure

10 below shows the power generation system response with the step load, i.e. the variation of system frequency, active power, voltage and reactive power. The RoCoF of this system is approximately 1.5 Hz/s.

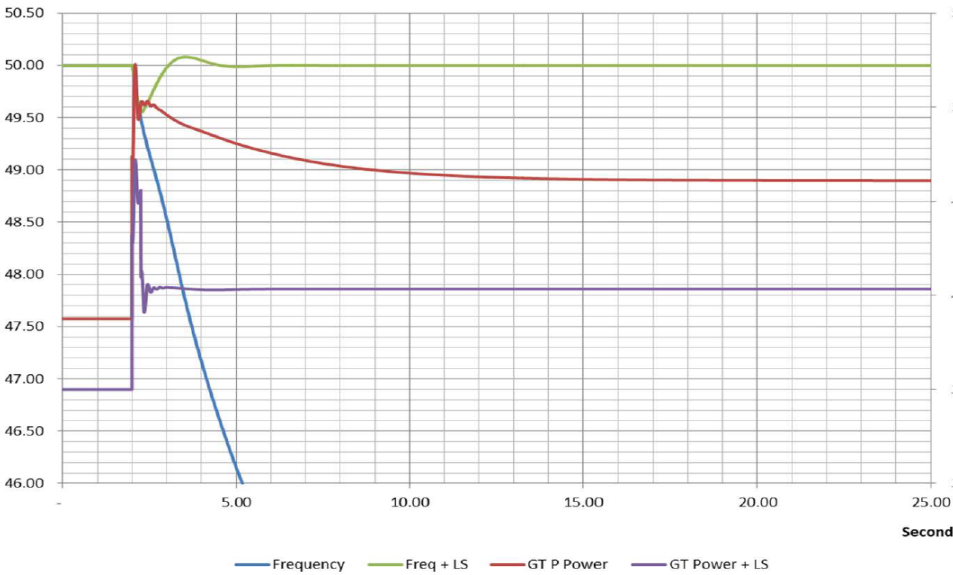


**Figure 10** Dynamic response of a grid upon loss of a generation

# Chapter 4

## Hybrid Power System Model

By definition, “modeling is the process of representing a real-world object or phenomenon as a set of mathematical equations”. It can be used to describe all the different kinds of systems, like mechanical, hydraulic, chemical, electrical systems (etc.) and while used for simulations, it can give a reliable and representative idea of their performance, characteristics and operation. It occupies an important part in engineering science, because it provides the means for testing systems, assessing their response, strengths and potential weaknesses, before they are actually constructed or at the level of the first tests, reducing the possibility of unfortunate events and failures of design and operation [29].

### 4.1 Model Background & Literature Review

Because of the broad interest in the field of microgrids and given the vast nature of this field there is extensive work carried out in modelling the microgrids. However most of the work out on this topic is either too narrowly focused in modelling one or two DERs like battery or inverter or CHP plant. For example T. Sun and D. Lubkeman [30] have focused heavily on CHP model, similarly MacNeill’s[31] work is focused offshore wind farm and H. A. Saleem [32] have focused on Diesel Gen Set. Also most of the simulation work involves very basic modelling techniques available via Matlab/Simulink®. Most of these models are 1<sup>st</sup> or 2<sup>nd</sup> order static models which have limited operational envelope to test the dynamics of the entire Hybrid Power Plant. Many of these models do not have integrated communication platforms to communicate

with PLC/microprocessor-based station/central microgrid controllers. Upon review of literature, it was also noted that the BESS models are either focused on Grid Connected Mode or Island mode operation, there is a need for more research on the aspect of resiliency help where BESS can in either of these modes and how will this mode switching impact the total Hybrid Power System operation and dynamics. Also, there is very little research done on the ability of load sharing among different inverter systems using droop control similar to conventional synchronous generators, also known as grid supporting inverter mode. While most of the work done in the area is focused on Inverter modelling, there is a big opportunity to research on how these different Inverter modes can be leveraged in Hybrid Power System and deliver integrated energy management.

In order to address the real-life application challenges, we have used high fidelity models developed in Typhoon's HIL simulator. We have tailored these models to Solar Turbines® existing microgrid equipment and have tried to simulate an exact replica of the microgrid facility at their Kearny Mesa Plant. Since we have access to the test facility, we will be able to validate our assumptions and test results by real testing on the power equipment also known as Power In Loop Testing.

We have identified multiple scenarios related to plant disturbance and operating condition. Most of these scenarios cover the wide spectrum from Island operation to Grid connection. We also simulated multiple electrical faults. Most faults in an electrical utility system with a network of overhead lines are one-phase-to ground faults resulting primarily from lightning-induced transient high voltage and from falling trees during severe storms are other causes of fault. These faults include the following, with very approximate percentages of

occurrence [33]. We were able to simulate all of these fault conditions using the line to neutral and line to line ground fault simulation.

Single phase-to-ground: 70%–80%

Phase-to-phase-to ground: 17%–10%

Phase-to-phase: 10%–8%

Three-phase: 3%–2%

In conventional networks, power flows from higher voltage level to lower voltage level and in case of fault short circuit current decreases as distance increases. Modern Microgrids have changed the concept and power could flow in both directions. Some of the prominent protection issues are: short circuit power, fault current level and direction, device discrimination, reduction in reach of over-current relays, nuisance tripping, protection blinding, etc.[32]. Figure 11 below is the overall schematic of the model consisting of following systems :

- 1) Inverter (500 KW)
- 2) Gas Turbine Generator (5 MW, Taurus 60<sup>®</sup>)
- 3) Step Up Transformer (600 V to 2.2 KV)
- 4) Auxiliary Transformer (480 V to 600 V)
- 4) Breaker (various time constants 50ms, 100ms, 200ms, 250 ms)
- 5) Power Management System (PMS) controller (Rockwell<sup>®</sup> PLC)
- 6) Energy Storage System (ESS) controller (Rockwell<sup>®</sup> PLC)

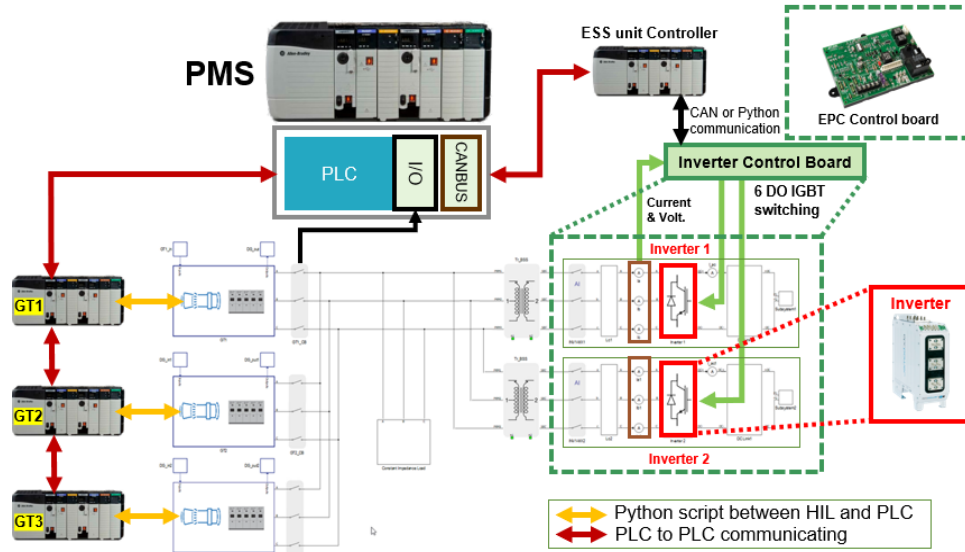


**Figure 11 HPS model simulated in typhoon simulator**

We have not modeled any cable/bus losses, we have also assumed a DC battery to be an ideal DC source. In this section the reader can go through the different models that were created using the Typhoon Hardware in Loop (HIL) simulator. Inverter and Gas Turbine Generator models are described in greater length. For the benefit of readers here are the three modes of Inverter[34] Operation that will be leveraged during the discussion of various testing scenarios:

## 4.2 Inverter Model

**Grid forming inverters:** Grid forming inverters are typically used in small, isolated networks, and their main objective is to regulate the network voltage and frequency. To this end, grid forming inverters are controlled as voltage sources, with fixed voltage amplitude  $|E|$  and frequency  $\omega$ . The active power  $P$  and reactive power  $Q$  are not directly controlled and are determined by the interaction of the inverter with the network. Typical applications are standby UPS systems, and island microgrids. Since the frequency  $\omega$  is set, the inverter usually cannot

operate in parallel to other grid forming inverters, unless an additional mechanism is used to match the frequencies. In power flow studies, single phase sinusoidal voltage waveform is represented as  $v(t) = |E| \sin(\omega t + \delta)$ , a grid forming inverter may be viewed as an infinite bus, and is represented as a reference bus, with a constant voltage amplitude  $|E|$  and angle  $\delta = 0$ . Grid forming inverters are also called Voltage Source Inverters (VSI).

Grid following inverters: Grid feeding/following inverters are operated as power sources and are mainly designed to deliver power to an energized grid. The active power  $P$  and reactive power  $Q$  are directly controlled, while the frequency  $\omega$  and voltage amplitude  $|E|$  are not directly controlled, and are determined by the interaction of the inverter with the grid. Typical applications are renewable energy systems and small grid-connected generators, which operate with specific active and reactive powers. As an example, in photovoltaic systems the active power is typically set by the source, and the reactive power is often set to zero. Grid feeding inverters are designed to operate in parallel to other inverters and generators. They cannot operate in isolation and require additional units to set the voltage magnitude and frequency. In power flow studies, a grid feeding inverter is represented as a P-Q bus, with constant active power  $P$  and constant reactive power  $Q$ . Grid feeding inverters are also called Grid Following Inverters, or inverters with P-Q control.

Grid supporting inverters: Grid supporting inverters operate somewhat similarly to synchronous generators: they deliver power to the grid, while contributing to the stability and reliability of the system. The frequency and voltage magnitude are controlled by a droop mechanism, such that there is a linear relationship between  $\omega$  and  $P$  and between  $|E|$  and  $Q$ . This type of control is very similar to active and reactive power control implemented on traditional synchronous machines, while regulating the frequency and voltage. Grid

supporting inverters may be connected in parallel to other generators or inverters and can also operate in isolation. In power flow studies, such an inverter cannot be represented as a standard bus. However, if the frequency  $\omega$  is known, and the voltage droop mechanism can be ignored, then the inverter is represented as a P-V bus with constant active power P and voltage amplitude  $|E|$ , similarly to a synchronous machine. Typical applications are energy storage

As described above the Inverter model selected is able to operate and simulate all of these 3 conditions mentioned above. For each of the modes a control strategy is outlined below. The Power control or current source mode, the voltage/frequency control or voltage source mode and grid supporting mode which allows a combination of both of the above modes are described.

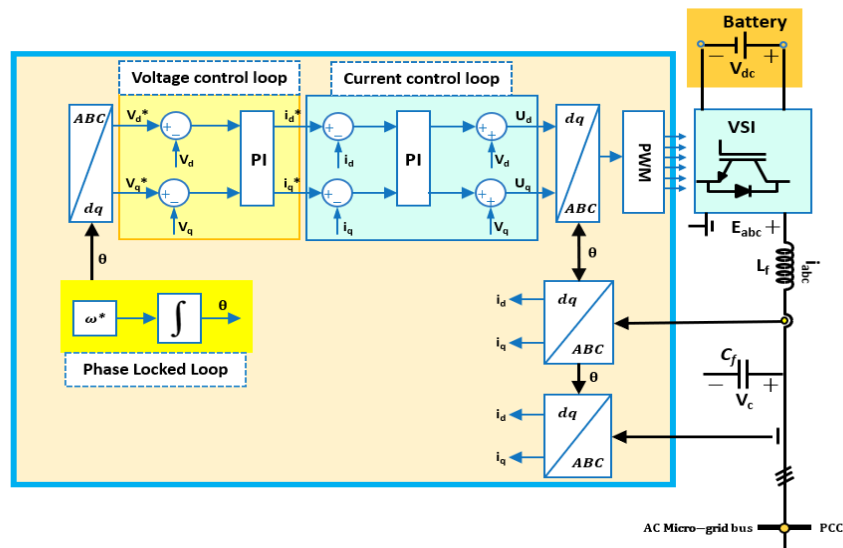
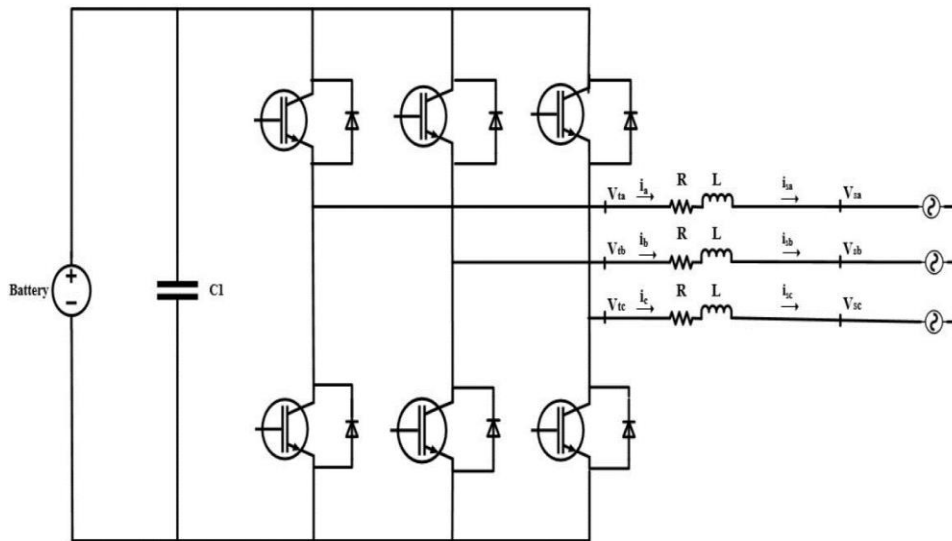


Figure 12 Grid connected inverter model block diagram

Grid Connected Inverter Mode: This mode is also known as Power control mode or current source mode. Based on the SOC of the batteries, the load demand and the export/import command from the SMC the BESS is being charged or discharged. In this mode BESS is contributing to the power flow but is not regulating the frequency. To accomplish this control

scheme two concurrent loops are implemented. Inner control loop which is controlling the inverter current and outer control loop that regulates the power. With the application of digital controllers, the synchronous reference frame control or d-q control has become very popular for controlling the grid-connected inverters. The basic concept of the d-q control is to perform a reference frame transformation from the stationary coordinate system (a-b-c coordinate) to a reference frame that is synchronously rotating with the a-b-c frame known as dq0[35] transformation.



**Figure 13 Grid connected inverter electrical diagram**

It's worth mentioning that in this Microgrid model the grid is assumed as an infinitely stable grid and hence it's considered as an ideal three-phase voltage source. Similarly, the DC batteries model has also been simplified and we are considering it to be an infinite DC source whenever commanded to discharge. SOC, temperature, cycling, heating and degradation impacts

for the battery have not been modeled and may be an area of future research. Voltages on the AC side of the inverter can be described as

$$\begin{aligned}
 V_{sa}(t) &= \hat{V}_s \cos(\omega t + \theta_0) \\
 V_{sb}(t) &= \hat{V}_s \cos \cos \left( \omega t + \theta_0 - \frac{2\pi}{3} \right) \\
 V_{sc}(t) &= \hat{V}_s \cos \cos \left( \omega t + \theta_0 - \frac{4\pi}{3} \right)
 \end{aligned} \tag{3.1}$$

where  $\omega$  is the angular frequency of the AC source,  $\hat{V}_s$  is the peak line to neutral voltage and  $\theta_0$  is the initial phase angle of the source.

The dynamics of the AC side of the circuit shown in figure 13 above could be described as follows.

$$\begin{aligned}
 L \frac{di_a}{dt} &= -Ri_a + V_{ta} - V_{sa} \\
 L \frac{di_b}{dt} &= -Ri_b + V_{tb} - V_{sb} \\
 L \frac{di_c}{dt} &= -Ri_c + V_{tc} - V_{sc}
 \end{aligned} \tag{3.2}$$

Where  $R$  and  $L$  are the series resistance and inductance by which each phase of the inverter is interfaced with the AC system. Variables in the abc system are transformed into the dq system (synchronous reference frame) using dq0 transformation. The terms in Equation 3.2 can be rewritten as following, to know more about the dq transformation reader can review referenced literature[36] that details how the  $\omega$  The term is introduced below.

$$\begin{aligned}
 L \frac{di_d}{dt} &= -Ri_d + L\omega(t)i_d + V_{td} - V_{sd} \\
 L \frac{di_q}{dt} &= -Ri_q - L\omega(t)i_q + V_{tq} - V_{sq}
 \end{aligned} \tag{3.3}$$

The power exchanged at the PCC could be derived as follows

$$\begin{aligned}
P(t) &= \frac{3}{2} [V_{sd}i_d + V_{sq}i_q] \\
Q(t) &= \frac{3}{2} [-V_{sd}i_q + V_{sq}i_d]
\end{aligned} \tag{3.4}$$

Now is the time to introduce a new control variable  $\omega(t) = \frac{d\rho}{dt}$  and

$$\begin{aligned}
V_{sd} &= \hat{V}_s \cos(\omega_0 t + \theta_0 - \rho) \\
V_{sq} &= \hat{V}_s \sin(\omega_0 t + \theta_0 - \rho)
\end{aligned} \tag{3.5}$$

$V_{sd}$  and  $V_{sq}$  are the voltage components of the AC source in the synchronous frame. In the equations above  $i_d$  and  $i_q$ , and  $\rho$  are the state variables and  $V_{td}$ ,  $V_{tq}$ , and  $\omega$  are the control variables. If  $\rho(t) = \omega_0 t + \theta_0$  then the  $V_{sq} = 0$ . Keeping  $V_{sq}$  at zero using a phased locked loop (PLL) controller the power exchanged with the AC source at the PCC can be written as:

$$\begin{aligned}
P(t) &= \frac{3}{2} V_{sd} i_d \\
Q(t) &= -\frac{3}{2} V_{sd} i_q
\end{aligned} \tag{3.6}$$

As  $V_{sd}$  is constant, the active and reactive power at the PCC can be controlled by  $i_d$  and  $i_q$ . Now it is time to define the reference values for  $i_d$  and  $i_q$  as

$$\begin{aligned}
i_{dref}(t) &= \frac{2}{3V_{sd}} P_{sref}(t) \\
i_{dref}(t) &= -\frac{2}{3V_{sd}} Q_{sref}(t)
\end{aligned} \tag{3.7}$$

Therefore, if a fast controller is applied on the VSC in such a way that  $i_d = i_{dref}$  and  $i_q = i_{qref}$ , then  $P_s = P_{sref}$  and  $Q_s = Q_{sref}$ , and therefore  $P_s$  and  $Q_s$  can be controlled independently by their reference values. It is worth a mention that  $i_{dref}$ ,  $i_{qref}$ , and  $V_{sd}$  are in steady state. By choosing  $P_{sref}$  and  $Q_{sref}$  As constant signals, the control of the sinusoidal abc variables has been modeled as the control of DC variables in a synchronous frame. The problem

of controlling active and reactive power which is exchanged between the VSC and AC voltage source at the PCC is simplified to controlling  $i_d$  and  $i_q$

Based on this decoupled d-q reference frame, the control system for the grid-connected inverter can be designed consisting of two cascaded loops, as shown in figure 14[37]. The inner loop regulates the d- and q-axis currents while the outer loop regulates the real and reactive power injections at PCC. The reactive power reference is generated by the voltage controller which is used to regulate the PCC voltage to its nominal value. The real power reference under the normal condition can be selected as a constant value to mitigate the negative influence caused by the intermittent PV/Wind generation on the grid.

The mismatched power between the renewable resources generation and the desired amount of real power injection into the grid is provided by the BESS whose control system regulates the dc-link voltage to be constant[38]. Now let's review how the d axis and q axis PI controllers are designed for this mode of operation. While the complete design and analysis of the PIC controllers for dq loop and PLL controller is beyond the scope of this thesis we have presented key aspects of this design below based on similar research on inverter modelling[39].

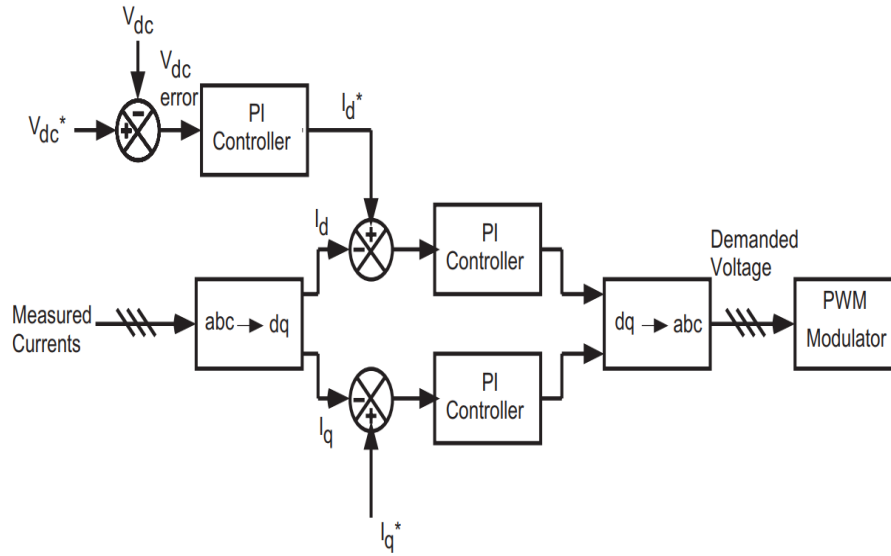


**Figure 14 id and iq controller model block diagram**

Identical control loops can be formed for the d axis and q axis, generally the value of gains and tuning constants for both the controllers are identical. Switching frequency of the inverter is also a very critical parameter as it impacts the sizing of the capacitors and inductors, it also has an overall impact on the cooling system requirements due to the excessive heat generated if switching frequency is set too high.

As shown in figure 15 below, we selected a variable switching method which varied from 2 microsecond to 8 microsecond.

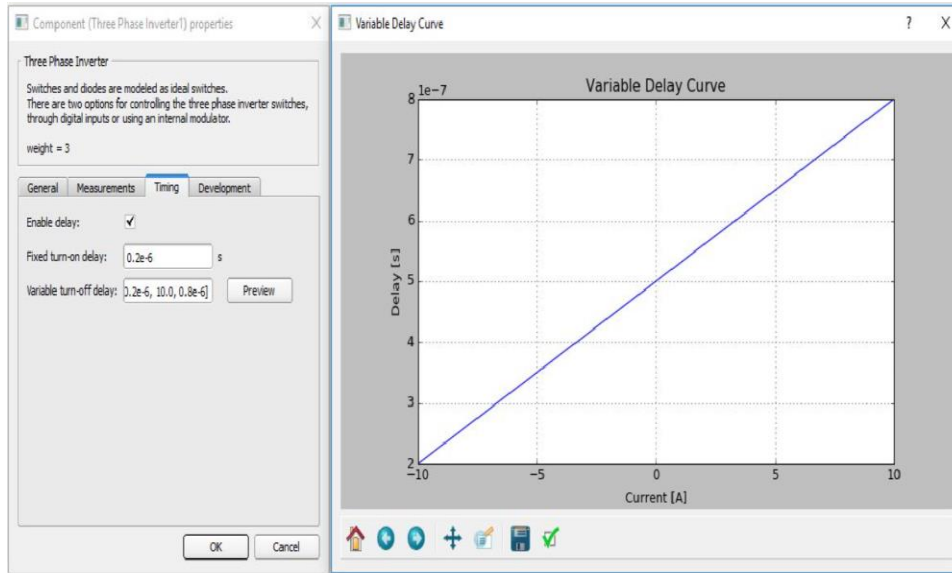


**Figure 15 Inverter switching frequency setting in model**

Model of Grid Forming Inverter : This is the stand alone mode of the operation which is widely known as Island mode of operation. This mode is also known as frequency control mode or voltage source mode. The operating frequency is not imposed by the grid anymore, but inverter is now capable of maintain the frequency  $\omega_m$ , at PCC. In this mode active and reactive power are not controlled by the inverter, inversely the active and reactive voltage components are controlled to change the frequency of the grid. Figure 14 shows the basic circuit diagram for a three-phase grid forming power converter. The control scheme consists of two control loops cascaded into the dq referential frame, an outer-loop voltage controller and an inner loop current controller. The outer-loop voltage controller provides a reference for the inner-loop current controller.

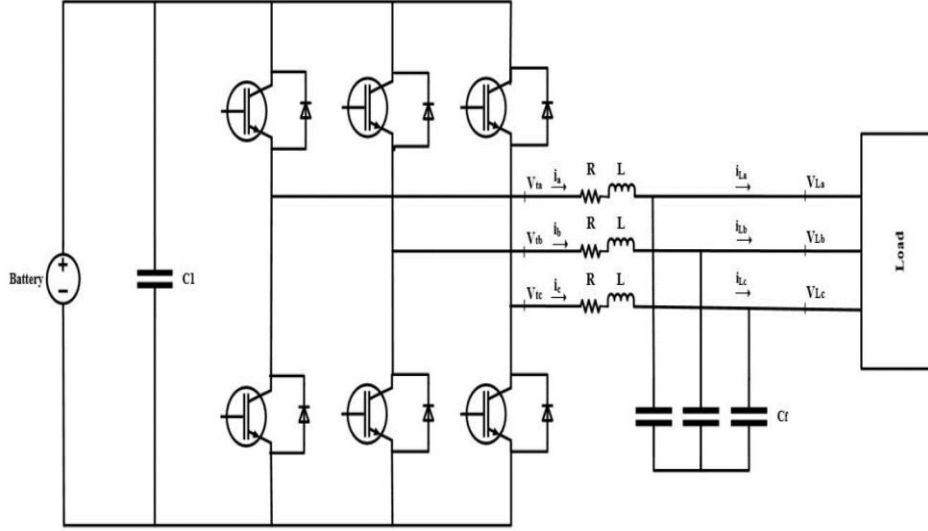


**Figure 16 Grid forming inverter electrical diagram**

In the proposed control scheme, the amplitude of the voltage at the PCC and current are measured and transformed to dc values by applying the Park dq transformation and compared to reference values. With the implementation of the control scheme, it is possible to decouple the active and reactive components to ensure the independent voltage regulation in imposing the frequency reference. Based on the choice of dq reference frame,  $i_d$  current has control over the active component while  $i_q$  current has control over the reactive component. In this mode, the inverter terminal is interfaced with the three-phase load via an RLC filter as depicted in figure 16 above. The filter is made of an RL series branch and a shunt  $C_f$ , here  $C_f$  provides a steady voltage at the node connected to the RL series branch. The current controlled inverter produces the active and reactive power ( $P_s, Q_s$ ) and  $C_f$  produces  $Q_c$ . Therefore, the active and reactive power which are fed into the load is  $P_s$  and  $Q_s + Q_c$  respectively.

From the current-controlled VSC, if we substitute  $V_s$  by  $V_L$ ,

Based on figure 16 above, the dynamic equations of the load voltages can be written as:

$$\begin{aligned}
C_f \frac{dV_{La}}{dt} &= i_a - i_{La} \\
C_f \frac{dV_{Lb}}{dt} &= i_b - i_{Lb} \\
C_f \frac{dV_{Lc}}{dt} &= i_c - i_{Lc}
\end{aligned} \tag{3.8}$$

Transforming Equation 3.8 from the abc frame to dq frame, we have:

$$\begin{aligned}
C_f \frac{dV_{Ld}}{dt} &= C_f \omega V_{Lq} + i_d - i_{Ld} \\
C_f \frac{dV_{Lq}}{dt} &= -C_f \omega V_{Ld} + i_q - i_{Lq}
\end{aligned} \tag{3.9}$$

Control objective here is to maintain the frequency and magnitude of the load voltage which are indirectly correlated with  $i_d$ , and  $i_q$  as shown in the equation above.

**Grid Supporting Inverter Model:** Grid-supporting power converters are designed to control the ac grid voltage and frequency of either a stand-alone or interconnected grid allowing import /export of the power to and from the grid. In these inverters there exists an approximate linear droop relation between the real power and frequency(P- $\omega$ ) and reactive power and voltage (Q-U) of traditional synchronous generators, known as droop curves. By emulating this output characteristics, grid-supporting inverters can share load proportional to their power capacities[40]. The PQ droop inverter adjusts its output power as a function of the variation of the microgrid's voltage and frequency. In this case, the inverter behaves like a power source and its control system is designed based on that of the Grid Following Mode inverter above[41]. On the contrary the  $\omega$ U-droop inverter behaves as a controlled voltage source and its control system is based on that of the Grid Forming Inverter above.

## 4.3 Gas Turbine Generator Model

Gas Turbine Generator (GTG) Model: GTG model described here is divided into three sections. Governor model that deals with fuel control, electrical model that deals with excitation control and generator control also referred to as Combined Generator Control Module (CGCM) and rotor model that deals with rotor speed and electrical load.

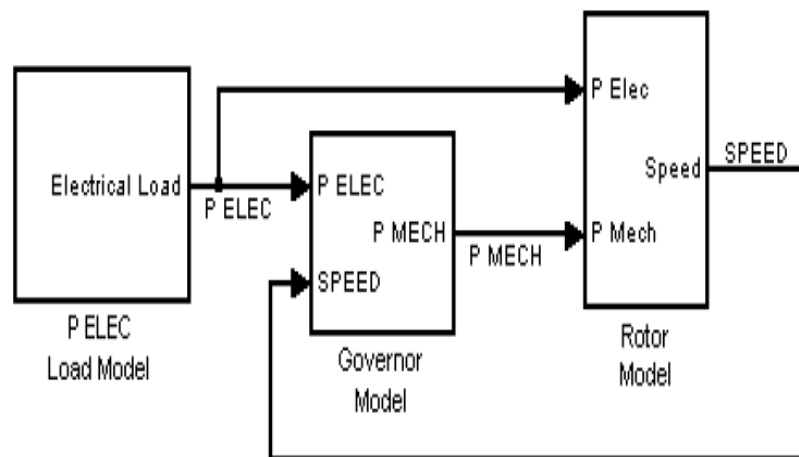


Figure 17 Simplified gas turbine generator model

### Governor Model

The Governor model has the following inputs and outputs:

#### Inputs

1. P ELEC – Electrical Load
2. SPEED – Rotor speed

#### Outputs

1. P MECH – Turbine Mechanical Power

The Rotor model has the following inputs and outputs:

## Inputs

1. P ELEC – Electrical Load
2. P MECH – Turbine Mechanical Power

## Outputs

3. SPEED – Rotor speed

The Load model has the following inputs and outputs:

## No Inputs

## Outputs

1. P ELEC – Electrical Load

As is typical in power system modeling, the governor model simulates the dynamics of the governor, fuel system, combustor and turbine. In this simple model shown below, the response of the fuel system, the combustor and the turbine are lumped into one first-order lag block. The time constant for this block is labeled  $T_{gt}$  and is called the turbine time constant.

The actual governor part of the model consists of the following components:

- Isochronous / Droop mode selection
- Speed control error
- Temperature control error
- Low value gate to select minimum error
- PID control

Descriptions of these components follow below.

Isochronous / Droop mode selection: This component puts the appropriate bias on the speed control based on whether isochronous or droop control mode is selected. GTG can be operated in 2 different modes: 1) Isochronous 2) Parallel/Droop. Isochronous Mode or Grid Forming

mode is also known as Island Mode. In this mode the GTG is participating in controlling the voltage and frequency of the power system. AVR is normally switched to Isochronous setting and the generator receives an active or reactive voltage set point from the SMC. Droop Mode is when the DGS is connected to the grid. DGS can participate in export import control of power; however the frequency of the generator is locked to the grid frequency. In this mode Droop Control is activated and DGS will act as power source, where the dispatch of power is generally co-related to the speed set point also known as droop curve. When droop mode is selected (Mode = 1) a bias based on the electrical load and droop setting is subtracted from the speed error. When isochronous mode is selected (Mode = 2) the bias is set to zero.

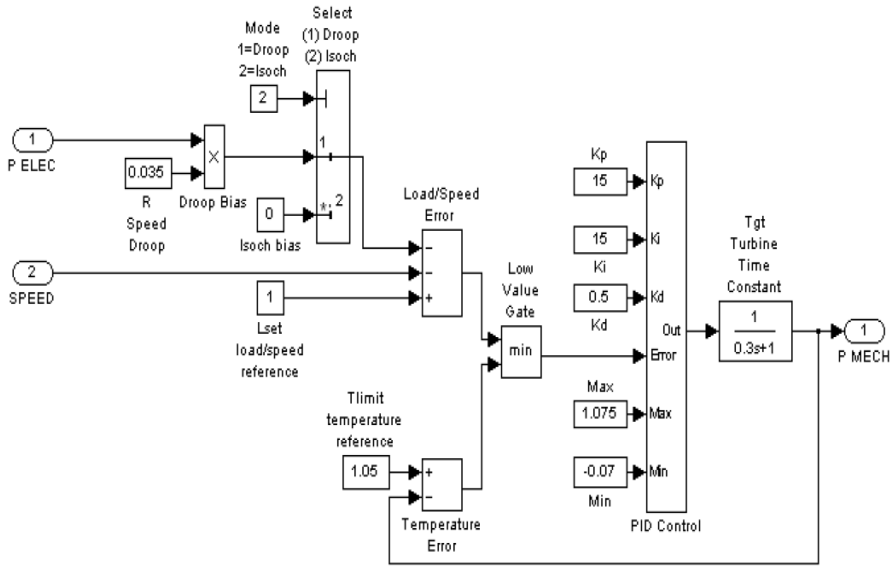


**Figure 18 Governor model of gas turbine generator set**

### Speed control error

This component calculates the error signal for speed control. The load/speed reference is compared to the actual speed and is biased by the isochronous/droop selected signal. The speed comes from the rotor model.

The load/speed reference,  $L_{set}$ , is a set point representing the operator set point for the load/speed control. A value of 1 represents rated speed. To run at rated speed at full load in droop mode, the load/speed reference needs to be set to  $1.0 + R$ , where  $R$  is the droop setting in per unit.

### Temperature control error

This component calculates the error signal for temperature control. The temperature reference is compared to the turbine temperature. In this simple model, per unit temperature is assumed to be the same as per unit turbine mechanical power. So 1 per unit temperature is the temperature when the turbine is running at generator rated real power. Zero per unit temperature is the temperature when the turbine is running at no load.

The temperature reference,  $T_{limit}$ , should reflect the temperature topping control setting for the conditions being simulated.

First, an adjustment to the temperature reference needs to be made to reflect the difference between the turbine power rating at the conditions being simulated (ambient temperature, elevation, fuel type, degradation, etc.) and the generator rated real power.

For example, if the generator rated real power is 5 MW but you are simulating conditions where the turbine capability is 5.5 MW, then the temperature reference should be set to  $5.5 / 5 = 1.1$ .

Second, an adjustment to the temperature reference needs to be made to reflect whether or not the temperature topping control has a peaking offset. Solar Turbines® offsets the temperature control when operating in island mode to allow short term over-firing during transients. The offset corresponds to about a 5% increase in per unit temperature reference. For example, if the generator rated real power is 5 MW but you are simulating conditions where the turbine capability is 5.5 MW, then the temperature reference before compensating for island mode peaking offset should be set to  $5.5 / 5 = 1.1$ . Factoring in island mode peaking offset results in a temperature reference of  $1.1 * 1.05 = 1.155$ .

Note that if the turbine runs above rated temperature for the ambient conditions for more than 20 seconds the turbine will be shut-down, but this is reflected in the model.

Low value gate to select minimum error. The low value gate outputs to the PID control the lowest error between the speed and temperature controls. In other words, the gate will cause the control loop that requires the least power output to be the input to the PID control.

#### PID control

The PID control is a typical Proportional plus Integral plus Derivative controller with high and low limits for the output and integral term anti-reset windup. Figure 19 shows the PID control subsystem.

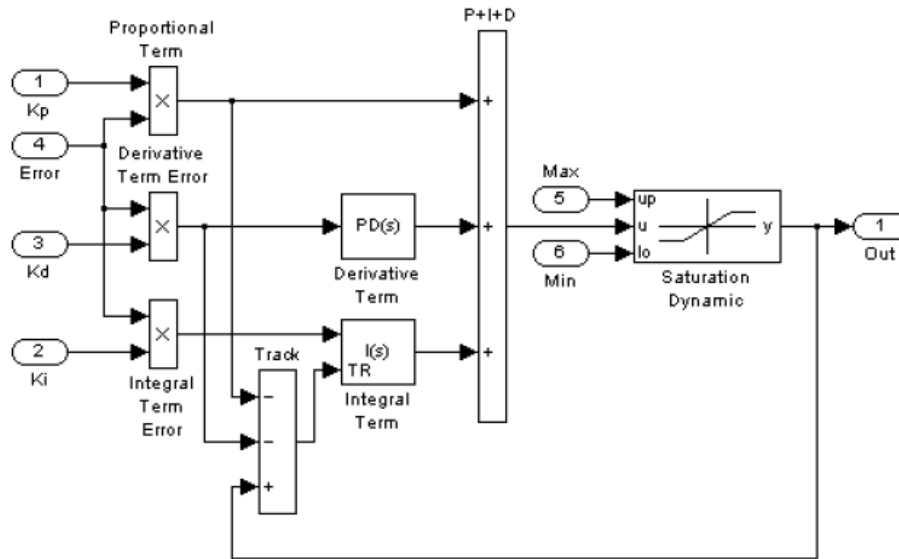


**Figure 19 PID control subsystem**

The following figure 20 shows the configuration of the derivative term, derivative block is configured as a controller of type PD but the proportional term is zeroed out.

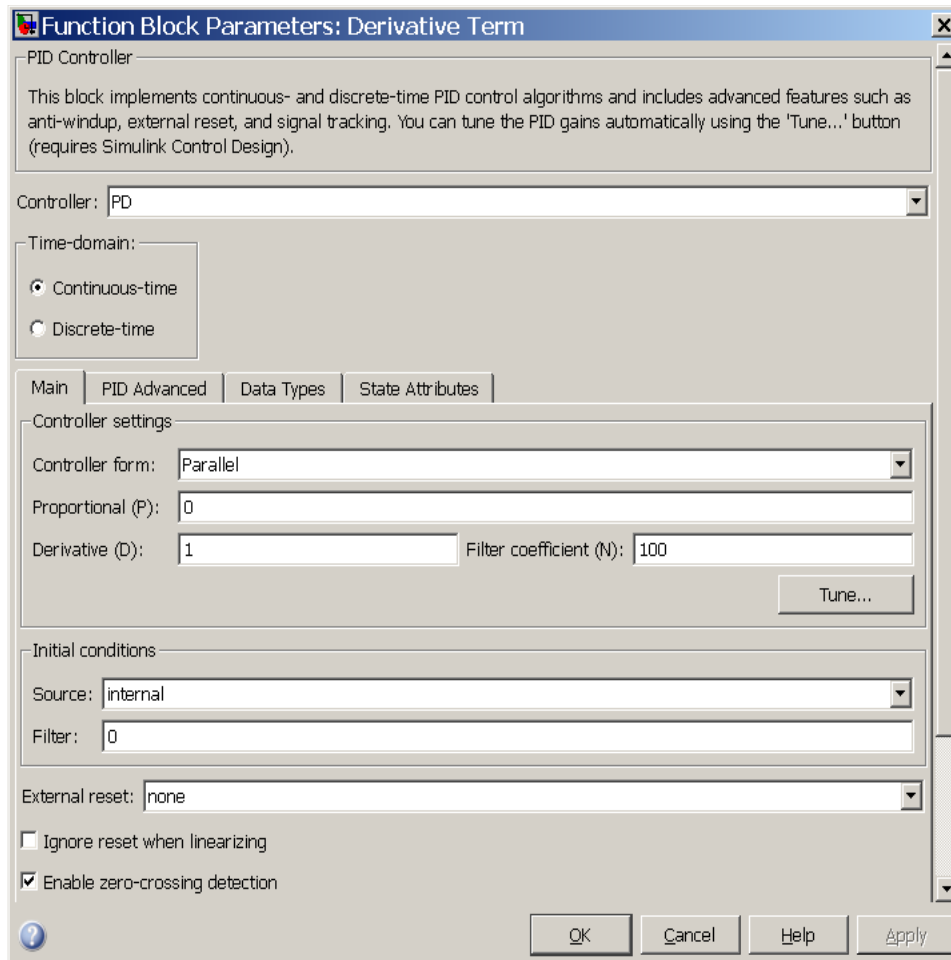


**Figure 20 Derivative term configuration**

The integral term configuration is shown in figure 21 below.

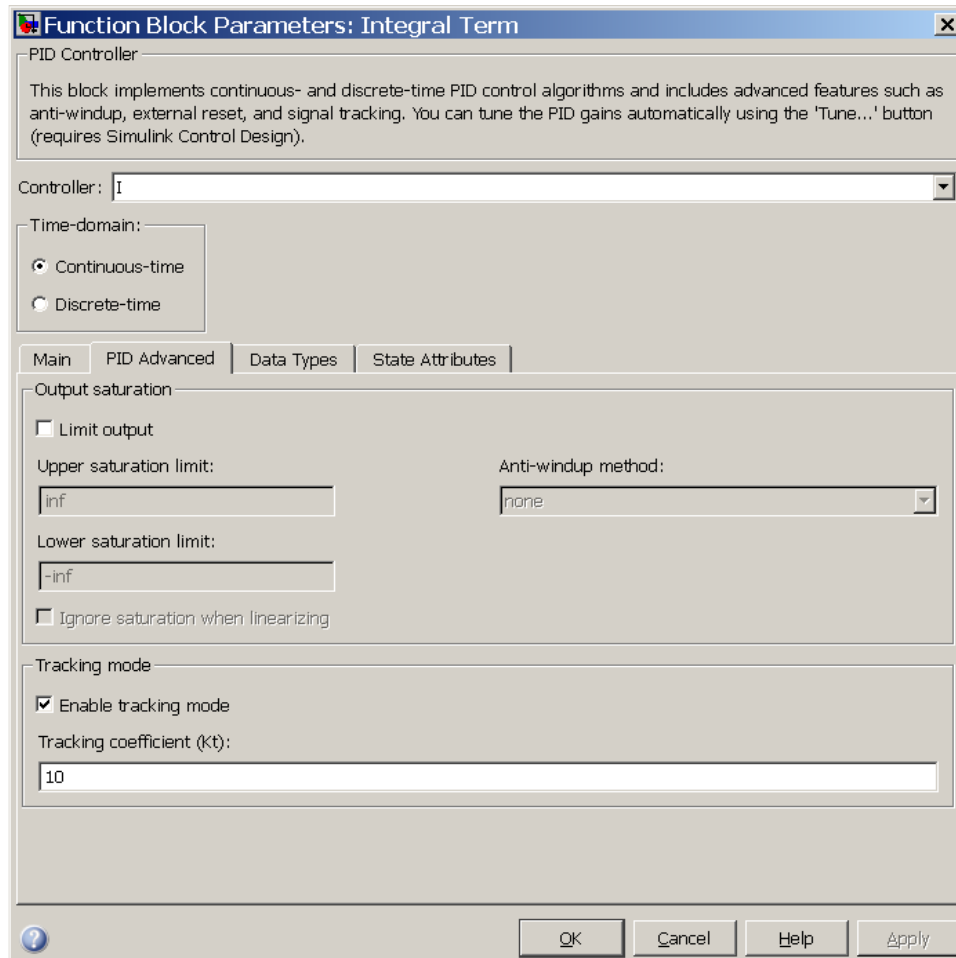


**Figure 21 Internal term configuration**

The integral term is set up to track the difference between the PID output and the sum of the proportional and derivative terms. This ensures the integral term will not wind up when the output is limited by the min or max limit.

The input parameters to the PID Control are

Error – Control error input

$K_p$  – proportional gain

$K_i$  – integral gain

$K_d$  – derivation gain

Max – PID control maximum output limit

Min – PID control minimum output limit

**Rotor Model :**

The rotor model is shown in figure 22, inertia is represented by the inertia constant H,

$$H = \frac{\text{kinetic energy at rated speed [MWs]}}{\text{rated power [MVA]}} \quad (2)$$

H has units kW-sec / kVA or equivalently MW sec / MVA

A typical value for the parameter H is 2 MW sec / MVA.

Since the industry standard is to per unitize H based on Generator MVA rating, and the rotor model has power per unitized based on Generator MW rating, H has to be scaled to convert MVA to MW as shown in figure 22.

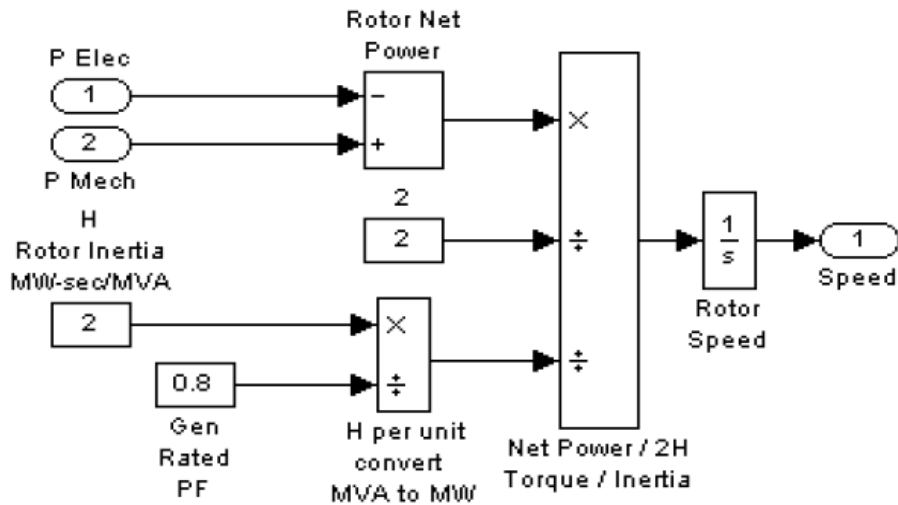


**Figure 22 Rotor model**

**Load Model :**

The load model is shown in figure 23, this model produces the Electrical Load signal as a function of time based on either a series of load steps or a motor starting load model. Starting motor model follows a preprogrammed motor KW vs time characteristic curve.

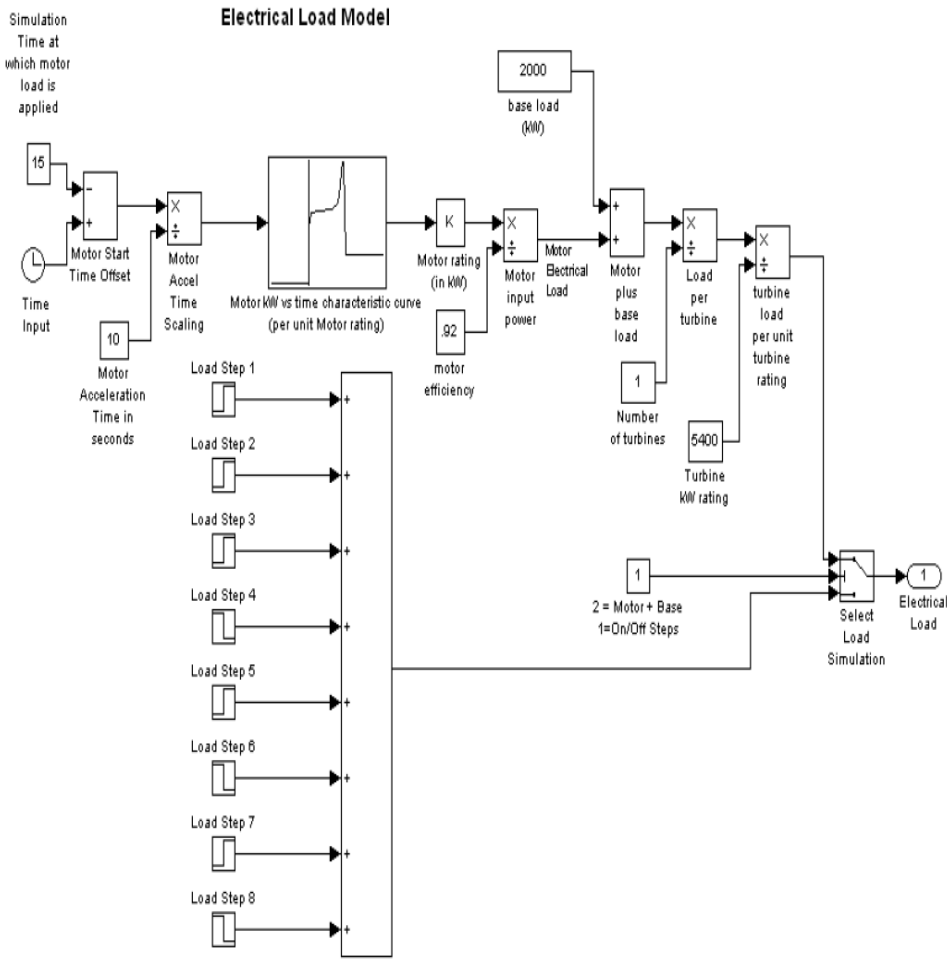


**Figure 23 Load model**

**4.4 Exciter Model**

Figure 24 shows the typical exciter model AC8B, this model is in accordance with IEEE 421.5.

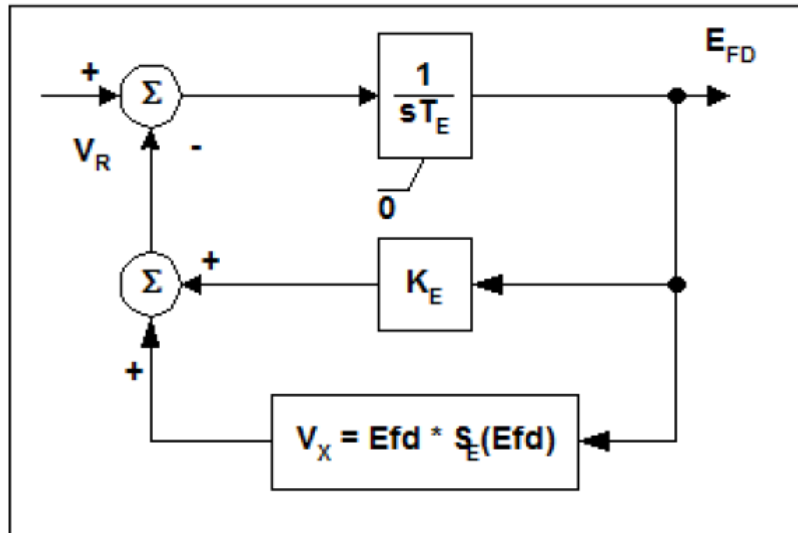


Figure 24 Exciter model of diesel generator set

The excitation control also known as The Automatic Voltage Regulator (AVR) or Combined Generator Control Module (CGCM), modulates the excitation field  $E_{fd}$  by changing the exciter field voltage  $V_r$  thus establishing the required terminal voltage  $V_X$  at the generator. It forms the key component of electrical system and has direct impact on the rotor field voltage  $E_{fd}$  which directly impacts the generator terminal voltage  $V_X$ . The constant  $K_e = 1$  for units with permanent magnet generators (PMG), or other means of power supply to the AVR power stage not extracted from the voltage at the generator terminals. The exciter saturation characteristic represented by equation  $V_X = E_{fd} * S_e(E_{fd})$  is a non- linear function with values typically defined in two points.  $T_e$  is exciter short circuit time constant.

Following are the exciter parameters set for typical GTG

**Table 3 Generator Exciter Settings**

The image shows a software dialog box titled "Component (IEEE AC8B Exciter) properties". The dialog is for configuring an "IEEE AC8B Exciter" model. It features a "General" tab with the following parameters and values:

Parameter	Value	Unit
Time constant $T_r$ :	0.020	s
Regulator proportional gain $K_p$ :	0.1	
Regulator integral gain $K_i$ :	0.1	
Major regulator gain $K_a$ :	300	
Major regulator time constant $T_a$ :	0.001	s
Exciter time constant $T_e$ :	0.1	s
Exciter gain $K_e$ :	1	
Demagnetizing factor $K_d$ :	0	
Rectifier loading factor $K_c$ :	0.1	
Initial terminal voltage:	0	pu
Initial field voltage:	0	pu
Execution rate:	inherit	

At the bottom of the dialog are three buttons: "Help", "OK", and "Cancel".

## 4.5 Transformer Model

Three-phase transformer is modeled as three single-phase transformers, meaning that only magnetic coupling between windings of the same phase are taken into account. If we take three single-phase transformers and connect their primary windings to each other and their secondary windings to each other in a fixed configuration, we can use the transformers on a three-phase supply. The magnetization inductance ( $L_m$ ) can be linear or with saturation, it is modeled on the primary side of the transformer. Core losses are modeled as resistance ( $R_m$ ) located on the primary side of the transformer. We can select the winding interconnections to be Star(Y) or Delta(D) on either side, for this model we selected Y connections on both primary and secondary. There are two types of tests that are performed to characterize a transformer. Both tests are performed on either the primary or the secondary side of the transformer. The tests are:

- short circuit test – exciting a set of three-phase windings while the other set of windings is short circuited, this defines short circuit voltage and current of transformer
- open circuit test – exciting a set of three-phase windings while the other set of windings is open circuited, this defines open circuit voltage and current of transformer

Measurement results obtained from these tests and other information given on the transformer's nameplate provide the necessary data for transformer characterization and modeling. Entire modelling of transformer is beyond the scope of this thesis however reader can get further details on this very well researched and documented power system component in reference [42].

The other important parameter to be reviewed as a part of transformer modelling is the amount of Inrush current during the energizing could be much higher than the full rated

current. It is short lived to a few cycles only. Inrush currents can be as high as 6 and 18 times the rated current. Magnitude of inrush current depends on several factors e.g. a) Primary voltage b)Transformer saturation curve c) Short circuit capacity of the network[43]. Lower the short circuit level, lower the inrush current. Inrush currents are reactive and can cause voltage drops. Inrush currents do not normally pose any challenge in grid connected mode as synchronous generators are designed to handle these high currents, However in Hybrid Power Plants, inverters are not designed to carry these. Typically, they can handle up to 2 to 3 times their rated current but not more and they will trip on overcurrent/voltage protection. There are multiple ways to get around this challenge, but the most important parameter is to ensure the transformer model is sized to handle the inrush current for the microgrid. The table below shows the critical parameter settings for the transformer used in this model.

**Table 4 Transformer Settings**

Parameter	Value	Description
$S_n$	2 MVA	Nominal Power of the Transformer
$f$	60	Frequency of the Transformer
$V_1$	2.2 KV	Primary Voltage of the Transformer
$V_2$	600 V	Secondary Voltage of the Transformer
$usc1$	4%	Short circuit voltage as % of nominal phase voltage
$ioc1$	0.70%	Open circuit no load excitation current as % of nominal current

All these subsystem models were simulated in real time and scenario testing done for various plant conditions follows in the next section of this report.

# Chapter 5

## Loopback Dynamical Simulation

The Loopback Dynamical Simulation allows remote testing of different conditions and environments before a package is launched and gives more accurate diagnostics when problems do arise. It opens the opportunity for integration with other distributed energy resources (DER) such as wind or solar. We evaluated 4 separate power flow models:

1. Governor Power Flow Model, Generator Driven by Mechanical Power
2. Governor Power Flow Model, Generator Driven by Rotor Speed
3. High Fidelity T60-7901 S Power Flow Model, Generator Driven by Mechanical Power
4. High Fidelity T60-7901 S Power Flow Model, Generator Driven by Rotor Speed

### 5.1 Introduction

Most Simulink models are based on static values and not capable of representing dynamic conditions, which means it does not realistically simulate the power flow of the generator set connected to the load/grid. However, most power system integrators and operators demand testing and modeling of the generator set with dynamic loads and want to verify the ability to change different plant operating conditions. We have tested our HPS architecture and algorithms using high-fidelity models which allow evaluation of the generator set to transient electrical variations.

For real time testing, dynamical simulation of station controls such as the power management system (PMS) is developed to test different features including load sharing, load shedding, spinning reserve and other PMS applications.

A Power Flow Model (PFM) is specifically used to simulate how the programmable logic controller (PLC), gas turbine, generator, and combined generator control module (CGCM) also known as Auto Voltage Regulator (AVR) interacts with one another during transients and its performance is measured under different step loads. All of these physical and logical components are modeled separately in the final high-fidelity PFM.

Traditional Simulink models of the electrical system have relied on a governor model driving a simplified version of the rotor, which is a low fidelity representation of how gas turbine and generator set would interact with one another. Though the model is a good representation, this governor power flow model is feeding the generator with mechanical power (PM), which does not follow the standard of driving the generator with rotor speed (NGP). Feeding with rotor speed provides better integration of fuel system dynamics with generator measurements. Hence another governor power flow model, where the governor model drives the generator with the NGP was used for HIL simulation.

## **5.2 Model Configuration**

A standalone Solar Turbines® SoLoNOx 1 Shaft model was used as part of validation for each of the power flow models developed. This model will be referred to as the standalone preferred governor model shown in figure 25.

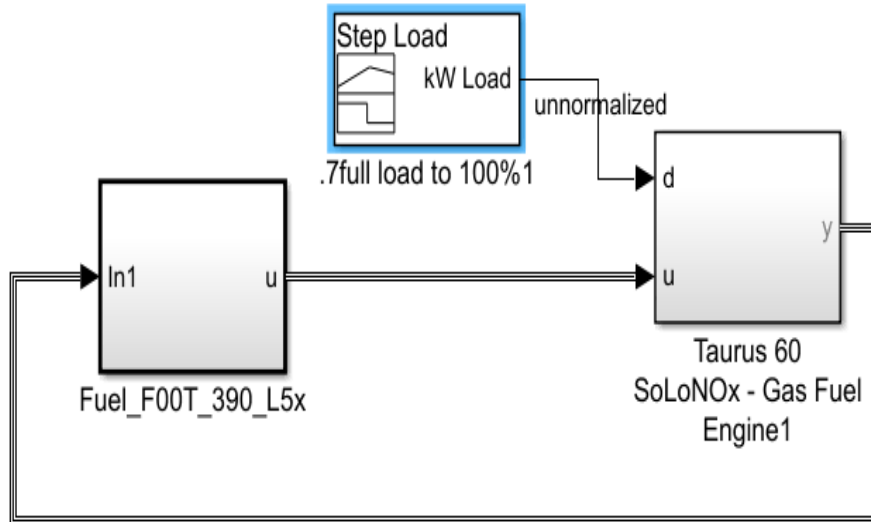


**Figure 25 Standalone preferred governor model**

The standalone T60-7901S model above consists of a model of the PLC (Fuel Control) and the Taurus 60 SoLoNOx<sup>®</sup> Gas Fuel Engine driven by an input step load signal. The model of the PLC is directly translated from the RSLogix5000<sup>®</sup> software to Simulink. The model of the Gas Engine is a high-fidelity model of the engine, and includes models of the compressor, fuel management system, gas burner, and rotor among other components as shown in figure 26 below.



operation, divided by 100. The generator parameters are designated such that it models a Taurus 60<sup>®</sup> KATO generator, 60 Hz, and rated at 7.875MVA, 13.8 kV and 6.3 kW.

The step load signal used in the standalone models (as seen in figure 25) is replaced by connection to a couple of Three-Phase Parallel RLC Load function blocks. These are connected to the generator via circuit breakers to model active and reactive power load sharing at times specified in the circuit breakers on the right side of figures to follow. The display shows relevant outputs from the generator to verify the signals, and it sends them to the CGCM/Exciter model, which are in yellow in figures to follow.

The standalone mode outputs mechanical power, so it can be integrated into the electrical system model as is. The preferred governor model is in the top left of figure 27.

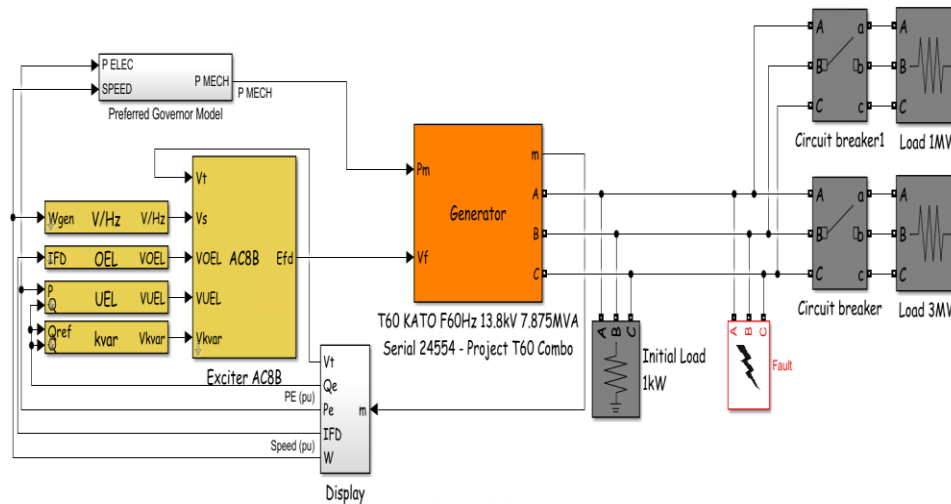


**Figure 27 Preferred governor power flow model, generator driven by mechanical power**

Inputs:

1. P ELEC – Electrical Load (pu)
2. SPEED – Rotor Speed (pu)

Outputs (one for each model):

1. P MECH – Turbine Mechanical Power (pu)
2. NGP - Gas Turbine Speed (percentage)

The second Preferred Governor model is very similar to the PM driven model above, but with extra computation within the Preferred Governor Model block to convert the output from P MECH to NGP. It also has an extra gain block which scales NGP to speed in pu to feed the generator.

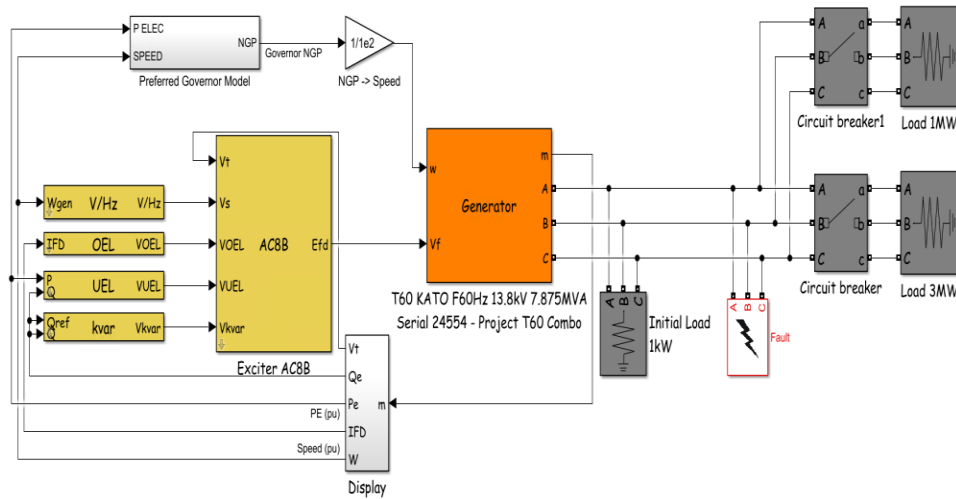


**Figure 28 Preferred governor power flow model, generator driven by rotor speed**

To output NGP, a conversion is performed on P MECH to mechanical power in horsepower. The input P ELEC is also converted to horsepower. The difference between the two is net mechanical power (PM), which should be zero at steady state.

## 5.4 High Fidelity T60-7901S Power Flow Models

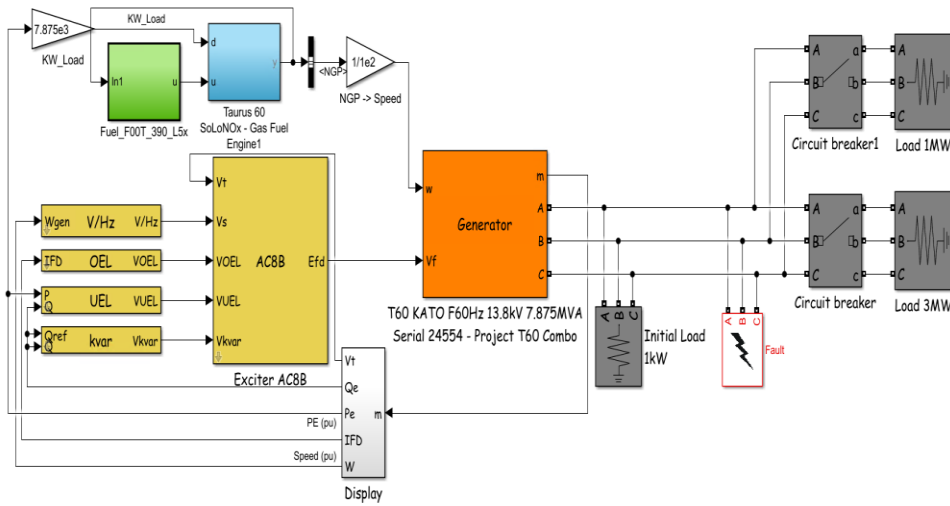


**Figure 29 High-fidelity electrical system model, speed driven**

For the speed driven high fidelity model, shown in figure 29, PE from the generator is connected to the gas engine and fed into the rotor model. It is used to compare the power in the engine (PM) as opposed to power in the turbine (PE), the difference of which is Net PM.

Since NGP was computed from the Net PM of the rotor, the calculation for PM in horsepower is available and converted to pu and output from the block. Thus, there are the options of PM and NGP for driving the generator. Because these align with the preferred governor models discussed before, they have been combined into the same .mdl Simulink file. The user can switch between the model they want to use with a switch, as shown below in the PM\_norm block for the PM driven power flow model in figure 30. Note that to save computation time, users should comment out the model that is not chosen by the switch.



plot in blue. The red lines are the setpoints, or what is allowable for the speed, and if the blue line denoting NGP goes beyond these bounds, alarms and shutdown procedures would be initiated. As the ambient temperature increases, the amount of load that the generator can support decreases. For this test cell, it can support up to 4.5 MW.

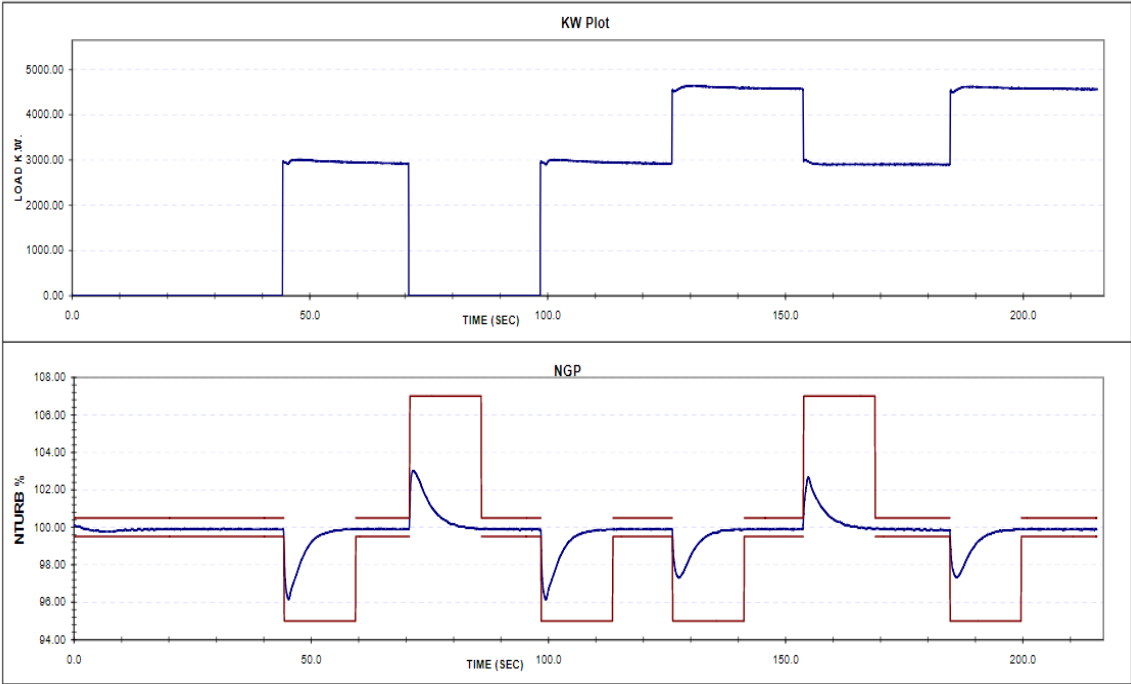


Figure 31 Load transient analysis

### 5.5.1 Preferred Governor Power Flow Models

If the user does not care about transients. The lightweight standalone preferred governor model suffices to give a simulation of the generator set. It runs much faster than real time but can do so because it is a low fidelity model which has oversimplified the computations required for the components involved in the PMS. The curve for the standalone model can be seen in black in figure 32, which follows the test cell data because it essentially black boxed the system, in a sense.

The governor power flow model is unaffected by ambient temperature as it simplifies temperature in a way that does not reflect this issue. It takes about 15 minutes to run a 7-minute simulation, which is double the real time. This is because the power flow model is still incredibly complex.

However, the standalone governor model was built without accounting for the exciter in the CGCM or the generator transients, so taking that block and integrating it into the power flow model results in some oscillations around the transients. After tuning the PID, the same defaults that allow for best performance. The speed driven and PM driven governor power flow models have the exact same results so that is why only one can be seen.

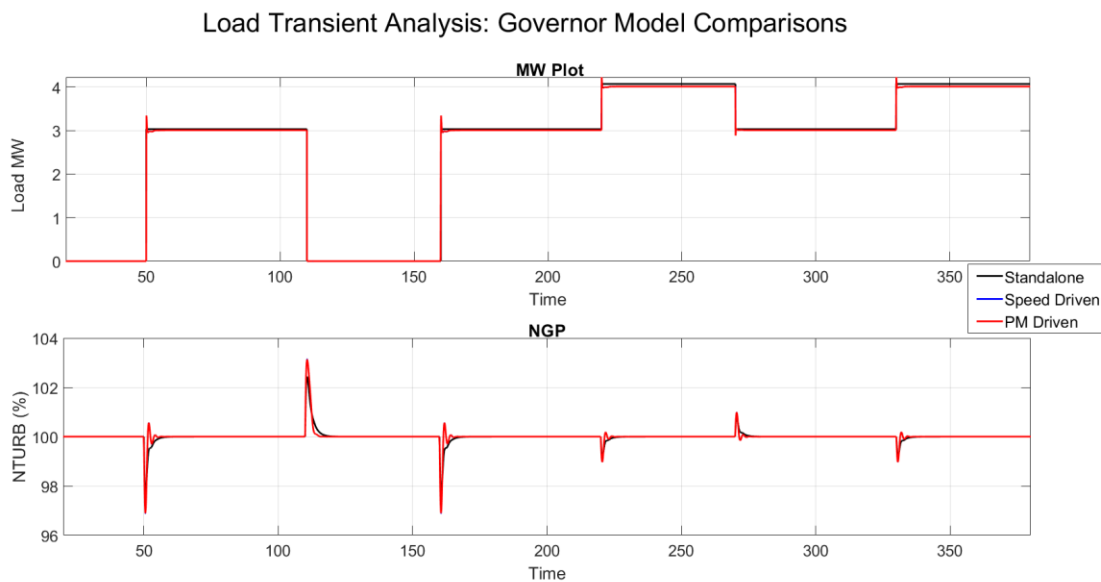


**Figure 32** Load transient analysis, governor power flow models

### 5.5.2 High Fidelity T60-7901S Power Flow Models

The speed driven and PM driven high-fidelity power flow models also have very similar results, so they overlap each other almost perfectly.

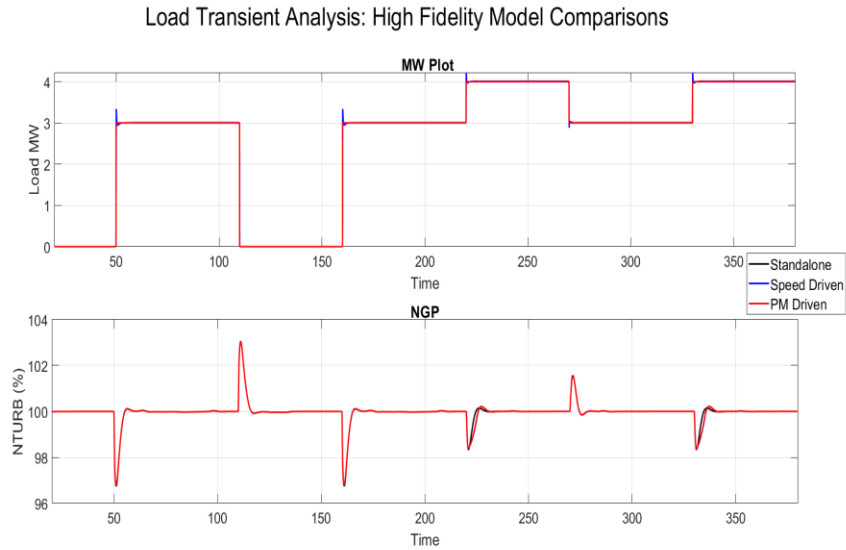


**Figure 33 Load transient analysis, high fidelity power flow models**

The high-fidelity model has complex computations which reflect each stage in the gas turbine and has the different temperature and pressure stations modeled within it. This means it will more accurately simulate the package in specific environments and conditions. This allows the initialization of the ambient temperature and pressures to factor in on the maximum load that is allowed on the generator set. It also means that computation time for the high-fidelity model could take around ten times that of the governor model.

While the high-fidelity power flow models both take much longer to simulate, their results most accurately align with the standalone T60-7901S model. The standalone model T60-7901S model took around 15 minutes to run the 7 minute simulation and incorporating it into the power flow model increased this amount as it did for the governor model when it was integrated into the power flow model.

### 5.5.3 Multiple Fidelity Comparison

The plots in figure 34 show a first load of 3MW and then a second load of 1 MW, as opposed to a second load of 2MW as in the test cell data. This is because the initialization of the

simulation was done with values that involve different ambient conditions than that of the test cell. The results from the governor power flow model comparisons in bottom part of figure 34 follow the load used on the high-fidelity model for a direct comparison.

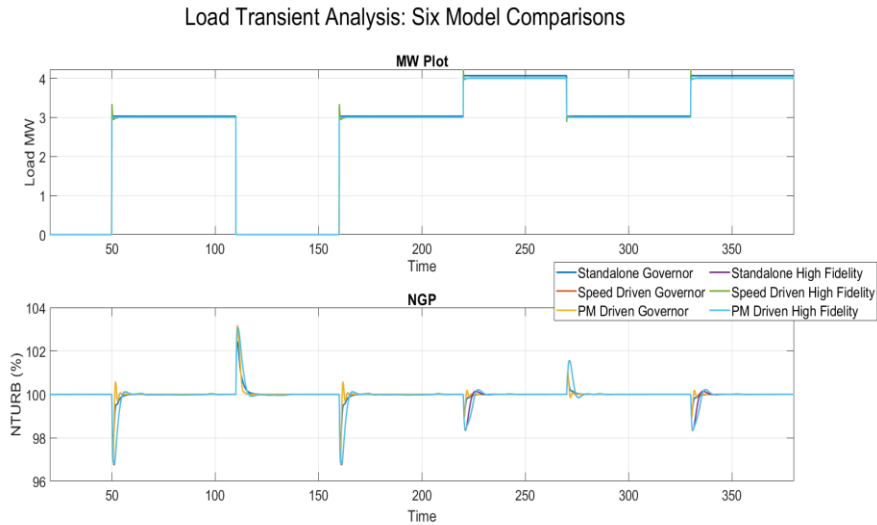


**Figure 34 Load transient analysis, multiple fidelity comparison**

The three governor models have sharper transitions and are not as accurate in modeling the transient behavior of the generator set. The high-fidelity models act as much better predictors of the responses and complex signals involved in the generator set as it operates in the electrical system.

The governor model which drives the generator with speed as opposed to mechanical power, is truer to real world operations of the generator set. The two high fidelity power flow models have been validated against the standalone and can be used for the loopback PLC once S5kSI is more stable.

## **5.6 Software Requirements**

Because the RSLogix5000<sup>®</sup> programming language used on the PLC is not designed as a standalone development tool, it lacks methods to test and validate the logic accurately. This is alleviated by using MATLAB's Simulink graphical modeling environment to design and simulate the models of the PLC, gas turbine, generator, CGCM, and loads. Then, to test the PLC logic with the power flow model, we need a communication path between Simulink and RSLogix5000<sup>®</sup>. Rockwell<sup>®</sup> Automation has a tool to interface between the PLC in the Simulink model and the actual PLC called the Studio 5000<sup>®</sup> Simulation Interface.

### **5.6.1 MATLAB<sup>®</sup> Simulink<sup>®</sup>**

The power flow models can be validated in the Simulink environment because the software allows modeling and simulation of complex physical and logical components. The Taurus 60<sup>®</sup> gas turbine, generator, and load are all physical systems that have specific parameters and complex relationships. The CGCM and PLC are logical systems that take input from the physical components and then output commands back to continue, start, or stop certain operations.

The different function blocks in the Simulink library, such as the signal builder block, can model load inputs which can be used to test the system and verify functionality of the logical components. In fact its performance aligns with the load function block, which is a more accurate and higher fidelity model of actual loads. In this sense, Simulink is very modular and a great way to rapidly prototype and compare expected results and model edge cases as necessary. Transfer functions allow modeling of expected behavior when systems become too complex.

The signals of the different models can be logged and easily compared in Simulink, allowing comparisons and verification that the models accomplish the same tasks despite using different inputs or outputs. It also allows models to be validated against test cell data, and for results to be saved for further review and comparisons. The Simulink model is created and used in MATLAB® version 9.4 R2018a, Simulink 9.1 for compatibility with the Studio 5000® Simulation Interface.

### **5.6.2 RSLogix 5000®**

RSLogix 5000® is the design and configuration software developed by Rockwell® Automation used for the PLC residing on the Allen-Bradley® ControlLogix-XT controller chassis. The PLC is used to supervise and control the package operation. It requires FactoryTalk access and is built on ladder logic, structured text, function block diagrams, and sequential function chart editors. The resulting software project file is composed of a task which consists of a series of programs, which are in turn made up of routines which are the actual control logic. This file is called the ACD file and resides on the controller.

However, the RSLogix 5000® programming language is lacking in its ability to test relationships and verify functionality. Edge cases often cannot be tested due to their existence being very limited, so the input required to execute the logic associated with these cases might not be used or tested. The ability to slowly step through and inspect the logic with the ladder logic can also be difficult, as the structure of the code can be hard to trace depending on the complexity involved. This makes standalone development as well as verification of logic in RSLogix 5000® strenuous. These complexities are combated by using the Simulink environment to model certain inputs to test the logic, and for designing of the code.

### **5.6.3 Studio 5000® Simulation Interface**

The Studio 5000® Simulation Interface (S5kSI) is used for communication between the PLC in the controller chassis and the power flow model to test the logic in the PLC. It is still not a mature interface system but has the end goal of having the ability to connect a Simulink model to a physical PLC to communicate with the model developed. The interface takes the controller tags and connects them over to the inputs and outputs of a block in the Simulink model of the PLC, to form a data exchange between the logic and the modeling software

# Chapter 6

## Results & Technical Analysis

### 6.1 Test Setup of loop back PLC and CHIL

CHIL (Controller hardware-in-the-loop) simulation is a technique where the controller is integrated into the test loop. Signals through sensors and actuators are simulated to test the controller actions, as shown in the test setup shown below. CHIL is leveraged to test algorithms. Most common CHIL tools include dSPACE®, Opal-RT®, Speedgoat®, Typhoon® HIL, ETAS®. For the purpose of this test Typhoon HIL was utilized. To allow for ease of troubleshooting and limited inverter board capacity only 2 x GTG were simulated connected to BESS. Actual PLC based controllers with plant specific software were connected in a loopback mode to emulate the entire dynamic operating spectrum, from start up, full load to shut-down. 2x50% Inverter control boards are used to simulate the inverter operation of grid following and grid forming mode. As shown in the figure 35 Units are sharing the load and when one unit goes down immediately BESS detects the loss of power and starts dispatching the power thus providing the needed spinning reserve.

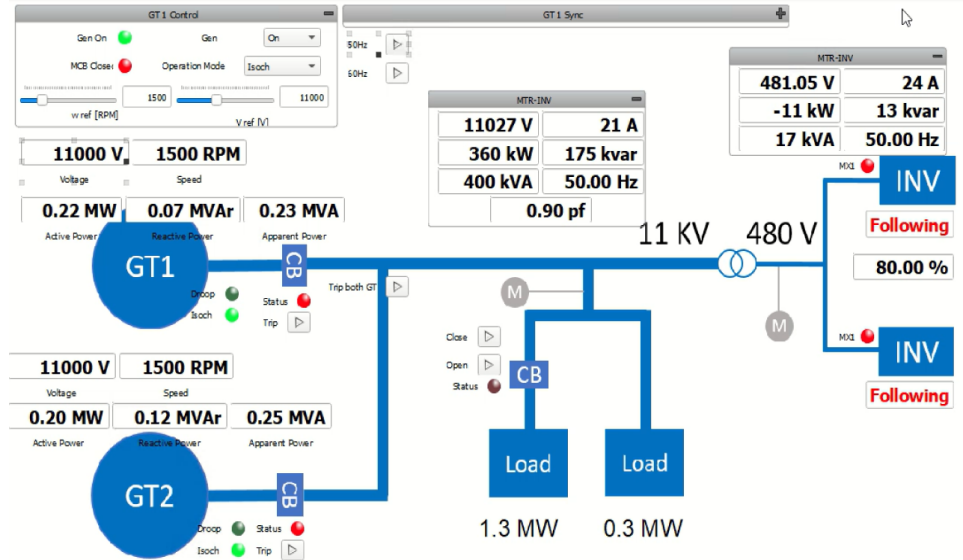


Figure 35 Controller hardware in loop (CHIL) simulation set up using GTG and BESS

Each GT and BESS unit controller, acting as a primary control loop is tuned to ensure that this transfer is managed within the 250 millisecond(ms) response time window available for maximum load. If unit control response time exceeds this window the Power Management System (PMS), operating as secondary control loop tertiary control. The diagram of a microgrid with hierarchical control structure is shown in figure 36.

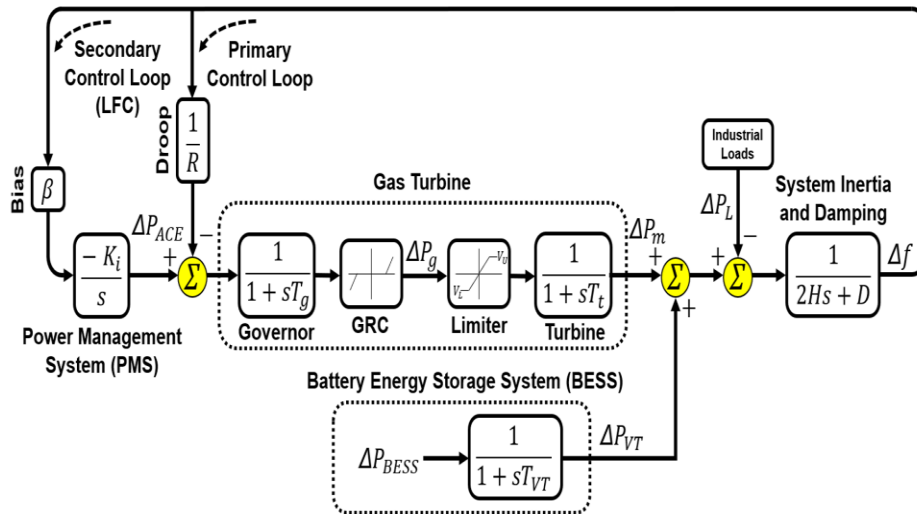


Figure 36 Primary and secondary control loops of hybrid power system

The central PMS controller implements tertiary control functions such as load-shedding, state estimation, and voltage-var control. The central controller can communicate with local controllers of energy resources in the microgrid to send dispatch signals and obtain status and measurement of local units. The stability control function is implemented in local controllers to achieve real-time power balancing and power sharing[17]. The dominant presence of Power electronics (PEL) interfacing significantly increases control complexities. In Microgrids with high renewable penetration, the absence of inertia and the relatively short lines of Microgrids infrastructure increase the difficulties of frequency and voltage control[44].

A key area in which energy storage is widely recognized as being necessary is to serve large transient loads, the ramp rates of some loads maybe beyond the dynamic range of gas turbines. In that case, storage, with fast charge and/or discharge rates is needed to buffer a gas turbine from the transient [24].

Before performing integrated system tests, CHIL is used to tune and test every generator by using their controllers. This provides the starting-point PID (Proportional Integral Derivative) constant values for each distributed controller[45]. A large variety of tests were conducted using the loop-back simulator and actual distributed controllers for various generation loading conditions. Some of the tests included generation tripping, load tripping, large load startups, single-phase and three-phase faults at various plant locations, loss of excitation and prime mover, arc-flash events triggering the opening of multiple breakers within the system.

Starting reliability is defined as the expected likelihood that a generating unit can successfully start on demand and/or within a given time period[46]. CHIL is used extensively to validate this starting reliability for the spinning reserve application. Since, there is always a trade-off between communication burden and performance[44], it is ensured in this hybrid

architecture that embedded inverter controls allow for grid forming and grid following mode changes locally without any central intervention.

Similarly local gas turbine controllers can perform generator and governor controls locally. The PMS controller manages and communicates with all the other plant components control decisions based on knowledge of all balance of plant inputs combined in a single optimization problem. The PMS controller thus provides the power and frequency set points only thus offering a very efficient and tightly integrated architecture.

#### BESS Short-circuit Test

We identified the following 4 scenarios for a Flexible HPS consisting of a Diesel Generator Set, Battery Storage System with Inverter, Non-controllable Load, Utility grid connection. The Interaction of these different DERs was controlled through a Station Microgrid Controller(SMC) and responses were recorded using Typhoon HIL Simulator. All the results are recorded and reviewed below. For the purpose of this thesis, we have carefully picked these 4 scenarios which have the most practical application in the industry and will also allow us to find the weakness in design or operating conditions of the proposed HPS. For the purpose of testing, we have assumed a solid-state breaker which will have 200 ms response time.

**Table 5 Scenario Testing Table**

	GTG #1	GTG #2	Load Breaker	Key Observations
Essential Load Scenario	1	1	0	Only essential loads are connected, load breaker is open, BESS can be requested to charge/discharge, inverter is Grid Following, it will follow the grid frequency. This is a standby mode where only essentials loads are powered during scheduled maintenance of the plant.
Full Load Scenario	1	1	1	BESS and GTG can participate in load dispatch, inverter is in Grid Following mode.
Black Start Scenario	1	1	1	First time BESS is connected online, it acts as a load, GTG 1 & 2 will charge the BESS and will maintain load frequency.
Spinning Reserve Scenario	0	1	1	When One GT trips, BESS will immediately pick up the load and participate in load frequency control. GTG and BESS are also load sharing. Inverter is in Grid Forming mode.

1= Breaker Closed

0= Breaker Open

Scenario 1 : This is a standby mode, wherein only the essential load is connected. Inverter is grid following and State Of Charge (SOC) is maintained for the BESS. As we can see from figure 37 when the PMS provides a control signal to charge and discharge the BESS, the PI controller in the inverter reacts and performs local control to match the phase angle. It's interesting to note that local load does not see any impact due to this energy transfer between GTG and BESS. Similarly, we can assume that if the battery SOC is below certain set point, SMC will provide a charge signal to the inverter and now inverter will act as a load and will be able to consume the power from the grid.

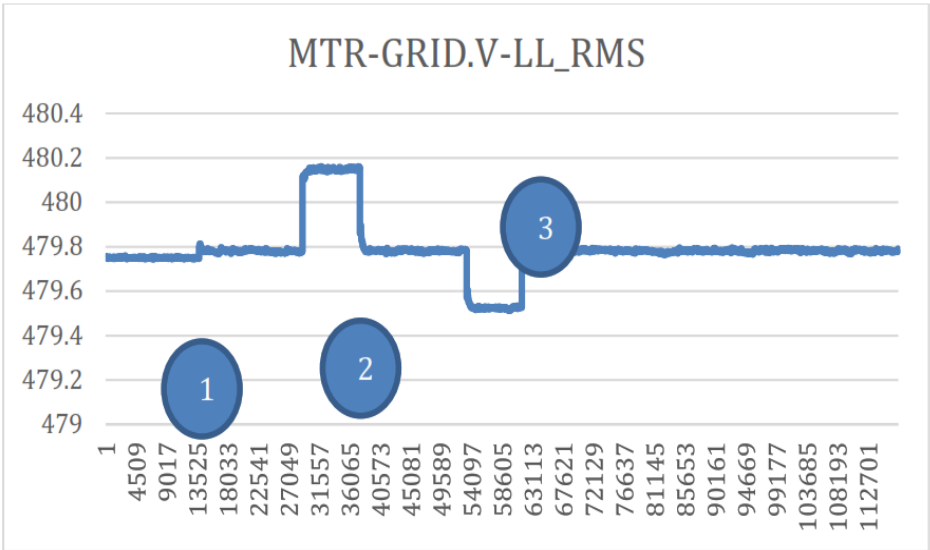


**Figure 37 Discharge-charge of BESS in scenario 1**

Discharge-Charge of BESS in figure 37 above shows the SoC of the energy storage system. Instance 1. Is when the inverter went online on grid following, 2. Discharging 100 kW, 3. Charging at 100 kW. This mode of operation is also known as Economic Dispatch/Demand Charge mode. Upon further analysis of the waveforms it is evident that switching frequency of the inverter and the gain of the PI controller can be tuned to ensure faster dispatch of the power to the grid.

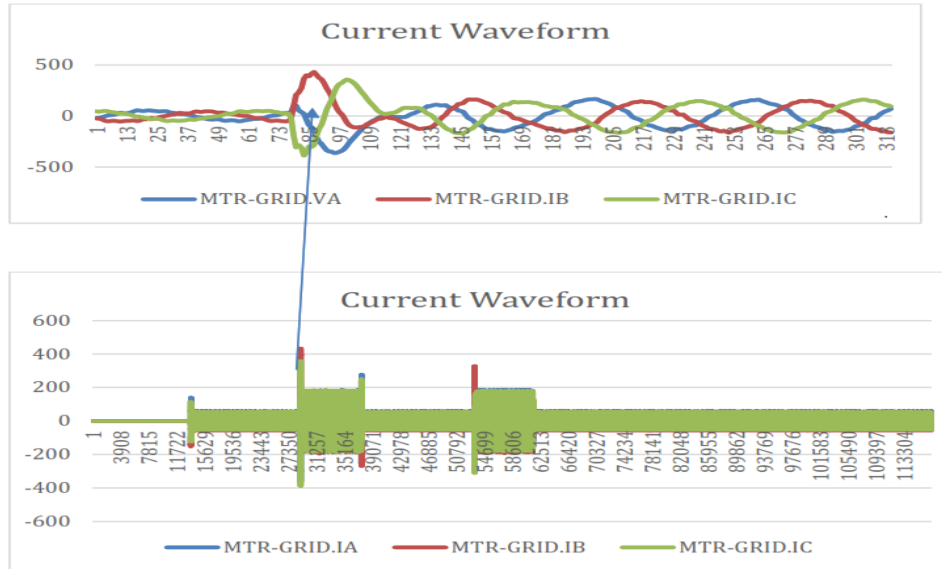


**Figure 38 Inverter PI controller performance**

Inverter PI Controller Performance in figure 38 above shows the waveform at Grid Connection Point. Inverter controls senses the phase difference and quickly reacts through PI control and adjust the error

Scenario 2 : As shown in figure 39 below, this is a grid connected mode, where the entire plant load is being fed by GTGs. Inverter is grid following and the PMS will perform the function of export and import including load sharing between GTG and BESS. Economic dispatch algorithms can be implemented at PMS based on tariff rates of the local utility and charge/discharge commands can be set for the battery and GTGs. It's also worth noting that BESS is acting as a spinning reserve, helping the plant to avoid running a standby GTG.

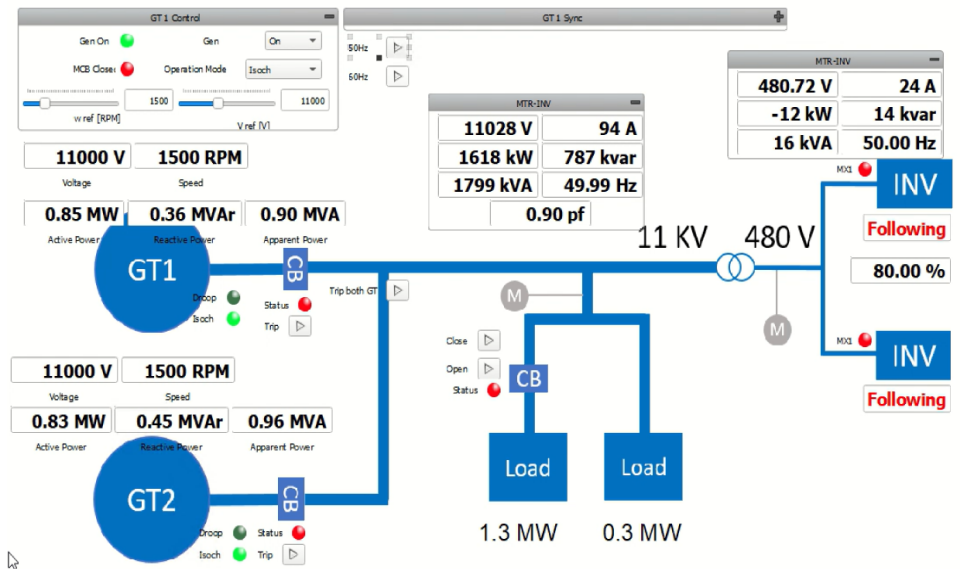


**Figure 39 Export-import control in scenario 2**

As seen from the figure 40 below, when the load breaker is closed, both the GTGs immediately ramp up and share the 1.6 MW load between them. Inverter is in grid following mode hence it is not participating load sharing unless it is commanded to do so by the PMS. GTG fuel control and governor model can be tuned to have a smooth operation upon the closure of the load breaker. As we can see from the frequency curve, upon closure of the load breaker the grid frequency drops to 49.2 hz, however the governor control of GTG is able to quickly adjust

the speed to limit the duration below the allowable reaction time for the plant, thus keeping the RoCoF below the load shedding limits.

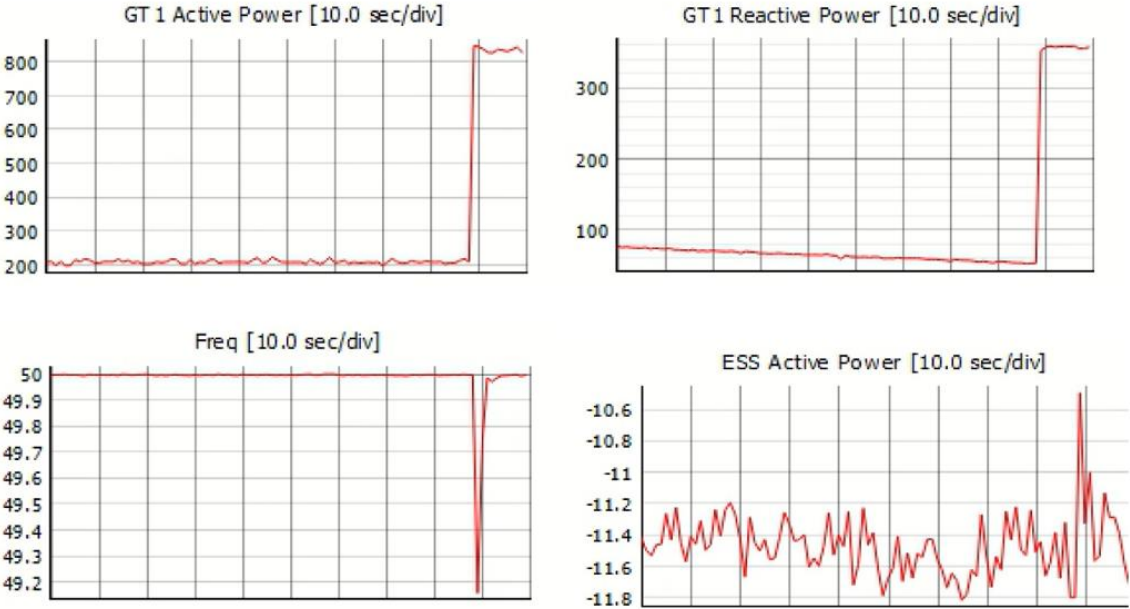


**Figure 40** When load breaker is closed,GT1/2 share 800KW under isochronous control mode

Scenario 3 : This is simulated version of the black start mode of the plant start up. When the first-time plant is started up, GTGs will be started and will be synchronized with the load. At this point of the time, the BESS is not fully charged, and it needs to be charged to the full capacity. While this charging of the BESS is being done, it acts as an additional load for the plant. Such operation is not very common, but it needs to be planned during the design basis for the project. The load capacity of the plant, GTG capacity and load profile of the plant will have significant impact on the sizing of the BESS. There is a lot of research being done on the optimum sizing of the BESS for multitude of applications. As we can see from the figure 41 below GTGs are generating 800 KW load each and feeding plant load of 1.6 MW, as soon as completely drained BESS is connected to the load and PMS commands inverter to fully charge the BESS, GTGs



**Figure 41 GTG 1 and 2 ramp-up to provide black start charging for BESS**

are able to sustain all of the microgrid load. The entire 2.6 MW load is now being supplied by the GTG. It is worth noting here that to allow for the fast charging of the inverter such full load

charging operation is designed in this plant operation. If GTGs are capacity limited, then inverter can be partially charged by varying the setup of the inverter for gradual charging. This is also an example of the variable load in a grid wherein Inverter will be in Grid Following mode. As shown in figure 42 below when BESS demands 1000 KW charge the grid frequency drops to 49.4 but quickly recovers as both GTGs pick up the load instantly. This test is also a very good set up to perform inverter short circuit test, where the inverter may discharge upto 1000 KW and switch to normal standby position when the fault is reset. Such electrical fault cannot be simulated in real life, however through simulation we are able to verify this function. As shown in the figure below as soon as ESS normalizes its power GTGs will quickly reduce their power to 800 KW each.

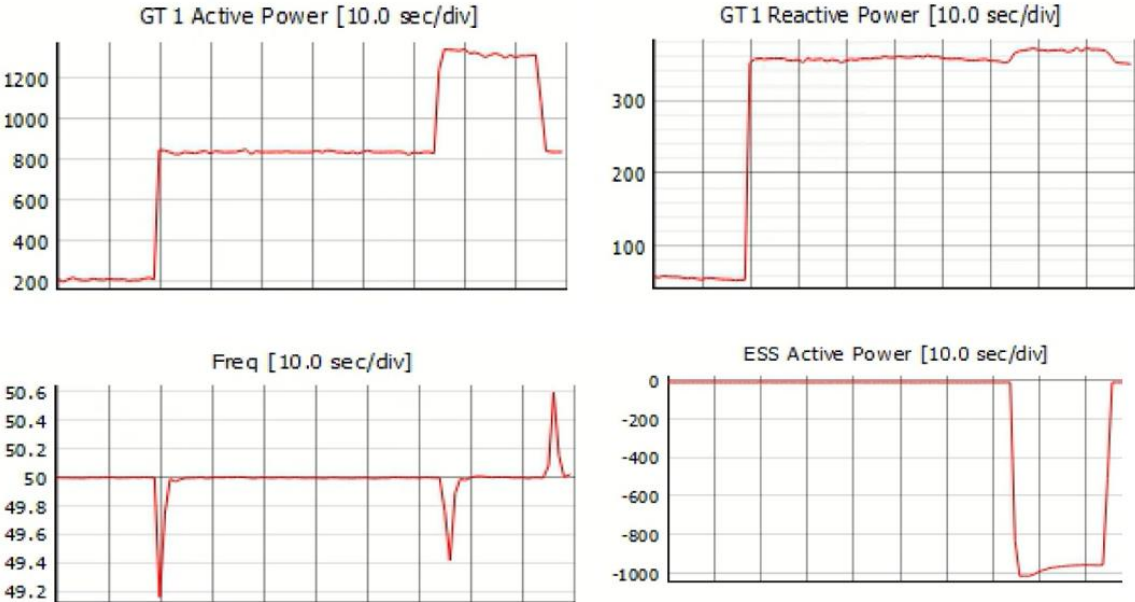


**Figure 42 BESS is fully discharged, GTG will load share and charge**

Multitude of fault simulations can be performed utilizing this test set up.

Scenario 4 : This is spinning reserve mode of operation. As shown in the figure 43 below, when GTG1 trips BESS can immediately dispatch the load shortfall.

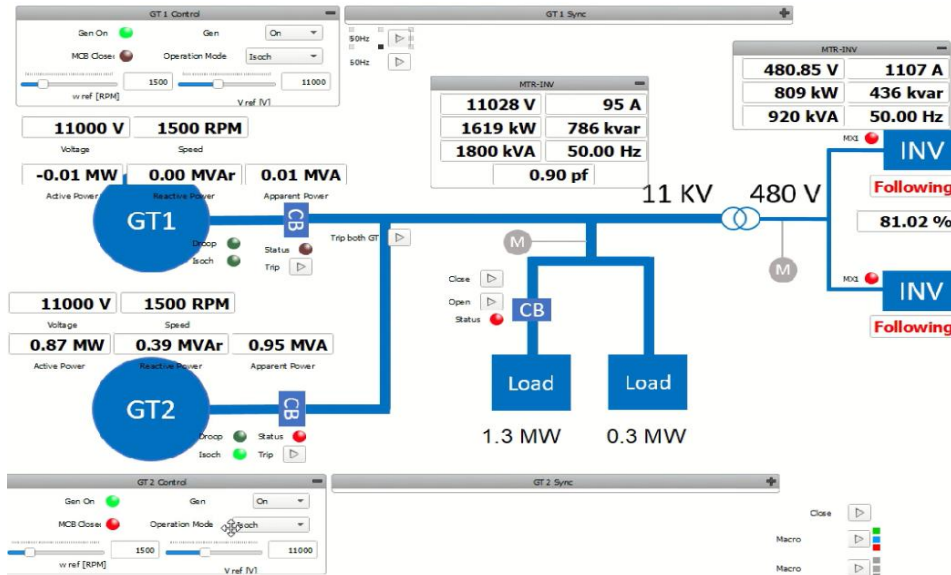


**Figure 43 Scenario 4, GTG 1 trips and BESS immediately takes over the load**

This is similar to an island operation mode where BESS and GTG are participating in load management of the microgrid, BESS is also participating in frequency control of the microgrid.

In this mode of operation, a droop curve similar to the synchronous generators is programmed in the inverter. As we can see from the figure 44 below, as soon as GTG1 trips, the frequency drops and GTG 2 tries to recover the shortfall, concurrently BESS is able to

dispatch the load and control the frequency back to nominal range.

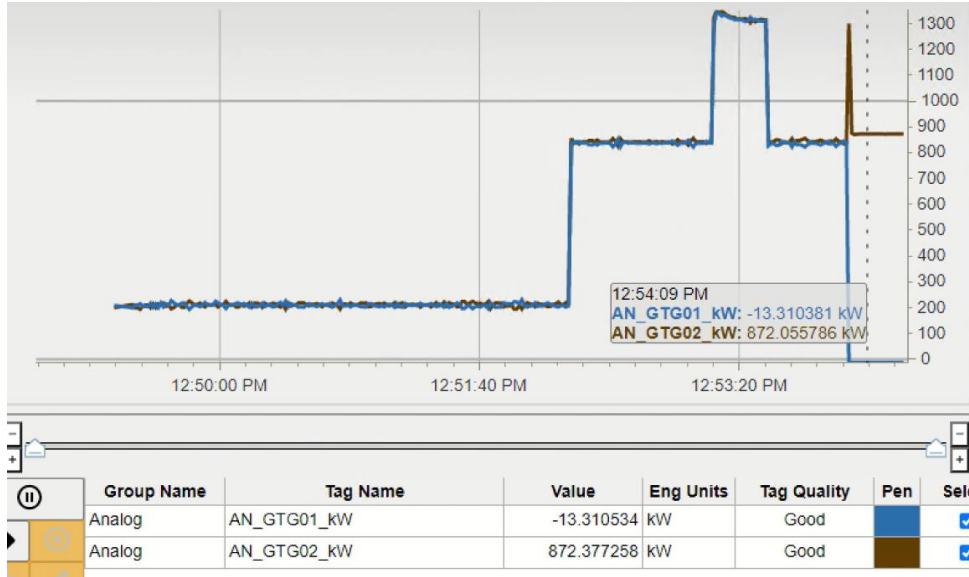


**Figure 44** GTG1 trips, GTG2 tries to pickup the load however BESS immediately takes over

We can also see from the figure 45 below that frequency drops upto 49.4 hz and BESS is very quick in recovering the frequency back to 50 Hz range.

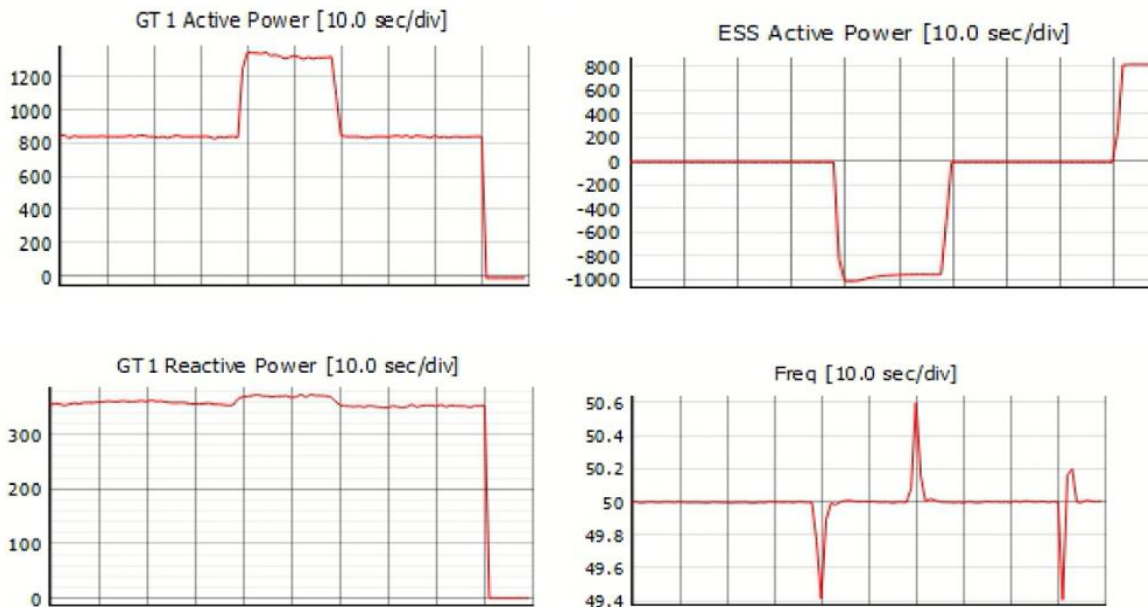


**Figure 45** Frequency drop with active frequency control from BESS

This mode is very similar to load sharing mode of generators, where multiple generators may be operating in parallel. Based on the slope of the droop settings BESS and GTG will respond to the changes in the load. There is substantial research being done in the area of Grid Supporting Inverters and how to make them suitable to create synthetic inertia on the grid. The biggest challenge in this mode of operation is the amount of current injection into the microgrid also leads to harmonic distortions which may be detrimental to other power equipment connected to the plant network.

This is considered as an ideal mode if we are islanding from the grid, we were able to simulate multiple islanding scenarios by creating different faults on the grid breaker and letting this mode sustain the microgrid. We can also perform reactive power control in this mode and it may require similar droop curve programming in the inverter. As shown in figure 46, the frequency regulation is most effective when BESS and GTG are participating in load management. Frequency control with BESS and GTG shows that BESS is able to provide much better and tighter frequency control compared to just by the GTG.

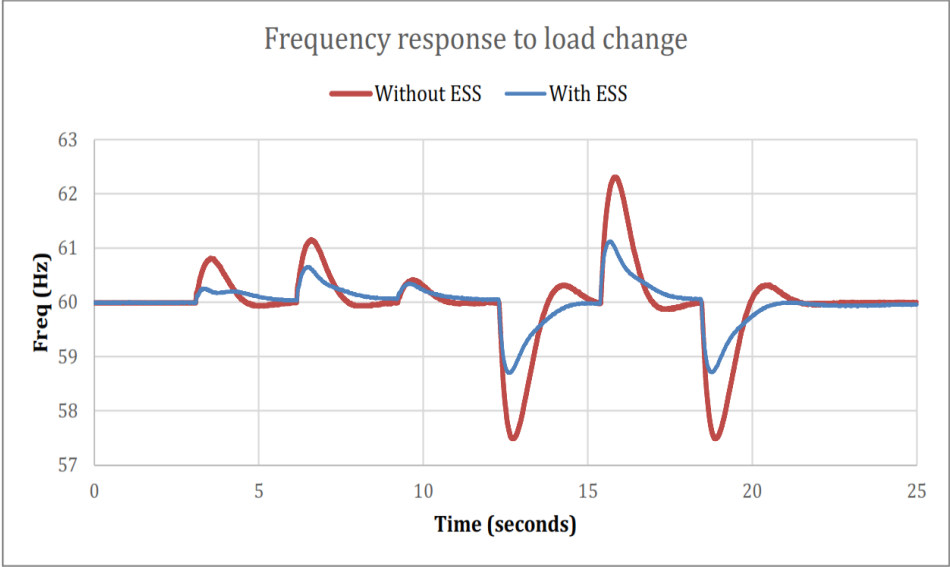


**Figure 46** Frequency control with BESS and GTG

It's noteworthy that in Scenario 2 where GTG governor control was managing the load, frequency dropped below 49.2 Hz, while in case of Scenario 4 frequency is well above 49.4 Hz, thus ramp rate of power discharge from BESS can help with quick response and support grid stability. While testing this Spinning Reserve mode it is interesting to note that depending upon the cost objective (fuel cost, operation cost etc) of the plant, it may make sense to keep the GTG partially or fully loaded while BESS can also help with peak shaving demand by the grid.

One of the improvisations that we recommend based on these result is to get an early warning of GTG failure through digital communication to the BESS and switch it to Grid forming mode. If you have multiple GTGs, BESS capacity should be big enough to cater to the plant load or have some form of load shedding mechanism in the PMS. We tried this algorithm in our PMC and the biggest advantage of this method is when the GTG is tripped we don't see an inrush current and the inverter does not trip on overcurrent.

Finally, we also wanted to verify multi tasking capability of the PMS with a view to see in case of plant disturbance if PMS will have enough bandwidth to perform all critical functions hence we also concurrently demanded charge/discharge signal from the PMS to BESS and its was evident that PMS was able to monitor and control multiple DERs without any data congestion.

Another very important observation was related to BESS and GTG controller tuning. Since inverter is in Grid Forming mode hence the frequency control is now a joint effort led by GTG and BESS, and this poses a serious problem which is highlighted in figure 47 below. As we can see below if we change the load or the voltage setpoint to the GTG, it reacts and delivers the power but this also starts a tug of war between the GTG and BESS for control. We

can see below that the frequency fluctuations were dramatic until we started to reduce the gain of the PI controller of the BESS. We also realized that for optimum performance of the microgrid it's extremely important for PMS to be able to perform the remote tuning of the control constants of local DERs.

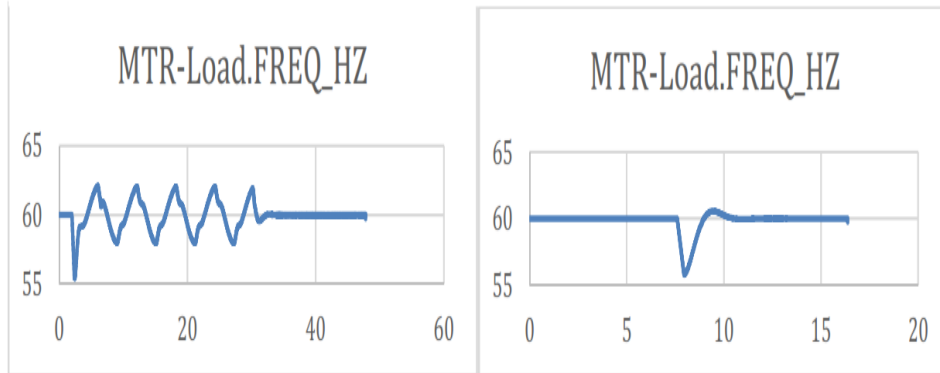


**Figure 47 Impact of gain adjustment of BESS on islanding**

Figure 47 above shows that by reducing the gain of the BESS inverter we are able control the frequency effectively. The figure on left shows frequency oscillation where DGS and BESS were out trying to take control, by reducing the gain of BESS we see a much smoother transition.

During this mode of operation one can leverage the GTG to perform the active power control and BESS can provide all of reactive power control. Such a control scheme needs further validation and testing on the real system, and it will be a very powerful economic tool for microgrid operators who have restrictions related to Power Factor and reactive power in their agreements. There is also a unique case of Power Factor control that can be managed in this mode of operation. For e.g there are certain machineries or devices in the plant which may operate closer to unity power factor and for such unique cases the Power Factor control can be provided by the BESS. Finally, one of the most promising modes of operation that can be

leveraged by this combination will be to put GTG in droop control and let BESS perform the frequency control of the grid, thus providing synthetic inertia.

While the above 4 scenarios do not test all the eventualities a microgrid can face, we were able to test many important and critical modes which will be used in different Hybrid Power System applications.

# Chapter 7

## Economic & Policy Analysis

### 7.1 Feasibility & Adoption

The objective of this project is to research, develop, and test modular fast-acting coordinated real-time power control with energy storage capability to enable HPS to provide fast grid support and improve power reliability of the electric grid. The modular design of the control algorithms and equipment should allow a variety of new and existing HPS in the 1-20 MWe size range to adopt the technology. It should also enable engagement of a CHP plant with the electricity grid operator through microgrid controls as defined by the IEEE P1547 and IEEE P2030.7 standards.

### 7.2 Policy Potential

HPS can be utilized in a variety of industrial facilities and commercial buildings with coincident power and thermal loads, however the installation of larger power systems (>20MW) has declined in recent years. Power Systems in the 1-20 MWe range that can operate as HPS have the potential to play a key role in increasing manufacturing efficiency while also supporting grid functions. There are many standalone diesel generators and gas generators based microgrids operational which have a lot of untapped standby power available and if these units can be combined into HPS they will provide a huge energy resource. There are currently 329 gas turbine CHP systems between 1-20 MWe providing over 2,300 MW of power in the U.S. today; these systems would be well suited for incorporation of HPS

technology which allows them to provide needed grid services. It is estimated that the export technical potential for industrial manufacturing sectors is 11,535 MW at 3,929 sites. A firm understanding of the potential market for HPS will be crucial in targeting manufacturing facility types and regions of the U.S. for future innovation and growth. Although the technical characteristics of manufacturing facilities generally support increased HPS deployment, there are potential economic and regulatory barriers that could affect market penetration. One main barrier relates to HPS ownership is the unclear value proposition for electric utilities. Many investor- owned electric utilities view customer-sited HPS as a source of revenue erosion due to traditional business models and regulations linking cost recovery and utility revenue to electricity sales. Legal/regulatory considerations, financing needs, and infrastructure requirements are also some impediments that need to be reviewed.

In HPS most of the power and thermal generation comes from conventional generation technologies, notably gas. Across a wide range of applications, conventional generation is the foundation of DER investment because these units mitigate the demand charge by peak shaving during peak hours and reduce the volumetric charge by displacing grid imported electricity during all hours. Solar PV, Wind and electric storage are viable and important, and indeed optimal in most cases, but serve to supplement natural gas investments rather than facilitate low-carbon microgrids. HPSs can benefit the microgrid owner, distribution system operator or utility, and society concurrently. Microgrids facilitate energy cost reductions, help integrate renewable energy sources, and can provide a host of services to the local distribution system. In theory, these benefits could be spread equitably among stakeholders and maximized with correct policy measures[47].

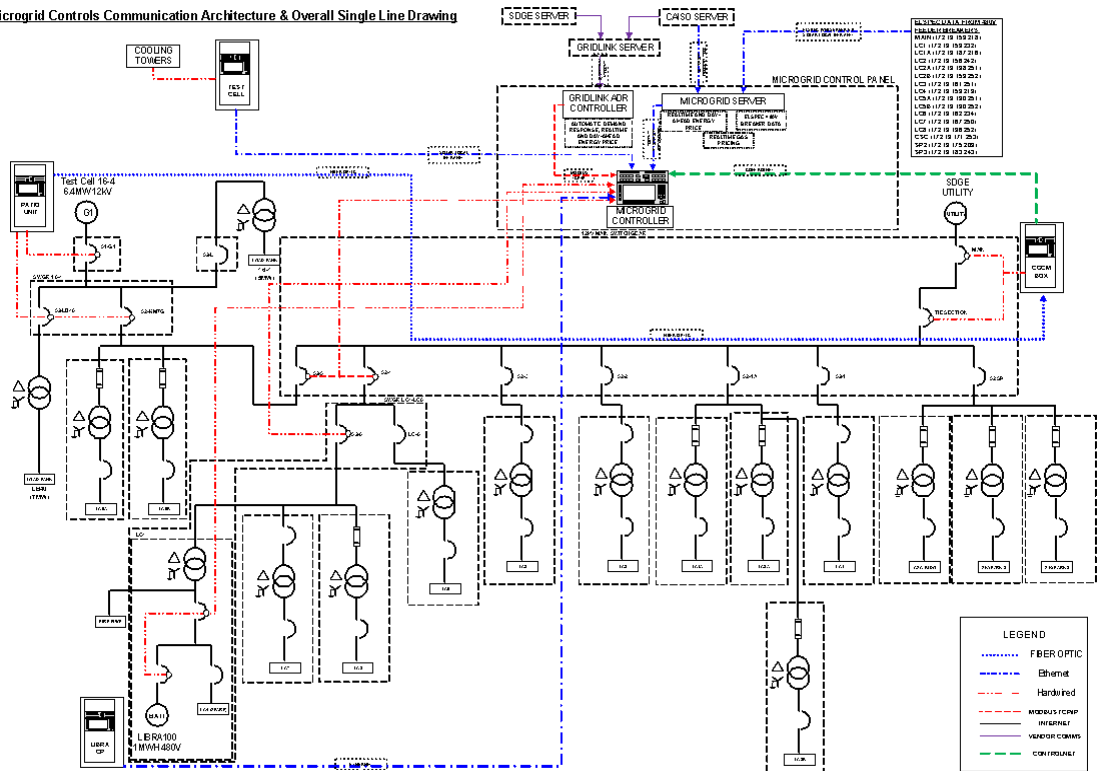
# Chapter 8

## Field Validation and Conclusion

### 8.1 Site Testing

Solar Turbines® Kearny Mesa manufacturing plant has three primary suitable test environments for this project: 1) the low and high voltage controls and power laboratory, 2) A 5.5MWe Taurus 60® power generation system grid-connected and fully instrumented for the collection of operation, performance, and emissions data, and finally 3) the facility microgrid including a manufacturing load and distribution fully instrumented for power flow and quality as well as a Solar LC1000 1MWe energy storage module.

Microgrid Controls Communication Architecture & Overall Single Line Drawing



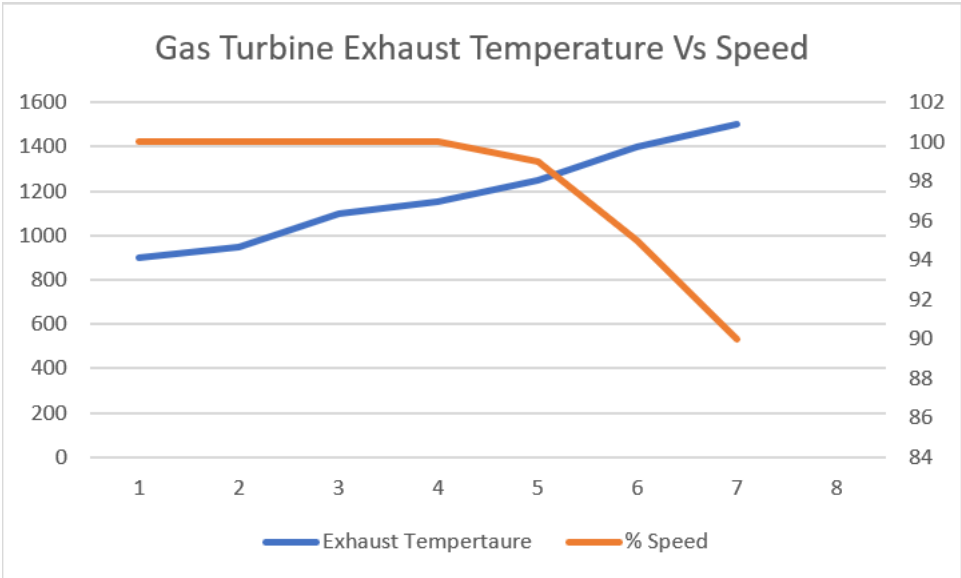
4

Figure 48 Solar Kearny Mesa facility one-line diagram

The Kearny Mesa facility is an example of a microgrid with T60 generator, Solar Energy Storage, Station Microgrid Controller (Real time pricing, economic dispatch, peak Shifting, load Shedding, load Sharing, grid / Island Capability), critical load (data center), and two emergency diesel gensets as shown in figure 48. All assets are network connected and are controlled and monitored. Based on all the simulation data collected from the HIL, we were able to validate the assumptions and fidelity of the models by testing various scenarios on the actual equipment. The key conclusions from this validation are listed below.

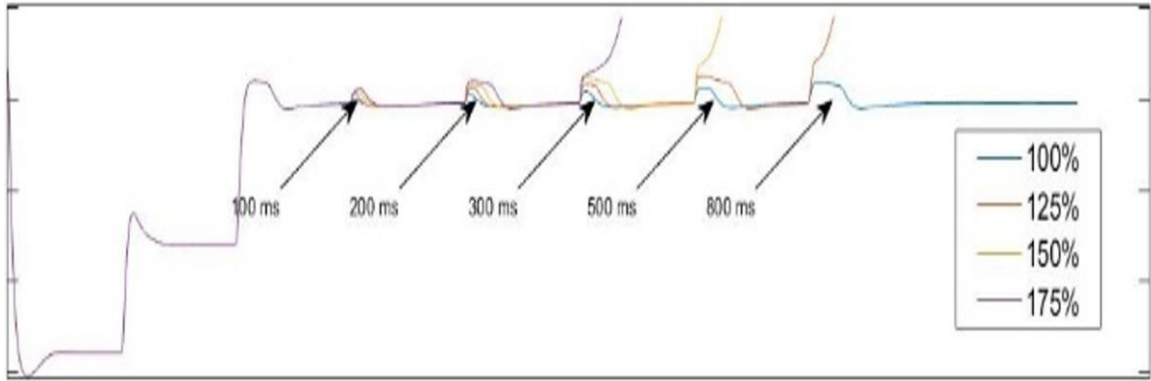
## 8.2 Results and Discussion

Figure 49 shows the results of a test whereby a Taurus 60<sup>®</sup> load is increased from 4MW to 6MW. The sudden increase is similar to 3 Taurus 60<sup>®</sup> operating in parallel at 4MW and suddenly one shutdown, transferring the load equally to the other two Taurus 60<sup>®</sup>. The units eventually shutdown on high exhaust temperature if there is no spinning reserve aid offered.



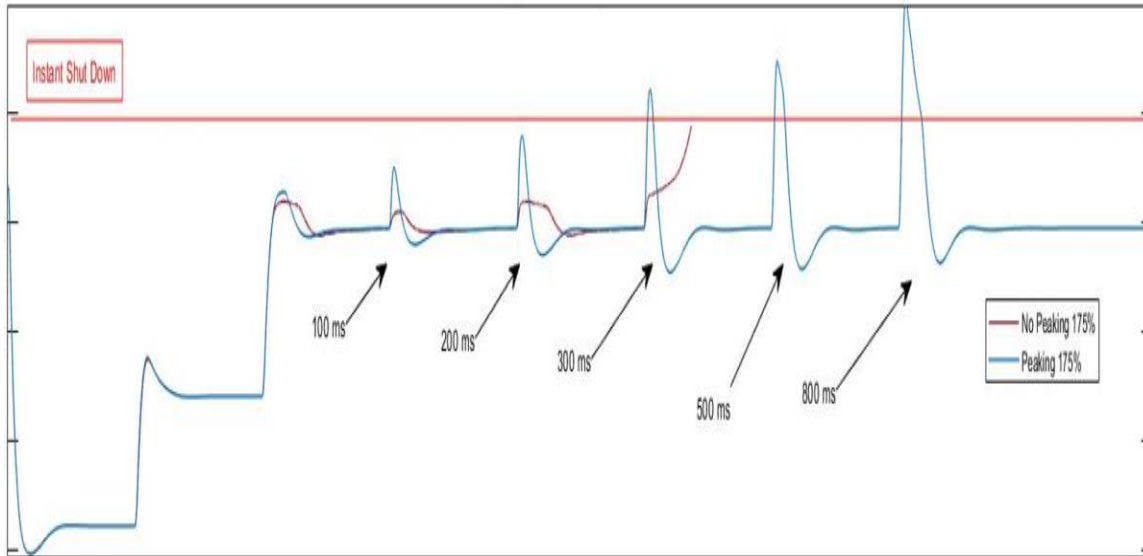
**Figure 49** Test showing exhaust temperature rise due to significant on-load ramp up

Figure 50 shows a similar analysis but with a series of load changes and response times identified in Table III. The turbines are configured not to accept large load changes instead it ramps up the governor response gradually, a control method that allows generators to respond in tandem with BESS to the large load changes in these scenario, the step change load is increased gradually and both the exhaust temperature and Turbine speed (N<sub>gp</sub>) are monitored for shutdown.



**Figure 50 Only gradual step load changes allowing better control for the plant**

Figure 51 shows the comparison between the response time when large load acceptance is enabled. It's noteworthy though that irrespective of the algorithms used, the speed at which the energy storage needs to be dispatched doesn't change that much. This test further validates our previous calculation for the 1.5 Hz/s RoCoF and validates that 250 ms will be ideal response time for the Gas Turbine and for the BESS to dispatch the 4 MW load. This will allow for the plant to avoid any protection trip or load shedding requirement and maintain stable grid operations



**Figure 51 System response without any gas turbine load acceptance limitation**

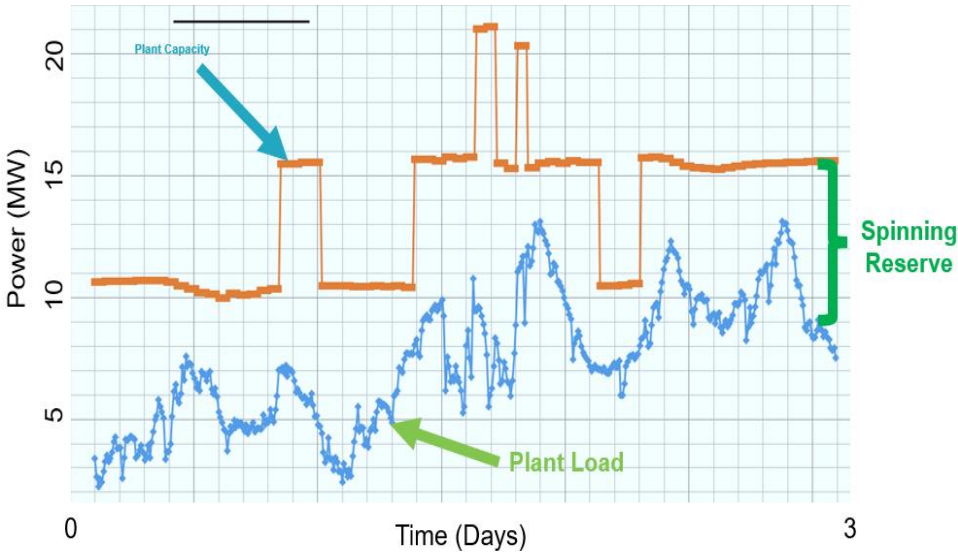
**Table 6 System load response**

Step Load Change	Response Time				
	100 ms	200ms	300ms	500ms	800ms
90% -> 100%	PASS	PASS	PASS	PASS	PASS
90% -> 125%	PASS	PASS	PASS	PASS	FAIL
90% -> 150%	PASS	PASS	PASS	FAIL	FAIL
80% -> 175%	PASS	PASS	FAIL	FAIL	FAIL

### 8.3 Conclusion

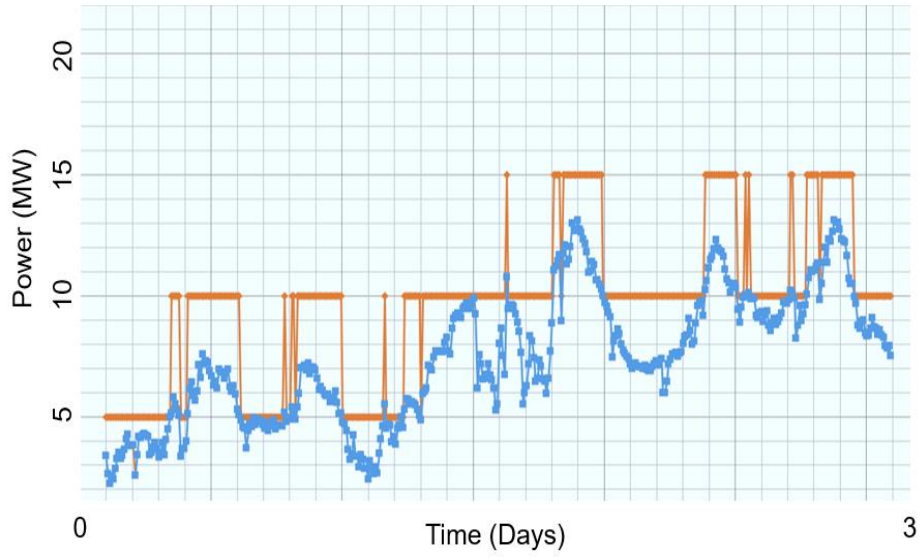
An integrated hybrid Gas Turbine Generator (GTG) system coupled with Battery Energy Storage System (BESS) shifts the operating philosophy from N+1 to a N+BESS system. This hybrid integration, coupled with advanced algorithms described in this dissertation can reduce capital expenditure (CAPEX) and Operating Expenditure (OPEX) of any system. Such hybrid power systems architecture allows better overall efficiency of the plant and leads to reduced CO2 emissions.

Figure 52 below is a sample of the plant load over 3 days. The blue line shows the plant load and how it varies on daily basis and is dependent on the operational needs. The orange line is the plant capacity. Step changes are indicative of a turbine is switched on. In this example, the capacity goes from 10MW to 20MW. What is very interesting is that the even when the load is at 50% of a single gas turbine, the plant is operating two units at approximately 25% part load turbine capacity. Gas turbines operate very inefficiently at part load increasing fuel consumption and emissions.



**Figure 52 Plant capacity without BESS**

On the contrary in figure 52 below, when GTG and BESS are integrated, GTGs can run closer to full load and BESS can immediately dispatch the needed power within the allotted reaction time window. This provides a much efficient operation and lower emission,



**Figure 53 Plant capacity with BESS**

This operation model provides significant savings in the carbon footprint of the plant.

Table below shows the overall savings due to efficiency and carbon tax.

**Table 7 Carbon Footprint and Operational Cost Reduction**

Item	Current Configuration	Proposed Configuration	Savings
KW Rating of GT	3 MW each	4 MW	
No of GTs operating	4 Nos	3 Nos	
% of Rated Load operation	75%	100%	
Fuel Consumption mmBTU/hr	40.21	51.1	
Annual Fuel Consumption mmBTU/Yr	345,806	439,460	
Total Fuel Consumption (\$5 mm/BTU)	1,383,224	1,318,180	
Annual Fuel Cost (\$)	\$6,916,120	\$6,590,900	\$325,220
Ton Co2/Yr	80,000 Tons	66,000 Tons	
Carbon Tax (50\$ /Ton)	\$ 4,000,000	3,300,000	\$700,000
Annual Saving (Fuel Cost and Carbon Tax avoidance)			\$1,025,220

Based on all the data collected as a part of this thesis, it is amply clear that BESS provides itself as an exceptional tool to leverage its capability in various operating conditions of a Hybrid Power Plant. The Grid Supporting Mode of inverter in which BESS can emulate as a synchronous generator is the most promising mode for seamless operation in Grid and Islanding conditions. Dynamic testing of integrating this mode with various DERs will help instill

confidence in the user community. It is still debatable if we can make the DER's more intelligent by embedding the Station Level Control capability at the Unit control level, thus completely getting rid of a Station Microgrid Controller. Such effort will require prior knowledge of the complete Microgrid installation and may not be suitable for existing plants which may require upgrade of their local controllers. Station Microgrid Controllers need to be fast, adaptive and highly integrated with local controllers hence using an open platform similar to PLC (Programmable Logic Controller) that allows for communication across different systems without prior knowledge of programming is very important. It's also critical that PMS has direct read/write capability to key tuning parameters of the DER including that of inverters. During the course of testing we had to tune multiple controllers and we realized that certain inverter manufacturers may not have such open architecture for remote connectivity. While the Inverter technology continues to evolve it is evident that it will play a big role in paving the way for integration of renewable energy into the grid. However, due to the intermittency of renewable energy, it has also brought harmonic challenges to the grid as a fluctuating power is continuously injected to the grid/microgrid. Efforts have to be devoted to the control of the feed-in grid current, which has to be synchronized with the grid voltage using a synchronization system[48].

## **ACKNOWLEDGEMENTS**

This work is supported by Solar Turbines<sup>®</sup>, A Caterpillar Company and University of California San Diego (UCSD).

## Bibliography

- [1] T. Porsinger, P. Janik, Z. Leonowicz, and R. Gono, “Modelling and Optimization in Microgrids,” *Energies* 2017, Vol. 10, Page 523, vol. 10, no. 4, p. 523, Apr. 2017, doi: 10.3390/EN10040523.
- [2] J. Undrill, “Primary Frequency Response and Control of Power System Frequency,” *Energy Anal. Environ. Impacts Div. Lawrence Berkeley Natl. Lab.*, no. February, 2018.
- [3] F. Katiraei, M. R. Iravani, and P. Lehn, “Micro-grid autonomous operation during and subsequent to islanding process,” *2004 IEEE Power Eng. Soc. Gen. Meet.*, vol. 2, p. 2175, 2004, doi: 10.1109/PES.2004.1373266.
- [4] H. M. Kim, Y. Lim, and T. Kinoshita, “An intelligent multiagent system for autonomous microgrid operation,” *Energies*, vol. 5, no. 9, pp. 3347–3362, 2012, doi: 10.3390/EN5093347.
- [5] C. D. Barley and C. B. Winn, “Optimal dispatch strategy in remote hybrid power systems,” *Sol. Energy*, vol. 58, no. 4–6, pp. 165–179, Oct. 1996, doi: 10.1016/S0038-092X(96)00087-4.
- [6] S. X. Tang, L. Camacho-Solorio, Y. Wang, and M. Krstic, “State-of-Charge estimation from a thermal–electrochemical model of lithium-ion batteries,” *Automatica*, vol. 83, pp. 206–219, Sep. 2017, doi: 10.1016/J.AUTOMATICA.2017.06.030.
- [7] A. G. Tsikalakis and N. D. Hatziargyriou, “Centralized control for optimizing microgrids operation,” *IEEE Power Energy Soc. Gen. Meet.*, 2011, doi: 10.1109/PES.2011.6039737.
- [8] A. Valibeygi, S. A. R. Konakalla, and R. De Callafon, “Predictive hierarchical control of power flow in large-scale PV microgrids with energy storage,” *IEEE Trans. Sustain.*

- Energy*, vol. 12, no. 1, pp. 412–419, Jan. 2021, doi: 10.1109/TSTE.2020.3001260.
- [9] D. Jones and M. Kelly, “Supporting Grid Modernization with Flexible CHP Systems,” 2017, Accessed: Sep. 11, 2022. [Online]. Available: <https://nccleantech.ncsu.edu/wp-content/>.
- [10] “Combined Heat and Power (CHP) Technical Potential in the United States,” 2016, Accessed: Sep. 11, 2022. [Online]. Available: [www.energy.gov/chp](http://www.energy.gov/chp).
- [11] A. Ulbig, T. S. Borsche, and G. Andersson, “Impact of Low Rotational Inertia on Power System Stability and Operation.”
- [12] E. M. G. Rodrigues, G. J. Osório, R. Godina, A. W. Bizuayehu, J. M. Lujano-Rojas, and J. P. S. Catalão, “Grid code reinforcements for deeper renewable generation in insular energy systems,” *Renew. Sustain. Energy Rev.*, vol. 53, pp. 163–177, 2016, doi: 10.1016/j.rser.2015.08.047.
- [13] I. Scott and S. H. Lee, “Battery energy storage,” *Large Energy Storage Syst. Handb.*, no. May, pp. 153–179, 2011.
- [14] B. Hartmann, I. Vokony, and I. Táci, “Effects of decreasing synchronous inertia on power system dynamics—Overview of recent experiences and marketisation of services,” *Int. Trans. Electr. Energy Syst.*, vol. 29, no. 12, Dec. 2019, doi: 10.1002/2050-7038.12128.
- [15] M. Kosmecki *et al.*, “A methodology for provision of frequency stability in operation planning of low inertia power systems,” *Energies*, vol. 14, no. 3, 2021, doi: 10.3390/en14030737.
- [16] T. Kerdphol, M. Watanabe, K. Hongesombut, and Y. Mitani, “Self-Adaptive Virtual Inertia Control-Based Fuzzy Logic to Improve Frequency Stability of Microgrid with

- High Renewable Penetration,” *IEEE Access*, vol. 7, pp. 76071–76083, 2019, doi: 10.1109/ACCESS.2019.2920886.
- [17] X. Feng, A. Shekhar, F. Yang, R. E. Hebner, and P. Bauer, “Comparison of Hierarchical Control and Distributed Control for Microgrid, Electric Power Components and Systems,” *Electr. Power Components Syst.*, vol. 45, no. 10, pp. 1043–1056, 2017, doi: 10.1080/15325008.2017.1318982.
- [18] H. Zhang, H. Sun, Q. Zhang, and G. Kong, “Microgrid Spinning Reserve Optimization with Improved Information Gap Decision Theory,” *Energies 2018, Vol. 11, Page 2347*, vol. 11, no. 9, p. 2347, Sep. 2018, doi: 10.3390/EN11092347.
- [19] M. U. Usama, D. Kelle, and T. Baldwin, “Utilizing spinning reserves as energy storage for renewable energy integration,” 2014, doi: 10.1109/PSC.2014.6808136.
- [20] H. Bevrani, “Robust Power System Frequency Control,” *Robust Power Syst. Freq. Control*, 2009, doi: 10.1007/978-0-387-84878-5.
- [21] A. Ulbig, T. S. Borsche, and G. Andersson, “Impact of low rotational inertia on power system stability and operation,” *IFAC Proc. Vol.*, vol. 19, pp. 7290–7297, 2014, doi: 10.3182/20140824-6-ZA-1003.02615.
- [22] J. Shair, X. Xie, and G. Yan, “Mitigating subsynchronous control interaction in wind power systems: Existing techniques and open challenges,” *Renew. Sustain. Energy Rev.*, vol. 108, no. March, pp. 330–346, 2019, doi: 10.1016/j.rser.2019.04.003.
- [23] R. M. Kamel, A. Chaouachi, and K. Nagasaka, “Detailed Analysis of Micro-Grid Stability during Islanding Mode under Different Load Conditions,” *Engineering*, vol. 03, no. 05, pp. 508–516, 2011, doi: 10.4236/ENG.2011.35059.
- [24] R. E. Hebner *et al.*, “Dynamic Load and Storage Integration,” *Proc. IEEE*, vol. 103, no.

- 12, pp. 2344–2354, Dec. 2015, doi: 10.1109/JPROC.2015.2457772.
- [25] H. Bahlwan *et al.*, “Sizing and operation of a hybrid energy plant composed of industrial gas turbines, renewable energy systems, and energy storage technologies,” *J. Eng. Gas Turbines Power*, vol. 143, no. 6, Jun. 2021, doi: 10.1115/1.4049652/1095483.
- [26] “Black System,” *BLACK Syst. SOUTH Aust. 28 Sept. 2016 – Final Rep.*, no. SEPTEMBER 2016, 2017.
- [27] C. W. Taylor, “Power system stability controls,” *Power System Stability and Control, Third Edition*. pp. 1-31-13–20, 2017, doi: 10.4324/b12113.
- [28] L. Díez-Maroto, L. Rouco, and F. Fernández-Bernal, “Fault ride through capability of round rotor synchronous generators: Review, analysis and discussion of European grid code requirements,” *Electr. Power Syst. Res.*, vol. 140, pp. 27–36, 2016, doi: 10.1016/j.epsr.2016.06.046.
- [29] “Modeling and Simulation of an Autonomous Hybrid Power System Stamatia Gkiala Fikari Masterprogrammet i energiteknik Master Programme in Energy Technology,” 2015, Accessed: Sep. 11, 2022. [Online]. Available: <http://www.teknat.uu.se/student>.
- [30] T. Sun and D. Lubkeman, “Modeling Combined Heat and Power Systems for Microgrid Applications,” doi: 10.1109/TSG.2017.2652723.
- [31] A. M. Macneill, “Offshore Power System Micro-Grid Design,” 2017.
- [32] H. A. Saleem, “Microgrid Modeling and Grid Interconnection Studies,” Accessed: Sep. 11, 2022. [Online]. Available: [https://trace.tennessee.edu/utk\\_gradthes](https://trace.tennessee.edu/utk_gradthes).
- [33] J. L. Blackburn and T. J. Domin, “Protective Relaying : Principles and Applications, Third Edition,” *Prot. Relaying*, Dec. 2006, doi: 10.1201/9781420017847.
- [34] Y. Levron and J. Belikov, “Lecture 1: Introduction to Power System Dynamics: Time-

- varying Phasors and Primary Frequency Control,” Accessed: Sep. 11, 2022. [Online]. Available: <https://a-lab.ee/projects/dq0-dynamics>.
- [35] F. Blaabjerg, R. Teodorescu, M. Liserre, and A. V. Timbus, “Overview of Control and Grid Synchronization for Distributed Power Generation Systems,” *IEEE Trans. Ind. Electron.*, vol. 53, no. 5, pp. 1398–1409, 2006, Accessed: Sep. 11, 2022. [Online]. Available: [https://www.academia.edu/9649353/Overview\\_of\\_Control\\_and\\_Grid\\_Synchronization\\_for\\_Distributed\\_Power\\_Generation\\_Systems](https://www.academia.edu/9649353/Overview_of_Control_and_Grid_Synchronization_for_Distributed_Power_Generation_Systems).
- [36] D. Baimel, J. Belikov, J. M. Guerrero, and Y. Levron, “Dynamic Modeling of Networks, Microgrids, and Renewable Sources in the dq0 Reference Frame: A Survey,” *IEEE Access*, vol. 5, pp. 21323–21335, Oct. 2017, doi: 10.1109/ACCESS.2017.2758523.
- [37] A. M. Bouzid, A. Chériti, and P. Sicard, “H-infinity loopshaping controller design of micro-source inverters to improve the power quality,” *IEEE Int. Symp. Ind. Electron.*, pp. 2371–2378, 2014, doi: 10.1109/ISIE.2014.6864990.
- [38] X. Wang, M. Yue, E. Muljadi, X. Wang, M. Yue, and E. Muljadi, “Modeling and Control System Design for an Integrated Solar Generation and Energy Storage System with a Ride-Through Capability Preprint Modeling and Control System Design for an Integrated Solar Generation and Energy Storage System with a Ride-Through Capability,” 2012, Accessed: Sep. 11, 2022. [Online]. Available: <http://www.osti.gov/bridge>.
- [39] E. Twining and D. G. Holmes, “Grid Current Regulation of a Three-Phase Voltage Source Inverter With an LCL Input Filter,” *IEEE Trans. POWER Electron.*, vol. 18, no. 3, 2003, doi: 10.1109/TPEL.2003.810838.
- [40] M. Theses and J. A. Mueller, “Scholars’ Mine Scholars’ Mine Small-signal modeling of

- grid-supporting inverters in droop Small-signal modeling of grid-supporting inverters in droop controlled microgrids controlled microgrids,” 2014, Accessed: Sep. 11, 2022.  
[Online]. Available:  
[https://scholarsmine.mst.edu/masters\\_theseshttps://scholarsmine.mst.edu/masters\\_theses/7335](https://scholarsmine.mst.edu/masters_theseshttps://scholarsmine.mst.edu/masters_theses/7335).
- [41] W. Guo and L. Mu, “Control principles of micro-source inverters used in microgrid,” *Prot. Control Mod. Power Syst. 2016 11*, vol. 1, no. 1, pp. 1–7, Jun. 2016, doi: 10.1186/S41601-016-0019-8.
- [42] L. M. R. Oliveira and ) A J Marques Cardoso, “MODELLING AND SIMULATION OF THREE-PHASE POWER TRANSFORMERS.”
- [43] M. Bello, A. Maitra, D. Montenegro, and D. Gusain, “Power system studies considerations for Microgrid design,” *2019 IEEE Work. Power Electron. Power Qual. Appl. PEPQA 2019 - Proc.*, May 2019, doi: 10.1109/PEPQA.2019.8851559.
- [44] A. Vasilakis, I. Zafeiratou, D. Lagos, and N. Hatziargyriou, “The Evolution of Research in Microgrids Control,” *IEEE Open Access J. Power Energy*, pp. 1–1, Oct. 2020, doi: 10.1109/oajpe.2020.3030348.
- [45] K. G. Ravikumar, B. Bosley, T. Clark, and J. Garcia, “Isochronous load sharing principles for an islanded system with steam and gas turbine generators,” in *2017 Petroleum and Chemical Industry Technical Conference, PCIC 2017*, Dec. 2017, vol. 2017-Decem, pp. 405–412, doi: 10.1109/PCICON.2017.8188761.
- [46] G. K. Toh and H. B. Gooi, “Starting up rapid-start units for energy and reserve contributions,” in *2010 IEEE 11th International Conference on Probabilistic Methods Applied to Power Systems, PMAPS 2010*, 2010, pp. 626–631, doi:

10.1109/PMAPS.2010.5529003.

- [47] R. Hanna, M. Ghonima, J. Kleissl, G. Tynan, and D. G. Victor, “Evaluating business models for microgrids: Interactions of technology and policy,” *Energy Policy*, vol. 103, pp. 47–61, 2017, doi: 10.1016/j.enpol.2017.01.010.
- [48] Y. Yang, L. Hadjidemetriou, F. Blaabjerg, and E. Kyriakides, “Benchmarking of phase locked loop based synchronization techniques for grid-connected inverter systems,” *9th Int. Conf. Power Electron. - ECCE Asia "Green World with Power Electron. ICPE 2015- ECCE Asia*, pp. 2167–2174, Jul. 2015, doi: 10.1109/ICPE.2015.7168077.